

NUTRIENT LOADING AND TRANSFORMATIONS IN THE
COLUMBIA RIVER ESTUARY DETERMINED BY HIGH
RESOLUTION IN SITU SENSORS

By

Melissa L. Gilbert

A THESIS

Presented to the Division of Environmental & Biomolecular Systems

and the Oregon Health & Science University School of Medicine

in partial fulfillment of the requirements for the degree of

Master of Science

September 23, 2011

School of Medicine
Oregon Health & Science University

CERTIFICATE OF APPROVAL

This is to certify that the Master's thesis of
Melissa Gilbert
has been approved

Joseph A. Needoba, Ph.D., Research Advisor
Assistant Professor

Antonio M. Baptista, Ph.D.
Professor

Fredrick G. Pahl, Ph.D., External Examiner
Professor, Oregon State University

Table of Contents

Certificate of Approval.....	ii
List of Figures	vi
List of Tables.....	vii
Acknowledgments	viii
Abstract.....	ix
Chapter 1.....	1
Introduction	1
1.0 History of the Columbia River	1
2.0 The Nitrogen Cycle and Eutrophication	3
3.0 Phosphorus Cycle	7
4.0 Silicic Acid Cycle.....	8
5.0 Nutrients in the Columbia River Basin and Plume.....	10
5.1 Columbia and Willamette Rivers.....	10
5.2 The Columbia River Estuary	11
5.3 The Columbia River Plume and Coastal Ocean	11
5.3.1 Transitional Phase.....	12
5.3.2 Upwelling phase	13
6.0 The Value of High Resolution Observations	13
7.0 Statement of Purpose	16
8.0 Figures.....	17
9.0 References	21
Chapter 2.....	28
Methods, Challenges, and Troubleshooting an Autonomous Profiling Nutrient Analyzer	28
1.0 Abstract	28
2.0 Introduction	29
3.0 Deployment Methods.....	30
3.1 Pre-Deployment	30
3.2 Deployment.....	33
3.3 Post Deployment	33
3.4 Data Analysis	34
4.0 Challenges	35
4.1 Turbidity	35
4.2 Dissolved Gasses.....	36
4.3 Deployment Conditions.....	37
5.0 Data Quality	38
5.1 Detection Limits.....	38
5.2 Laboratory Analyzed Grab Samples on the APNA	38
5.3 Laboratory Analyses compared to In Situ Data.....	39
6.0 Troubleshooting.....	43
6.1 Reagent pumps do not appear to be pumping.....	43
6.2 Reagent pumps are not delivering proper quantity of fluid.....	45
6.3 Nitrate channel is noisy after deployment	46
6.4 Pressure compensation bulb is harder than normal.....	46
6.5 Error in file while downloading.....	47

6.6 Corrupted ANA.*** files	47
7.0 Conclusions	48
8.0 Figures.....	50
9.0 Tables.....	64
10.0 References	69
Chapter 3.....	70
Nutrient Loading and Transformations in the Columbia River Estuary Determined by High Resolution In Situ Sensors.....	70
1.0 Abstract	71
2.0 Introduction	72
3.0 Materials and Methods.....	75
3.1 Study Area	75
3.1.1 Estuary Sampling Location: SATURN-03.....	76
3.1.2 River Sampling Location: SATURN-05.....	77
3.1.3 CMOP Campaign.....	77
3.2 Instrumentation on Observatory Platforms	77
3.2.1 Autonomous Profiling Nutrient Analyzer (APNA).....	77
3.2.2 Cycle-PO4	79
3.3 Bench Top Nutrient Sampling Methods.....	80
3.4 Data Analysis	81
3.4.1 Conservative Mixing End Member Calculation.....	81
3.4.2 Calculation of Ocean End Member Salinity	83
3.4.3 Nitrate: Change in River Concentration.....	83
3.4.4 Phosphate: Change in River Concentrations.....	84
3.4.5 Statistical Analysis.....	84
4.0 Results.....	85
4.1 Seasonal Patterns at SATURN-03	85
4.1.1 Salinity	85
4.1.2 Nutrients.....	85
4.2 Seasonal River and Ocean End Members at SATURN-03	87
4.3 Summer 2010 at SATURN-03.....	89
4.4 Neap Tide Versus Spring Tide Outwash at RM-17	91
5.0 Discussion	92
5.1 River to Ocean Nutrient Gradients and Transformations.....	93
5.1.1 Nitrate.....	94
5.1.2 Phosphate	97
5.1.3 Ammonium.....	99
5.2 Denitrification and DNRA.....	102
5.3 Remineralization Within the Estuarine Turbidity Maximum (ETM)	103
5.4 Lateral Bay Remineralization	104
6.0 Conclusions	105
7.0 Acknowledgments	107
8.0 Figures.....	108
9.0 Tables.....	118
10.0 References	120
Chapter 4.....	129

Conclusions and Future Direction	129
1.0 Conclusions	129
2.0 Future Direction.....	130
Appendix A.....	134
Silicic Acid Data and Results	134
Appendix B	144
Autonomous Profiling Nutrient Analyzer Procedures	144
1.0 Pre Deployment Procedure	144
1.1 Cadmium column preparation	144
1.2 Reagent Pump Calibration.....	145
1.2.1 Flow meter Readings	145
1.2.2 Total Flow Measured	145
1.2.3 Pump Calibration.....	145
1.2.4 Analyzing the Data	146
1.2.5 Update ANA.CFG file	146
1.3 Reagent Preparation	147
1.4 Standard Preparation	149
1.5 Pre Deployment Inlet Calibration	150
1.5.1 Inlet Calibration.....	150
1.5.2 Data Processing	151
1.6 AUTO Mode Testing	151
1.6.1 Upload a new ANA.SSF file	151
1.7 Field Instructions – for deployment at SATURN-03.....	152
2.0 Post Deployment Procedure.....	153
2.1 Data Download	153
2.2 Post-Deployment Inlet Calibration	153
2.3 Data Processing.....	154
2.4 System Cleaning	155
2.4.1 Flow Cell Cleaning	155
2.4.2 Cadmium column cleaning.....	155
3.0 MatLab OHSUAutoAnalysisV2 in depth analysis.....	156
3.1 Introduction.....	156
3.2 Methods—APNA Data Analysis	156
3.3 Line by Line Analysis	156
3.3.1 Program 1: APNADDataAutoProcessor.m.....	156
3.3.2 Program 2: Nutrient Sub files.....	157
3.3.3 Program 3: Debubble_d.m	160
3.3.4 Program 4: PlateauSelectorV2.m	160
3.3.5 Program 5: APNADDataGUI	162
3.4 Matlab Data Processing Manual	163
4.0 Discrete Sample Processing.....	165
4.1 APNA Prep.....	165
4.2 Running Discrete Samples	165
4.3 Discrete Data Processing	166

List of Figures

Figure 1.1 Map of Columbia River Basin.....	17
Figure 1.2 Aquatic Nitrogen Cycle.....	18
Figure 1.3 Redox Ladder.....	19
Figure 1.4 Sample Biasing.....	20
Figure 2.1 Flow Check and Pump Calibration Log Sheet.....	50
Figure 2.2 Reagent Pump Calibration Data.....	51-53
Figure 2.3 Inlet Calibration Log Sheet.....	54
Figure 2.4 Inlet Calibration Data.....	55-56
Figure 2.5 MatLab Primary GUI.....	57
Figure 2.6 MatLab Secondary GUI.....	58
Figure 2.7 Discrete Analysis Log Sheet.....	59
Figure 2.8 APNA, SUNA, AA Nitrate Comparison 11/9/2010.....	60
Figure 2.9 APNA, AA, Cycle-PO4 Comparison 11/9/2010.....	61
Figure 2.10 APNA, SUNA, AA Nitrate Comparison 12/22/2010.....	62
Figure 2.11 New and Old SUNA Slope and Intercept Comparison.....	63
Figure 3.1 Map of the Lower Columbia River.....	108
Figure 3.2 Raw Data Profile.....	109
Figure 3.3 Conservative Mixing.....	110
Figure 3.4 Seasonal Raw Data.....	111-112
Figure 3.5 Seasonal Averages.....	113-114
Figure 3.6 Summer Raw Data.....	115
Figure 3.7 Summer End Member Data.....	116
Figure 3.8 RM-17 Tide Outwash Data.....	117
Figure A.1 RM-17 Silicic Acid Tide Outwash Data.....	138
Figure A.2 Silicic Acid End Members at SATURN-03.....	140
Figure A.3 Silicic Acid Versus Salinity Plot Plume Survey.....	143

List of Tables

Table 2.1 APNA Grab Sample Data 11/9/2010.....	64
Table 2.2 APNA and AA Comparison 11/9/2010.....	65
Table 2.3 APNA Grab Sample Data 12/22/2010.....	66-67
Table 2.4 APNA and AA Comparison 12/22/2010.....	68
Table 3.1 Ocean End Member Salinity.....	118
Table 3.2 Comparison of Nutrient Concentrations Across Reaches.....	119
Table A.1.a Silicic Acid Data from RM-17 Neap Tide Outwash.....	135
Table A.1.b Silicic Acid Data from RM-17 Spring Tide Outwash.....	136-137
Table A.2 Silicic Acid End Member Data From SATURN-03.....	139
Table A.3 Silicic Acid Data from the Columbia River Plume.....	141-142

Acknowledgments

I would like to express my gratitude to my thesis committee; Joseph Needoba, Antonio Baptista, and Fredrick Prah for all of their efforts. I would also like to thank all of those at Oregon Health & Science University as well as the Center for Coastal Margin Observation and Prediction that helped with instrumentation and my research activities. These include: Grant Law and my summer intern Ezra-Mel Pasikatan helped to develop MatLab code for APNA data processing, Sarah Riseman for help with nutrient analysis, and the Astoria field team for their help with APNA deployments. I would also like to thank the Captain and crew of the R/V Wecoma and R/V New Horizon as well as the chief scientists Frederick Prah and Tawnya Peterson. I would also like to thank all of the graduate students, especially Michelle Maier and Leslie Slasor, who I worked closely with throughout this project. Finally, I would like to thank all of the administrative staff who made this a fantastic experience. My utmost appreciation lies with Joseph Needoba for the numerous hours he has spent working with me over the past two years on this project, as he has gone above and beyond my expectations.

Abstract

We present results from a high temporal resolution observational study of nutrient loading and biogeochemical transformations in the Columbia River estuary, OR. During 2010, three autonomous nutrient sensors (Satlantic SUNA, SubChem Systems Inc. APNA, WET Labs Cycle-PO4), measured nitrate + nitrite, ammonium, ortho-phosphate, silicic acid, and nitrite across different seasons in the lower Columbia River and estuary. Large salinity ranges and conservative behavior of nutrients during daily flood-ebb mixing allowed for river and ocean end members to be calculated from estuary-based measurements. The results revealed the importance of the estuary as a “bioreactor” for inorganic nutrients despite relatively short water residence times. High concentrations of ammonium and phosphorus were identified in the estuary compared to the river during late summer, suggesting that elevated rates of nutrient remineralization were localized in the lower estuary and likely reflect organic matter accumulation and decomposition in the estuarine turbidity maximum and lateral bays. Furthermore, we have identified a synchronicity of large pulses of dissolved silicic acid and ammonium into the estuary during spring tide high turbidity periods, which was likely released from dissolution of benthic diatom-rich sediment within the lateral bays.

Chapter 1

Introduction

1.0 History of the Columbia River

The Columbia River drainage basin is the second largest in the continental United States (Fig. 1.1). It covers 567,000 km² in seven states and 102,300 km² in British Columbia, Canada (BPA 2001). Covering areas west of the Cascade Mountains to the Pacific coast, this large area consists of a variety of climate zones including desert, moist, and temperate maritime. Prior to 1909 and the building of any dams, the peak river discharge was upwards of 15,500 m³/s, and up to 60% of the annual runoff occurred during the early spring (BPA 2001). Currently, 29 major dams and many smaller water impoundments are located throughout the Columbia River and all of its major tributaries. According to NOAA stream flow data, the daily discharge during the spring freshet has decreased by 44% between 1858 and 1999 due to dams. The dams do not provide long term storage capacity; therefore, a reduction in spring discharge is offset by an increase in discharge during other periods of the year. Despite alterations to river flow and habitat impacts, the dams are vital to the people residing in the Columbia River basin. Including being one of the largest hydroelectric systems in the world, these dams provide flood control, irrigation, navigation and recreation to the community (BPA 2001). Today, 6% of the basin's water is diverted for use as irrigation (BPA 2001). A

total of 7.1 million acres are irrigated by this water, including over half a million acres of agricultural, urban, and recreational land as well as forest nurseries (BPA 2001).

There is no doubt that dams are important for the economy of the Pacific Northwest, but there have been significant ecological impacts associated with alterations in river flow. These impacts include: an increase in water temperature by $\sim 1^{\circ}\text{C}$ (Moore 1968), reduced suspended particulate matter (van Winkle 1914; Sullivan 1997), increased salinity penetration (Jay 1984), and an increase in phytoplankton growth (Sullivan et al. 2001). Alterations in flow and the building of dams also decreased sediment transport by creating what is known as the “artificial-lake effect” in which sediment settles out of the water column into large pools of water created behind dams. The Willamette River sediment load decreased by 35% from virgin flow to 1970-1999, and the total sediment load in the Columbia River decreased by 61.5% from virgin flow to 1970-1999 (Bottom et al. 2005). This has resulted in decreased shallow water habitats for salmon (Bottom et al. 2005). Thus, dramatic declines in the native populations and habitat of the Columbia River salmon have been documented over the past century (Bottom et al. 2005).

The main focus of this study was on the lower Columbia River, specifically from SATURN-05 (River Mile 53), to the Columbia River plume. The transition from SATURN-05 to the plume is dramatic and at most times of the year water can travel this distance in only a few days (Sommerfield 1999). Tidal effects can reach as far up the river as the Bonneville Dam (River Mile 141) (Bottom et al. 2005), while salt intrusions vary from tide to tide, but never reach the fresh water tidal flats of Cathlamet Bay (Simenstad et al. 1990a). The Columbia River estuary has a strong estuarine turbidity maximum (ETM), which has been identified as an important site for biogeochemical

reactions, and was the focus of a 10 year National Science Foundation (NSF) program during the 1990s. The traditional view of the Columbia River plume is that during winter, downwelling winds push the plume northward along the coast and during summer, upwelling winds push the plume southwest away from the coast (Hickey 1989). However, recent findings have shown that the coastal plume can be bi-directional and much more complex than previously thought (Hickey et al. 2005; Hickey et al. 2010).

2.0 The Nitrogen Cycle and Eutrophication

Nitrogen gas (N_2) is the most abundant element in the earth's atmosphere and is vital to life; however, nitrogen gas is biologically unavailable to most organisms. The strong triple bond takes a significant amount of energy to break into reactive nitrogen (Nr) forms, and until the industrial revolution and the invention of the Haber-Bosch process, Nr could only be formed by a few types of bacteria (Galloway et al. 2003). Since the 1960's, the global use of Nr from the Haber-Bosch process for food production and other industrial activities has resulted in both beneficial and detrimental changes for humans and the environment. Although humans are now able to sustain a larger global population due to Nr availability, the effects of nitrogen pollution are far felt through direct and non-point sources. Excess Nr in the air and drinking water can cause a variety of respiratory illnesses, reproductive problems, and cancer (Townsend et al. 2003). Although indirect effects of excess Nr are more difficult to determine, increased coastal hypoxia (Galloway et al. 2003; Rabalais et al. 2001) and eutrophication (NRC 2000) are two well documented consequences.

The industrial production of Nr is not going to stop in the near future, thus it is imperative that we understand how it cascades through the environment (Galloway et al.

2008) and where it can be converted back into N_2 . Altering river systems through channelization and dams has significantly impacted nitrogen cycling within aquatic systems by altering water and particle residence times (Galloway et al. 2003). Many studies have documented the effects of dams and other structures on nutrient loading and export to coastal zones (Aviles and Niell 2007; Goldyn and Szlag-Wasielewska 2005; Paul 2003; Benndorf and Putz 1987). The destruction of tidal flat areas, decreased residence time, and increased concentrations of anthropogenic Nr in nitrogen limited rivers, estuaries and coastal waters has been shown to cause excess primary production, eutrophication, and even coastal hypoxia (Rabalais et al. 2001; Bricker et al. 2007). Quantifying estuarine nitrogen fluxes and nitrogen removal has received a lot of consideration because estuaries are the last region of removal for natural and anthropogenic Nr before it enters the marine environment where increased Nr can cause coastal hypoxia (Rabalais et al. 2001).

During organic matter respiration, most organisms prefer to use O_2 as an electron acceptor because it yields the highest energy per mole of organic matter (Seitzinger 1988). However, when O_2 is depleted in the environment, other electron acceptors can be utilized. One alternative process is denitrification, where nitrate is the electron acceptor. Denitrification has been measured in sediment, ground water, rivers, wetlands, estuaries, and coastal marine systems. During organic matter respiration, bacteria convert nitrate to nitrogen gas thus converting Nr to an unusable form (1.1) (Fig. 1.2).

1.1

Another process that can remove Nr nitrogen from the environment is anaerobic ammonium oxidation (anammox). Anammox has recently been shown to compete with

denitrification in anoxic environments (Dalsgaard et al. 2003). Annamox occurs through the oxidation of ammonium and the reduction of nitrite (1.2) (Fig. 1.2).

1.2

The utilization of free ammonium can create an ammonium deficiency in the environment (Dalsgaard et al. 2003).

Another Nr transformation pathway that occurs in anoxic environments and has been recently identified as a key component in the nitrogen cycle is dissimilatory nitrate reduction to ammonium (DNRA). The microbially mediated process of DNRA does not remove Nr from the environment, but reduces nitrate to ammonium (1.3) (Fig. 1.2).

1.3

In contrast to denitrification, which removes Nr nitrogen from the environment, DNRA conserves Nr by converting nitrate into a less mobile form of Nr (Rütting et al. 2011). The resultant ammonium from DNRA is still active in the environment and can be utilized again.

In aquatic ecosystems, organic matter remineralization releases nutrients including ammonium and phosphate into the water column and sediment. Regardless of the electron acceptor, inorganic ammonium and phosphate are products of organic matter remineralization (1.4) (Fig. 1.2).

1.4

Remineralization releases nutrients back into the environment at Redfield ratio, 16N:1P (Redfield et al. 1963), and does not change the oxidation state of the nitrogen.

In aerobic environments, ammonium that was released from organic matter remineralization and DNRA can be oxidized through the process of nitrification.

Nitrification is a microbially-mediated reaction in which ammonium is oxidized to nitrite and nitrate (1.5) (Fig. 1.2).

1.5

During nitrification, ammonium is oxidized from an oxidation state of -3 to nitrate, an oxidation state of +5. Both ammonium oxidizing bacteria and ammonium oxidizing archaea are responsible for this process. Nitrification is an important step in the nitrogen cycle, as it leads to the production of nitrate which can then be consumed by denitrification, thus removing Nr from the environment.

Increasing Nr inputs into the coastal ecosystem is the leading cause of coastal eutrophication (Rabalais et al. 2001). This may lead to hypoxia and thus allow for denitrification and anammox to occur within the water column itself. Removing more Nr within the water column may seem like a positive outcome, but there are many harmful processes associated with increased hypoxia that likely outweigh the benefits of increased Nr removal. In some coastal systems, increased eutrophication could eventually cause a permanent hypoxic/anoxic zone in the water column, in which the microbial preference for electron acceptors (redox ladder) causes distinct zones in the water column (Fig. 1.3).

Denitrification, DNRA and anammox play a large part in a system's nitrogen speciation and the percent of nitrogen that is removed as N_2 . Estuaries can remove up to 40-50% of the dissolved inorganic nitrogen inputs from a river depending on water residence times (Seitzinger 1988). Although estuaries can remove large quantities of nitrogen from the system, eutrophication is still being observed all over the world. Sixty-six percent of estuaries studied in the 2004 National Oceanic and Atmospheric Administration (NOAA) National Eutrophication Assessment were classified as moderate

to highly eutrophic (Bricker et al. 2007). The Columbia River estuary was among the list of estuaries with insufficient data to assess its eutrophic condition (Bricker et al. 2007). Thus, more research is needed in the Columbia River, estuary, and plume on a seasonal as well as high temporal resolution scale to identify the impacts and potential for eutrophication from nutrient loading in the watershed.

3.0 Phosphorus Cycle

Phosphorus is a key element to life. Along with nitrogen, phosphorus has been added to fertilizers to aid in crop growth, but unlike nitrogen, phosphorus is not made industrially. The only source of phosphorus is from mining. Other than runoff from agriculture, the major source of bio-available phosphorus is continental rock weathering. Correll (1998) pointed out that even with the input from agriculture, phosphorus is still the limiting nutrient in many rivers and lakes. Phosphorus is transported both in surface water and subsurface ground water (Reddy et al. 1999). However, only 5-10% of the phosphate transported to the ocean is in the dissolved bio-available form of ortho-phosphate (Froelich 1988), and very little phosphorus is introduced to the ocean via the atmosphere (Benitez-Nelson 2000). Other forms of phosphorus include: dissolved organic phosphorus, particulate inorganic phosphorus, and particulate organic phosphorus. Dissolved inorganic phosphorus can be utilized by phytoplankton in the Redfield ratio of 16N:1P and transformed into organic phosphorus (Redfield et al. 1963). Photosynthesis and respiration can also change the pH and thus change the chemical properties of water and may cause phosphorus precipitation (Reddy et al. 1999). Phosphorus can undergo many other transformations besides uptake and release from photosynthesis. A large pool of bio-available inorganic phosphorus is adsorbed to particles. Although

phosphorus that is sorbed is not prone to desorption (Froelich 1988), turbid estuaries can cause phosphorus desorption from suspended particles in the transition from fresh to salt water (Deborde et al. 2007). This process is known as the phosphate buffer mechanism (Carritt et al. 1954; Froelich 1988). Mineralization within the ETM can also release dissolved inorganic phosphorus that would thus be available downstream (Deborde et al. 2007). Unlike nitrogen, which is very complex and controlled by mostly biological processes, phosphate is controlled by chemical processes which can be complex in environments such as estuaries.

4.0 Silicic Acid Cycle

The main source of silicic acid to lakes and rivers is continental rock weathering. However, once silicic acid is in an aquatic system, it can be recycled through the food web numerous times. There are two main forms of silicic acid in the aquatic environment: dissolved silicic acid (DSi) and biogenic silica (BSi). DSi is biologically available while BSi has been sequestered by phytoplankton and plants. It is widely known that anthropogenic sources of nitrogen and phosphorus are increasing in lakes, causing eutrophication (Benndorf and Putz 1987). However, the silicic acid budget is not substantially affected by anthropogenic sources. With increased N and P in the water, diatom growth is now being limited by silicic acid in the surface waters during periods of summer stratification (Conley and Malone 1992). Alterations in Si:N and Si:P ratios has caused substantial impacts to many systems. If all of the silicic acid sequestered is not regenerated by the next season, a long term sink may form in which DSi is lost from the system and buried in the sediment as BSi, as has been documented previously in the Great Lakes (Schelske 1985). If DSi loss exceeds supply, eventually the ecosystem may

become silicic acid limited. Ultimately, the final stage of silicic acid depletion causes alterations to the phytoplankton assemblage that favors phytoplankton that do not utilize silicic acid in their cell walls (Conley et al. 1993). Decreases in DSi can happen rapidly (20-40 years) and lead to changes in the phytoplankton community structure and ultimately affect higher trophic levels in the food chain (Schelske et al. 1983). Although some lakes enriched with nitrogen and phosphate become silicic acid limited, it has been shown by Welch et al. (1989) that not all lakes enriched in nitrogen and phosphate lose DSi to the sediment. Unlike lakes, natural rivers and coastal marine systems with short residence times do not lose silicic acid to burial because silicic acid is renewed on an annual basis through natural rock weathering and transport (Conley and Malone 1992). In the recent past, human alterations to the natural flow of rivers has caused significant impacts to the silicic acid budget. Some dams have decreased silicic acid transport to the coastal ocean by creating the “artificial-lake-effect” (van Bennekom and Salomons 1981). Other dams and river structures have altered wetland habitat, which play a major role in the cycling of silicic acid. Seepage of DSi from wetlands and tidal flats (Grunwald et al. 2010) has been shown to be vital to diatom growth during periods of DSi limitation (Struyf et al. 2005). Whitney et al. (2005) suggested that the alteration of river flow by dams throughout the Columbia River basin reduced the Si transport to the North Pacific Ocean, and suggests that effects on the ecosystem can be felt as far north as the Alaska Gyre. DSi concentrations in the Columbia River and estuary are as high as the global mean riverine average (150 μM) (Conley 1997), and thus DSi limitation is not a concern within the estuary itself, but alterations to river discharge have already proven to be influential on coastal ecosystems.

5.0 Nutrients in the Columbia River Basin and Plume

5.1 Columbia and Willamette Rivers

Nutrient cycles within the Columbia River and Willamette River have distinct temporal and spatial patterns (Sullivan et al. 2001). Nutrient concentrations in the Columbia River reach a maximum in the winter, decrease during the spring, and reach their lowest during late summer. Nitrate concentrations reach an average of $\sim 25 \mu\text{M}$ during winter and decline to $\sim 5 \mu\text{M}$ during late summer (1978-1994 USGS) (Sullivan et al. 2001). Silicic acid concentrations can reach over $200 \mu\text{M}$ during winter but remain relatively high during summer ($100\text{-}150 \mu\text{M}$) (Sullivan et al. 2001; Bruland et al. 2008). High silicic acid concentrations year round is unique compared to many other rivers (Conley 1997). While many rivers around the world are becoming silicic acid limited during spring and summer and their Si:N ratio is decreasing to less than 1:1 (Conley 1997; Cloern 2001), the Columbia River's Si:N ratio remains between 20 and 50 during the summer (Bruland et al. 2008). Phosphate concentrations can reach as high as $1 \mu\text{M}$ during the winter and are near zero during the summer, but are never fully depleted (1978-1994 USGS) (Sullivan et al. 2001). Assuming a Redfield ratio 16N:1P (Redfield et al. 1963), phosphate would be the limiting nutrient in the Columbia River. However, there is always measurable phosphate in the river, which suggests that nutrients are not limiting phytoplankton growth (Sullivan et al. 2001).

The Willamette River is a major input into the lower Columbia River. During winter high flow periods, the Willamette River can make up as much as 30-35% of the total Columbia River flow, while in low flow summer periods the Willamette contributes 0-15% (USGS stream flow data). Thus, quantifying nutrient patterns in the Willamette is

imperative for understanding nutrient biogeochemistry in the Columbia River. Prahl et al. (1998) showed that nutrient concentrations in the Willamette River were much higher than the main stem of the Columbia River during June of 1992 (10x higher ammonium and phosphate, 75x higher nitrate + nitrite, 2.5x higher silicic acid). Despite significantly higher nutrient concentrations in the Willamette River, nutrient concentrations in the mainstream Columbia River were only slightly enriched downstream of the Willamette River due to relatively low summer discharge (Prahl et al. 1998). Many small tributaries also flow into the Columbia River and could have a potential impact on nutrient concentrations in the mainstem Columbia River. While silicic acid was shown to be enriched in tributaries along the Columbia River, some were also enriched in nitrate, phosphate, and ammonium. However, the tributaries did not increase nutrient concentrations in the mainstem Columbia River because of lack of flow (Prahl et al. 1998).

5.2 The Columbia River Estuary

Nutrient dynamics in the Columbia River estuary are poorly understood. This is mainly due to the physical complexity of the estuary's circulation and mixing regime that prevent effective monitoring. Bruland et al. (2008) demonstrated conservative mixing of nitrate and silicic acid within the estuary that suggests few removal or addition processes are occurring, and attributed this to the short residence time of the water within the estuary.

5.3 The Columbia River Plume and Coastal Ocean

Significantly more research has been done to understand biogeochemical cycles and physical mixing of nutrients in the Columbia River plume and coastal ocean than has

been done inside the estuary. The Columbia River plume (defined as a salinity of 10-25 psu) is made up of 30-50% river water (Bruland et al. 2008) and can be a significant source of nutrients to the coastal ocean during portions of the year. However, during periods of upwelling, deep waters rich in nutrients are much higher than the Columbia River nutrient supply (Bruland et al. 2008).

5.3.1 Transitional Phase

Transitional time periods usually occur during the spring months when wind direction is variable. This can cause alternating downwelling and upwelling conditions along with a bi-directional plume (Hickey et al. 2005; Hickey et al. 2010). During transitional downwelling periods, the plume nitrate concentration can be as low as 2 μM , while during periods of transitional upwelling, nitrate concentrations within the surface plume can reach as high as 16 μM (Bruland et al. 2008). Although nitrate concentrations in the Columbia River are low during the spring transitional period, they are vital to sustaining coastal plume phytoplankton blooms during transitional downwelling wind shifts (Hickey and Banas 2008). Kudela et al. (2010) suggests that nitrate concentrations entering the plume from the Columbia River during periods of upwelling relaxation are substantial enough to serve as a “biological refuge and bioreactor” for up to 3-4 days. Nutrient limitation at the edge of the plume was apparent during this time, and a shift in phytoplankton community structure was observed, in which organic carbon can be transferred to higher trophic levels (Kudela et al. 2010). Thus, the Columbia River may serve as a “buffer”, sustaining productivity during transitional phases (Kudela et al. 2010).

5.3.2 Upwelling phase

Upwelling usually occurs during summer months when southerly winds push the Columbia River plume southwest of the mouth. During upwelling, the plume is usually characterized by high nitrate concentrations which are entrained from deep ocean waters into the surface plume (Hickey et al. 2010). Entrainment of deep water high in nitrate mainly occurs during flood tides, while during ebb tides, surface plume water mixes with warmer nutrient poor coastal surface waters (Lohan and Bruland 2006). Plume nitrate is mainly controlled by upwelling, while the Columbia River input controls silicic acid concentrations in the surface plume due to extremely high concentrations year round (Bruland et al. 2008). Near-shore plume waters are not nitrate limited due to tidal influences (Lohan and Bruland 2006), but as plume waters age and move away from the mouth of the Columbia River, the water becomes nitrate limited within a matter of hours due to phytoplankton uptake (Lohan and Bruland 2006; Bruland et al. 2008; Hickey et al. 2010; Kudela and Peterson 2009). The unique plume environment with entrained nitrate from deep ocean waters and silicic acid from the Columbia River allows for diatom growth within the plume (Lohan and Bruland 2006). Although nitrate is fully depleted by the time the plume has aged, evidence of high silicic acid from the Columbia River is still evident in surrounding coastal surface waters (Lohan and Bruland 2006).

6.0 The Value of High Resolution Observations

Scientists around the world now recognize the importance of high resolution observations in the marine environment. Networks of high resolution sensors are being built all over the world, and are now a vital part of coastal and open ocean research. Observational networks such as MARS in Monterey Bay, California (MBARI),

NEPTUNE Canada off Vancouver Island (University of Victoria), and SATURN in the Columbia River Estuary (CMOP), are currently producing massive amounts of high resolution data. This information is enabling the transition of studies from large scale events to understanding small scale events such as tidal effects, internal waves, and estuarine turbidity maximums. Through the use of these high resolution sensors, it has become apparent that under-sampling can cause major biases to data sets and significantly influence scientific conclusions. Figure 1.4 shows how choosing the correct sampling frequency is vital to a research project. The red line represents 23 random samples, while the black line and dots are nitrate samples taken every 1.5 hours at SATURN-03 mid water depth (8.2 m). It is clear that the majority of the fluctuations were missed by random sampling. Although 1.5 hour sampling shows a much more dynamic and complete record than the random samples, it may not even be enough to capture every detail of a rapidly changing system like the Columbia River.

Previously, most studies that aimed to identify nutrient transformations in an estuary conducted shipboard transects. Nutrient concentrations were plotted versus salinity and any deviations from a linear regression drawn from the river end member to the ocean end member were considered sources or sinks within the estuary. An example of this method in the Columbia River was a study by Bruland et al. (2008) in which nitrate and silicic acid mixing was observed by measuring concentrations from the river to the plume. However, this single set of observations did not allow for a cause-effect to be deciphered. It would require significant resources to identify and monitor nutrient transformations for any length of time in a dynamic estuary via shipboard transects.

In this study, we provide a unique approach to identify nutrient transformation patterns in a tidally driven estuary using in situ sensors. We used high resolution in situ sensors such as the APNA, SUNA, and Cycle-PO4 that measured nutrients at an hourly resolution. Paired with physical data such as salinity, which mixes conservatively in the estuary, we were able to identify nutrient transformations based on the premise that water will mix conservatively given a short enough time scale and a small enough geographical location. High resolution data allowed for river-ocean mixing to be analyzed for every tidal cycle by calculating conservative mixing regressions from nutrient versus salinity plots. These regressions yielded river and ocean end members which could then be analyzed on a temporal scale or compared to other high resolution data at other locations in the estuary. This novel approach revealed some of the first evidence of nutrient transformations within the tidally driven Columbia River estuary.

7.0 Statement of Purpose

Although we are beginning to understand of the physical and biogeochemical processes of nutrients in the Columbia River plume, limited nutrient data is available within the Columbia River estuary itself, which limits regional assessments of water quality. Not unlike many other estuaries, rapidly changing nutrient concentrations within the Columbia River estuary have been observed due to high water velocities, short water residence time and large tidal variations. Harsh winter weather conditions make it very difficult for manual sampling in both the coastal ocean and estuary. This study was aimed to overcome these challenges and provide a detailed high resolution data set of nutrient concentrations within the estuary during different seasons to aid in answering the question: “How effective is the Columbia River estuary-plume system as a bioreactor for transformation and removal of river-borne nutrients and biogenic inputs?” (Source: <http://www.stccmop.org/research>). New technologies employed in this study yielded a high resolution nutrient data set without having to preserve or analyze samples in the laboratory. Despite many challenges and large gaps in the data set, observations of tidal nutrient dynamics were observed during several times of the year. This study was a milestone in the calculation of accurate nutrient budgets within the Columbia River, estuary, and plume. Nutrient data can also aid in understanding biogeochemical processes of the estuarine turbidity maximum. However, this study has made it clear that hourly nutrient data from one location is not sufficient to answer many of these questions. To fully comprehend the temporal and spatial variations of inorganic nutrients within such a dynamic estuary, high resolution tidal data is needed from multiple locations, depths and seasons throughout the river to plume transition.

8.0 Figures



Figure 1.1. A Map of the Columbia River watershed (Musser 2008).

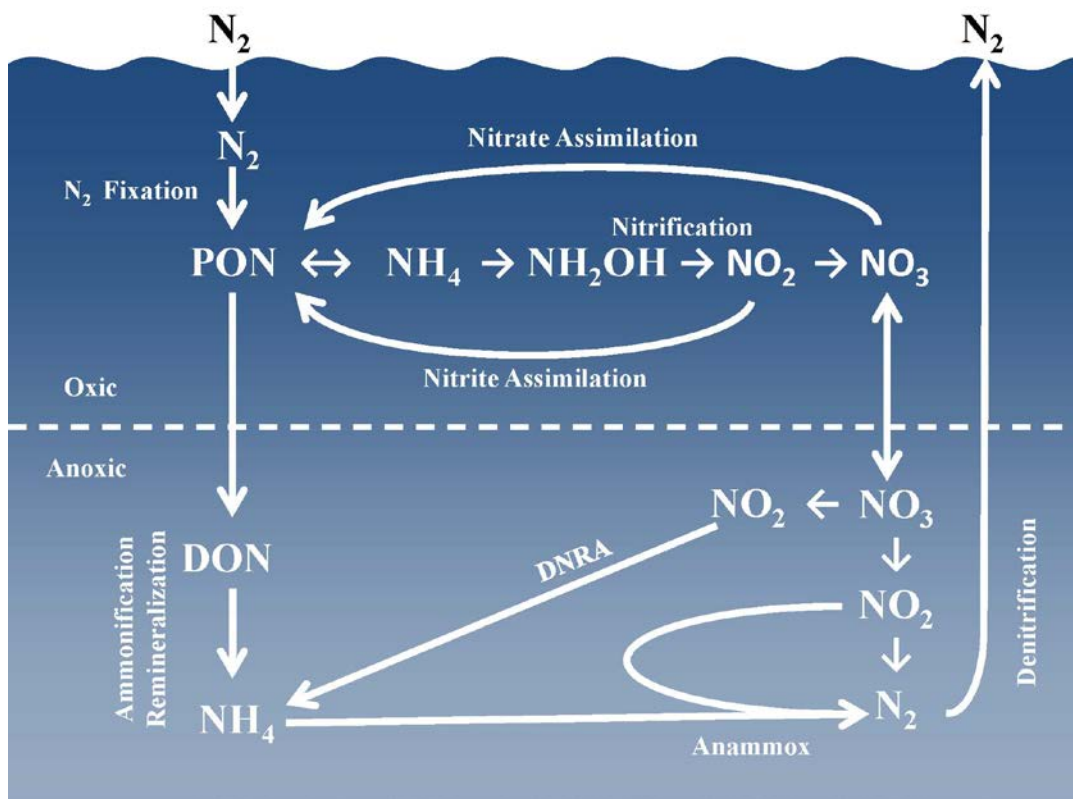


Figure 1.2. The aquatic nitrogen cycle.

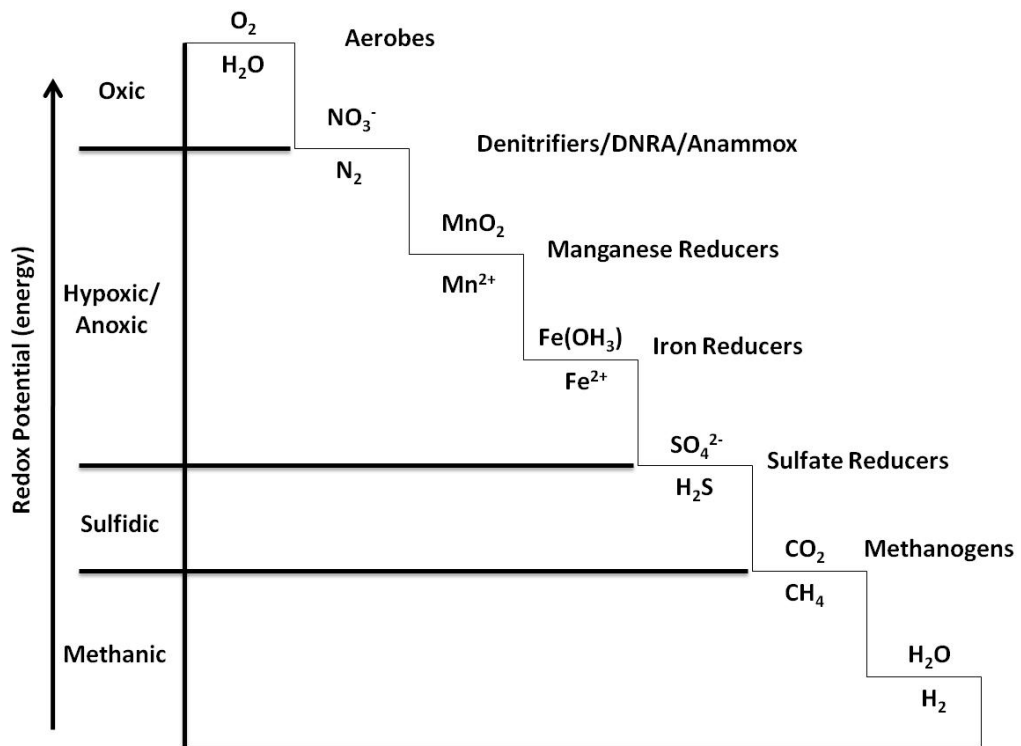


Figure 1.3. The redox ladder.

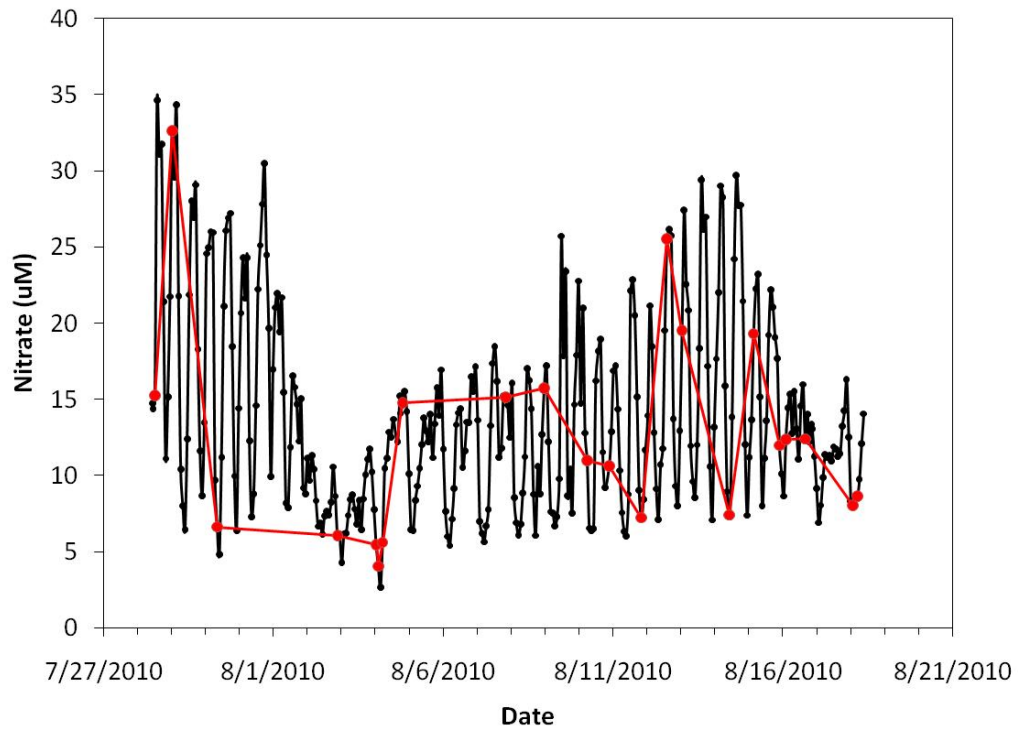


Figure 1.4. Sampling bias when under sampled.

This data was collected with the APNA from SATURN-03 mid water depth (8.2 m) in the Columbia River estuary. The black dots are samples collected every 1.5 hours and the red dots are random samples selected to show how the data can be biased if not sampled on the correct frequency.

9.0 References

Aviles, A., & Niell, X. F. (2007). The Control of a Small Dam in Nutrient Inputs to a Hypertrophic Estuary in a Mediterranean Climate. *Water Air Soil Pollution* , 180, 97–108.

Benitez-Nelson, C. (2000). The biogeochemical cycling of phosphorus in marine systems. *Earth-Sci. Reviews* , 51, 109–135.

Benndorf, J., & Putz, K. (1987). Control of eutrophication of lakes and reservoirs by means of pre-dams - I. Mode of operation and calculation of the nutrient elimination capacity. *Water Research* , 21 (7), 829-838.

Bonneville Power Administration (BPA), Bureau of Reclamation, and U.S. Army Corps of Engineers. (2001). *The Columbia River System Inside Story*. Federal Columbia River Power System, Second Edition DOE /bp-3372.

Bottom, D. L., Simenstad, C. A., Burke, J., Baptista, A. M., Jay, D. A., Jones, K. K., et al. (2005). *Salmon at River's End: The Role of the Estuary in the Decline and Recovery of Columbia River Salmon*. U.S. Department of Commerce, NOAA Technical Memorandum NMFS-NWFSC-68.

Bricker, S. B., Clement, C. G., Pirhalla, D. E., Orlando, S. P., & Farrow, D. G. (1999). *National Estuarine Eutrophication Assessment: Effects of Nutrient Enrichment in the Nation's Estuaries*. NOAA. Silver Spring: National Ocean Service Special Projects Office and the National Centers for Coastal Ocean Science.

Bricker, S., Longstaff, B., Dennison, W., Jones, A., Boicourt, K., Wicks, C., et al. (2007). *Effects of Nutrient Enrichment In the Nations's Estuaries: A Decade of Change*. Silver Spring, MD: NOAA Coastal Ocean Program Decision Analysis Series No. 26 National Centers for Coastal Ocean Science.

Bruland, K. W., Lohan, M. C., Aguilar-Islas, A. M., Smith, G. J., Sohst, B., & Baptista, A. (2008). Factors influencing the chemistry of the near-field Columbia River plume: Nitrate, silicic acid, dissolved Fe, and dissolved Mn. *Journal of Geophysical Research: Oceans* , 113, C00B02.

Carritt, D. E., & Goodgal, S. (1954). Sorption reactions and some ecological implications. *Deep Sea Research* , 1, 224-243.

Cloern, J. E. (2001). Our evolving conceptual model of the coastal eutrophication problem. *Marine Ecology Progress Series* , 210, 223-253.

Conley, D. J., & Malone, T. C. (1992). Annual cycle of dissolved silicate in Chesapeake Bay: implications for the production and fate of phytoplankton biomass. *Marine Ecology Progress Series* , 81, 121-128.

Conley, D. J., Schelske, C. L., & Stoermer, E. F. (1993). Modification of the biogeochemical cycle of silica with eutrophication. *Marine Ecology Progress Series* , 101, 179-192.

Conley, D. (1997). Riverine contribution of biogenic silica to the oceanic silica budget. *Limnology and Oceanography* , 42 (4), 774-777.

- Correll, D. L. (1998). The Role of Phosphorus in the Eutrophication of Receiving Waters: A Review. *Journal of Environmental Quality* , 27, 261-266.
- Dalsgaard, T., Canfield, D. E., Peterson, J., Thamdrup, B., & Acuna-Gonzalez, J. (2003). Anammox is a significant pathway of N₂ production in the anoxic water column in Golfo Dulce, Costa Rica. *Nature* , 422, 606-608.
- Deborde, J., Anschutz, P., Chailou, G., Etcheber, H., Commarieu, M., Lecroart, P., et al. (2007). The Dynamics of phosphorus in turbid estuarine systems: Example of the Gironde estuary (France). *Limnology and Oceanography* , 52 (2), 862-872.
- Froelich, P. N. (1988). Kinetic control of dissolved phosphate in natural rivers and estuaries: A primer on the phosphate buffer mechanism. *Limnology and Oceanography* , 33 (4, part 2), 649-668.
- Galloway, J. N., Aber, J. D., Erisman, J. W., Seitzinger, S. P., Howarth, R. W., Cowling, E. B., et al. (2003). The Nitrogen Cascade. *BioScience* , 53 (4), 341-356.
- Galloway, J. N., Townsend, A. R., Erisman, J. W., Bekunda, M., Cai, Z., Freney, J. R., et al. (2008). Transformation of the Nitrogen Cycle: Recent Trends, Questions, and Potential Solutions. *Science* , 320, 889-892.
- Goldyn, R., & Szelag-Wasielewska, E. (2005). The Effects of Two Shallow Reservoirs on the Phyto- and Bacterioplankton of Lowland River. *Polish Journal of Environmental Studies* , 14 (4), 437-444.
- Grunwald, M., Dellwig, O., Kohlmeir, C., Kowalski, K., Beck, M., Badewien, T. H., et al. (2010). Nutrient dynamics in a back barrier tidal basin of the Southern North Sea:

Time-Series, model simulations, and budget estimates. *Journal of Sea Research* , 64 (3), 199-212.

Hickey, B. M. (1989). Patterns and processes of circulation over the shelf and slope. In M. R. Landry, & B. M. Hickey (Eds.), *Coastal Oceanography of Washington and Oregon* (pp. 41-109). Amsterdam, The Netherlands: Elsevier Press.

Hickey, B. M., & Banas, N. S. (2008). Why is the Northern End of the California Current System so Productive? *Oceanography* , 21 (4), 91-107.

Hickey, B. M., Kudela, R. M., Nash, J. D., Bruland, K. W., Peterson, W. T., MacCready, P., et al. (2010). River Influences on Shelf Ecosystems: Introduction and synthesis. *Journal of Geophysical Research C: Oceans* , 115 (2), art. no. C00B17 .

Hickey, B., Geier, S., Kachel, N., & MacFadyen, A. (2005). A bi-directional river plume: The Columbia in summer. *Continental Shelf Research* , 25, 1631-1656.

Jay, D. (1984). *Circulatory Processes in the Columbia River Estuary*. Astoria, OR: Available from Columbia River Estuary Study Taskforce.

Kudela, R. M., & Peterson, T. D. (2009). Influence of a buoyant river plume on phytoplankton nutrient dynamics: What controls standing stocks of productivity. *Journal of Geophysical Research* , 114, C00B11.

Kudela, R. M., Horner-Devine, A. R., Banas, N. S., Hickey, B. M., Peterson, T. D., McCabe, R. M., et al. (2010). Multiple trophic levels fueled by recirculation in the Columbia River plume. *Geophysical Research Letters* , 37, L18607.

- Lohan, M. C., & Bruland, K. W. (2006). Importance of vertical mixing for additional sources of nitrate and iron to surface waters of the Columbia River plume: Implications for biology. *Marine Chemistry* , 98, 260-273.
- Moore, A. M. (1968). Water Temperatures in the Lower Columbia River. *Geological Survey Circular* , 551.
- Musser, K. (2008). <http://en.wikipedia.org/wiki/File:Columbiarivermap.png>
- National Research Council (NRC). (2000). *Clean Coastal Waters: Understanding and Reducing the Effects of Nutrient Pollution*. Washington, DC: National Academy Press.
- Paul, L. (2003). Nutrient elimination in pre-dams: results of long term studies. *Hydrobiologia* , 504, 289–295.
- Prahl, F. G., Small, L. F., Sullivan, B. A., Cordell, J., Simenstad, C. A., Crump, B. C., et al. (1998). Biogeochemical gradients in the lower Columbia River. *Hydrobiologia* , 361, 37-52.
- Rabalais, N. N., Turner, E. R., & Wiseman, J. W. (2001). Hypoxia in the Gulf of Mexico. *Journal of Environmental Quality* , 30, 320-329.
- Reddy, K. R., Kadlec, R. H., Flaig, E., & Gale, P. M. (1999). Phosphorus Retention in Streams and Wetlands: A Review. *Critical Reviews in Environmental Science and Technology* , 29 (1), 83-146.
- Redfield, A. C., Ketchum, B. H., & Richards, F. A. (1963). The influences of organisms on the composition of sea-water. In M. N. Hill (Ed.), *The Sea* (pp. 12-37). New York: John Wiley & Sons.

- Rütting, T., Boeckx, P., Müller, C., & Klemetsson, L. (2011). Assessment of the importance of dissimilatory nitrate reduction to ammonium for the terrestrial nitrogen cycle. *Biogeosciences Discussions* , 8, 1169-1196.
- Schelske, C. L. (1985). Biogeochemical silica mass balances in Lake Michigan and Lake Superior. *Biogeochemistry* , 1, 197-218.
- Schelske, C. L., Stoermer, E. F., Conley, D. J., Robbins, J. A., & Glover, R. M. (1983). Early eutrophication in the lower Great Lakes: new evidence from biogenic silica in sediments. *Science* , 222, 182-188.
- Seitzinger, S. P. (1988). Denitrification in freshwater and coastal marine ecosystems: Ecological and geochemical significance. *Limnology and Oceanography* , 33 (4, part 2), 702-724.
- Sommerfield, W. N. (1999). *Variability of residual properties in the Columbia River estuary: Pilot application of emerging technologies*. Beaverton : Masters Thesis. Oregon Graduate Institute of Science and Technology.
- Struyf, E., Damme, S. V., Gribsholt, B., & Meire, P. (2005). Freshwater marshes as dissolved silica recyclers in an estuarine environment (Schelde estuary, Belgium). *Hydrobiologia* , 540, 69-77.
- Sullivan, B. E. (1997). Annual Cycles of Organic Matter and Phytoplankton Attributes in the Columbia and Willamette Rivers, with Reference to the Columbia River Estuary. Oregon State University: Masters Thesis.

Sullivan, B. E., Prahl, F. G., Small, L. F., & Covert, P. A. (2001). Seasonality of phytoplankton production in the Columbia River: A natural or anthropogenic pattern?

Geochemica et Cosmochimica Acta , 65 (7), 1125-1139.

Townsend, A. R., Howarth, R. W., Bazzaz, F. A., Booth, M. S., Cleveland, C. C.,

Collinge, S. K., et al. (2003). Human health effects of a changing global nitrogen cycle.

Frontiers in Ecology and the Environment , 1 (5), 240-246.

van Bennekom, A. J., & Salomons, W. (1981). Pathways of nutrients and organic matter from land to ocean through rivers. In J.-M. B. Martin (Ed.), *River inputs to ocean systems* (pp. 33-51). Rome: UNEP/UNESCO.

van Winkle, W. (1914). *Quality of the Surface Waters of Washington*. Government Printing Office.

Welch, H. E., Legault, J. A., & Kling, H. J. (1989). Phytoplankton, nutrients, and primary production in fertilized and natural lakes at Saqvaqujac, N.W.T. *Canadian Journal of Fisheries and Aquatic Sciences* , 46, 90-107.

Whitney, F. A., Crawford, W. R., & Harrison, P. J. (2005). Physical processes that enhance nutrient transport and primary productivity in the coastal and open ocean of the subarctic NE Pacific. *Deep-Sea Research II* , 52, 681-706.

Chapter 2

Methods, Challenges, and Troubleshooting an Autonomous Profiling Nutrient Analyzer

1.0 Abstract

In this study we used the SubChem Systems Inc. Autonomous Profiling Nutrient Analyzer (APNA) to identify nutrient transformations along the Columbia River estuary-plume gradient. The APNA's ability to simultaneously measure five nutrients (nitrate + nitrite, nitrite, ortho-phosphate, silicic acid, and ammonium) as well as its high resolution capability allowed us to quantify river and ocean end member nutrient concentrations. The Columbia River estuary proved to be a much more dynamic environment than previous APNA applications; therefore, method adaptation for the effects of high dissolved gasses, high turbidity, and high water velocities was crucial. As the first high resolution multi-nutrient study in the Columbia River, strict calibration and quality control protocols were developed. Methods were developed for pre and post deployment calibrations, laboratory grab sample analysis, and data processing. A valuable data processing program was developed, which significantly reduced data processing time. Laboratory analyzed grab samples were used to verify in situ data quality. The following chapter outlines calibration procedures, deployment procedures, data analysis procedures, environmental challenges, common malfunctions, and steps for troubleshooting to aid in future deployment preparations.

2.0 Introduction

Unlike many in situ nutrient sensors that only measure one nutrient at a time (i.e. Satlantic SUNA, WET Labs, Cycle-PO4), the APNA (SubChem Systems Inc.) measures multiple nutrients simultaneously, which provides a comprehensive characterization of the aquatic ecosystem. The APNA uses a continuous (non-segmented) flow technique to measure in situ inorganic nutrients. Colorimetric absorbance methodologies are used for nitrate + nitrite (nitrate), nitrite, ortho-phosphate, and silicic acid, while fluorescence is used for ammonium. The APNA used in this study was specifically designed for nutrient concentration ranges in coastal systems such as the Columbia River. Short (1 cm) flow cells were installed for nutrients with a high range in concentration (silicic acid, nitrate) and long (5 cm) flow cells were installed for nutrients with a low concentration (ortho-phosphate, nitrite). For specific reagent recipes see the APNA Operating Manual and Appendix B of this document.

Characterizing tidal/daily scale nutrient transformations in any system is not trivial; however, the physical and chemical properties of the lower Columbia River and estuary include rapid water velocity and changing salinities which make high resolution sampling a necessity for accurate assessment of nutrient concentrations. As one of the most dynamic environments the APNA has ever been deployed in, methods had to be adapted to overcome complex environmental conditions in the Columbia River estuary. Higher levels of dissolved gasses and turbidity in the Columbia River estuary compared to previous deployment locations posed difficulties. We conducted laboratory studies to identify filters that would yield a high filtering capacity while decreasing dissolved gas adsorption. To ensure accurate in situ data, strict calibration and deployment protocols

were followed. Grab samples were analyzed in the laboratory on both the APNA (when not deployed) and an Astoria Analyzer and compared not only to in situ APNA data, but other in situ sensors as well.

This chapter outlines specific rationale behind calibration, deployment, record keeping and data analysis procedures. Explanations are given for altered factory recommended protocols. Common malfunctions along with troubleshooting steps are provided. Step by step procedures for pre-deployment, deployment, post-deployment, and data analysis can be found in Appendix B of this document. Further troubleshooting information and APNA repair history can be found in section 5 of the APNA Operating Manual.

3.0 Deployment Methods

3.1 Pre-Deployment

Prior to each deployment specific protocols were followed to ensure quality data. Data log sheets were developed to keep accurate and complete records, as quality records were extremely useful during troubleshooting. Prior to making reagents, flows and reagent pumps were calibrated to ensure precise reagent delivery and proper channel flow. Data was recorded on Flow Check and Pump Calibration log sheets to guarantee accurate and complete records (Fig. 2.1). See Appendix B for calibration protocol. Once data for this calibration was recorded on the log sheet, it was entered into a pre-made data processing template (Fig. 2.2). See Appendix B for data processing protocol. If calibrations were not linear or did not seem reasonable the calibration was repeated.

Microfluidic pumps, like the APNA's reagent pumps, can deliver variable quantities of fluid with changes in orientation; therefore, it was imperative that during

pump calibrations the APNA's spatial orientation (vertical/horizontal) was the same as it was during deployment. The factory does not deem a pump calibration necessary with each deployment. However, to ensure high quality data I performed this calibration prior to each deployment or at least bi-monthly. The most current pump calibration was kept in the APNA Operating Manual for reference during field deployments.

After all flows and pumps were calibrated, and all reagents were made, a pre-calibration was performed. See APNA Operating Manual for reagent preparation recipes and Appendix B for reagent preparation notes. There were two types of calibrations that could be performed on the APNA. The first was a standard addition calibration. This type of calibration required the CAL reagent pump be connected to a reagent bag filled with a mixed standard. The CAL reagent pump was turned on at different pump rates and mixed with the continuous sample stream. Changes to the delivery rates provided different standard dilutions. Although this type of calibration can run autonomously, small changes in the CAL reagent pump delivery rate can effect final standard concentrations. Standard addition calibrations were useful during deployments because they revealed inconsistencies in the measurement: changes in a calibration peak height indicated varying sample flow rates and thus calibration drift.

A laboratory inlet calibration was more accurate than the standard addition pump method. For an inlet calibration, standards were made by hand and run through the sample intake line. An extensive log sheet that included: reagent lot numbers, standard lot numbers, standard prep times, flow rates, system psi, file names, etc. was completed with each calibration (Fig. 2.3). See Appendix B for inlet calibration procedures. This log sheet not only aided in laboratory troubleshooting, but simplified remote

communication troubleshooting with SubChem Inc. because all vital information was organized in one location. If an inlet calibration was conducted on a different day than the pump calibration, flow rates of each channel were confirmed again prior to the inlet calibration.

To make inlet calibration data processing easier, a template was created where slopes and intercepts for each channel were derived quickly (Fig. 2.4). See Appendix B for data processing instructions. If calibration slopes were not linear, or if slopes did not appear consistent with previous calibrations, the calibration was repeated.

As our confidence in APNA data increased, Auto Mode sampling schemes changed slightly over time. In situ sampling started as baseline, sample, calibration, sample, baseline, but eventually the second sample and baseline were eliminated and the sampling schemes was condensed to baseline, sample and calibration. The factory does not recommend a calibration spike with each sample in environments where nutrient concentrations remain fairly stable. However, in the highly dynamic Columbia River estuary nutrient concentrations changed significantly within minutes. Therefore, we decided a calibration spike with each sample was appropriate.

Another non necessary, but helpful protocol was pre-deployment blanks. This was not implemented in early deployments, but proved to be a useful tool in determining in situ data quality. Pre-deployment blanks were checked before each APNA deployment to verify all blanks read 0 μM using slopes and intercepts generated from the pre-deployment calibration. For pre-deployment blank procedures see Appendix B.

3.2 Deployment

Although the APNA is designed to be submerged, we opted to keep it above water owing to the deployment platform. For this project the APNA was deployed at SATURN-03, where it was housed in a structure at the end of a pier. Due to deployment longevity and water pump constraints, we could only sample from one depth. The APNA sampled from a small reservoir filled from a pump located at 8.2 m depth. Mid water depth was chosen because it gave the largest salinity range and was the best representation of the whole water column. At SATURN-03, the APNA was connected to a continuous power supply as well as a network computer, which allowed for remote data observation. Easy land access, power supply, and data telemetry made this site ideal for our pilot study with the APNA. For specific deployment procedures see Appendix B.

Deployments lasted up to 1 month. Ideally the APNA would be deployed until one or more reagents have been fully consumed. However, conditions are rarely ideal. Pump failures, environmental conditions, internal leaks, clogged filters and other malfunctions significantly decreased deployment length. Although many deployments conducted up to this point were cut short for reasons listed above, some were successful and ended when reagents ran low.

3.3 Post Deployment

Upon return to the laboratory a post-calibration was performed using the same protocol as the pre-calibration. Although many deployments ended early due to failures listed above which prohibited a post-calibration, calibrations were done when possible. Other post deployment procedures included data downloading, system cleaning, and

cadmium column repacking. For post-deployment procedures see the APNA Operating Manual and Appendix B of this document.

3.4 Data Analysis

One of the biggest challenges that the APNA posed was data analysis. Deployments typically yielded 100-400 samples. Each sample contained data for five nutrients. SubChem Inc. provided us with basic processing tools that included a MatLab program for in situ data. This program selected baseline, sample and calibration peaks strictly based on time. Correction of individual data files for misplaced peaks was time consuming. For example, changes in nutrient concentration altered optimal sample peak times, making this program cumbersome to use in the Columbia River estuary where large nutrient concentrations ranges were observed daily.

A goal of my project was to build upon this data processing program and create a program that worked for our sampling environment. We proposed this project be done by a CMOP research experience for undergraduates (REU) summer intern. The student created the program based on a derivative (slope) peak selection method. The derivative-based selection along with a graphical user interface (GUI) reduced post data processing time significantly. For a line by line analysis and description of the new data processing program see Appendix B. The primary GUI allowed each channel's data to be viewed in one window (Fig. 2.5). Samples were color coded based on data quality (Fig. 2.5). A secondary GUI could be launched from the primary GUI by clicking on an individual data point (Fig. 2.6). In the secondary GUI window, baseline, sample, and calibration spike locations could be easily altered with slider bars. This new data processing

program was not only significantly more user friendly, but cut data analysis time from over one week to about one day.

4.0 Challenges

Turbidity and dissolved gasses posed significant challenges to deploying the APNA in the Columbia River estuary. Deployment conditions such as freezing air temperatures and periodic power outages also posed significant concerns. Through trial and error we provided some suggestions on how to manage these adversities; however, the solutions suggested here are optional and further alterations and enhancements should be made to improve APNA data quality.

4.1 Turbidity

A few major differences exist between the ocean, where APNA's have typically been deployed, and the Columbia River estuary. High sediment loads in the estuary tended to clog filters very quickly making pre-filtering samples difficult. When choosing a filter the delicate balance between filtering capacity and purging time had to be considered carefully. As filter housing capacity increased, more water was needed to purge the system before each sample decreasing the filter lifetime. The volume of water that was needed to flush a filter had to be as small as possible to preserve filter lifetime due to high turbidity.

Filter maintenance was crucial to a successful deployment. Clogged filters caused decreased sample flow, which altered calibrations and calculated sample concentrations. Clogged filters caused serious damage to the APNA when flow was not restored quickly. As filters clogged and flows decreased or ceased, reagents were pumped into the sample

lines at full strength and were not diluted with sample. Undiluted reagents caused corrosion and end cap damage.

4.2 Dissolved Gasses

Dissolved gases in the Columbia River estuary proved to be challenging. As water was pumped from depth to the surface at SATURN-03 gasses were released. Since samples are heated to 30° C in the APNA, further gases were released into the sample stream. These gasses caused bubbles in the sample stream which made data noisy and unusable.

After a few unsuccessful deployments, laboratory testing was conducted to identify a reasonable filtering option for the Columbia River estuary's environmental conditions. Water temperatures, filters, and filter housings were tested in the laboratory to identify a possible solution to this problem. Raw river water was collected and brought to the laboratory for testing. The first test was done using a factory suggested 10 μ M ultra-high molecular weight polyethylene filter cup. Bubbles formed on the outside of the filter and vibrations forced bubbles through the filter into the sample stream. In an attempt to reduce the amount of gas bubbles forming, a 47 mm 10 μ M filter was placed in a filter housing. At room temperature, bubble adsorption decreased and thus the number of bubbles entering the instrument decreased. At colder temperatures, a few bubbles formed on the inside of the sample line tubing, and some formed on the 47 mm 10 μ M filters which were pulled through. Although there was still some dissolved gas release at cold temperatures, it was manageable compared to the original filters and seemed to be the best filtering option, as the inlet had the least amount of surface area for the dissolved gasses to adhere to.

It was determined that two 47 mm filter housings in parallel with a 30 μ M nylon mesh pre-filter and a 10 μ M filter was the best compromise. This filtration setup decreased the number of bubbles that were pulled through the APNA and had a reasonable lifetime with the Columbia River's high turbidity loads. These two parallel filters lasted about one week during slow flow summer periods and 3-5 days during high flow, high turbidity winter periods.

4.3 Deployment Conditions

The APNA was made to be submerged in water that does not freeze. One of the challenges we faced while deploying the APNA above water at SATURN-03, was freezing air temperatures. Sample intake lines and reagent lines were small and quickly froze when air temperatures dropped below freezing. This caused expansion of fluid in plastic connectors and caused significant damage to the APNA's end cap. When deploying the APNA un-submerged in cold environments it was vital to retrieve the APNA if freezing temperatures were expected, as freezing temperatures caused significant damage.

Power outages from severe coastal storms and other unexpected events were of significant concern. To ensure the APNA was not damaged during power surges, it was plugged into a surge protector and an uninterruptible power supply (UPS). If power was lost for a prolonged period of time in which the UPS could not sustain the APNA or the APNA's power had to be cycled for any reason, all autonomous coding were loaded under the AUTO ON command to guarantee that the APNA would continue sampling once power was restored.

5.0 Data Quality

5.1 Detection Limits

A minimum detection limit (MDL) study was conducted on 10/19/2010 in conjunction with an inlet calibration. This study was done using the environmental protection agency (EPA) procedure to calculate an instrument's MDL (CFR). A large quantity (1 L) of a mixed standard was made. A baseline (no reagents) and sample (standard plus reagents) were measured seven times. According to EPA standards, the calculated MDL must not be greater than the standard used, and the standard used must not be more than ten times the MDL. A concentration of 1.0 μM was used for nitrate, and an MDL was calculated to be 0.14 μM . A concentration of 0.5 μM was used for nitrite, and an MDL was calculated to be 0.11 μM . A concentration of 0.5 μM was used for ortho-phosphate, and a MDL was calculated to be 0.28 μM . A concentration of 10.0 μM was used for silicic acid, and a MDL was calculated to be 2.0 μM . A concentration of 0.5 μM was used for ammonium, and a MDL was calculated to be 0.61 μM , which did not pass EPA MDL regulations.

5.2 Laboratory Analyzed Grab Samples on the APNA

Although typically a field instrument, methods were developed to run grab samples under ideal laboratory conditions for additional quality control. Unlike the Astoria Analyzer, which required a few ml of sample and took about 2 minutes to run one sample, the APNA required a minimum of 100 ml and took about 10 minutes to run one sample. A large portion of the increased run time for APNA grab samples was due to a baseline requirement for each sample as well as a stable flat peak once reagents were

added. Therefore, it was not practical to run large quantities of grab samples on the APNA.

Log sheets were created for APNA grab sample processing to ensure all appropriate information was recorded (Fig. 2.7). Data processing spread sheets were created to streamline data processing. See Appendix B for grab sample (discrete) procedures and data analysis protocol.

5.3 Laboratory Analyses compared to In Situ Data

APNA deployments from December 2009 – November 2010 revealed a discrepancy between in situ SUNA data and in situ APNA data. To understand these differences a preliminary study was conducted at SATURN-03 on 11/9/2010. During this study, samples were collected at SATUN-03 from near surface (2.0 m), mid water (8.2 m), and near bottom (13.0 m) at four different times throughout the day. Water was filtered for APNA and Astoria Analyzer laboratory analysis (See Chapter 3.3 Bench Top Nutrient Sampling Methods). APNA samples were analyzed using discrete sample processing procedures (See Appendix B, Table 2.1). Standards were run at the beginning and end of each run as well as after every 5-6 samples to account for any drift in baseline, sample peak height, or cadmium column reduction efficiency.

APNA and Astoria Analyzer laboratory analyzed grab samples were compared (Table 2.2). Samples agreed if they were within 3 MDL's or less than 15% relative standard deviation. Although many samples agreed, many did not despite appropriate standard curves and standard checks on both the Astoria Analyzer and the APNA. After much consideration, we have not been able to determine why APNA and Astoria Analyzer nitrite and silicic acid concentrations were different. Identical stock standards

were used for both APNA and Astoria Analyzer analyses. APNA and Astoria Analyzer standard curves were linear. APNA blank checks were at or below detection limits and standard check recoveries were typically between 90-110% (Table 2.1). One difference between APNA and Astoria Analyzer silicic acid was colorimetric methodologies. The APNA used oxalic acid, ascorbic acid, and sodium molybdate to form color while the Astoria Analyzer used molybdic acid, tartaric acid, and stannous chloride as reagents. These methodology differences should not have any effect on the final concentrations derived, but the different should be noted.

APNA and Astoria Analyzer nitrate data was compared to in situ SUNA data (Fig. 2.8). This revealed that SUNA nitrate concentrations were consistently higher than APNA and Astoria Analyzer concentrations for all near surface, mid water and near bottom samples. Although a direct comparison could not be done between grab samples and the in situ SUNA data because sample times were not the same, it was clear that in most cases the SUNA was significantly different than laboratory analyzed grab sample concentrations. With only a few data points from each depth, it was difficult to determine if any relationship existed. Therefore, this study revealed the importance of a more in-depth analysis of in situ versus laboratory analyzed samples (described below).

APNA and Astoria Analyzer laboratory analyzed ortho-phosphate data was compared to in situ Cycle-PO₄ data (Table 2.2, Fig. 2.9). Although Cycle-PO₄ appears higher than both APNA and Astoria Analyzer grab sample concentrations, all samples were within 3 MDL's; therefore, were not considered different.

This preliminary study raised questions not only about the accuracy of the SUNA data, but discrepancies between discrete samples from the APNA and Astoria Analyzer.

To further enhance APNA laboratory analyzed grab sample quality control, it was proposed that an external quality control (QC) standard be analyzed with each discrete sample run. This extra QC standard will provide further support and improve confidence of laboratory analyzed APNA samples. We also proposed a more in depth comparison of the SUNA, APNA, and Astoria Analyzer to resolve questions derived from the limited data in this study.

The more intensive study proposed included SUNA and APNA data, as well as grab samples taken every 15-30 minutes over the course of one or more days. This in-depth analysis was conducted on 12/22/2010, where grab samples were collected every 30 minutes from mid water (8.2 m) depth at SATURN-03. A total of 18 samples were collected throughout the day. During sample collection the APNA and SUNA were sampling mid water (8.2 m) every 30 minutes at SATURN-03. Grab samples were filtered for both APNA and Astoria Analyzer laboratory analysis (See Chapter 3.3 Bench Top Nutrient Sampling Methods). Grab samples were run on the APNA on 6/23/2011 (Table 2.3). Nitrate cadmium column recovery was 87%; therefore, all data, including the nitrate standards, were corrected for poor recovery. No correction to nitrite data was necessary because all standards were within acceptable limits. Ortho-phosphate, silicic acid, and ammonium recoveries were not all within 90-110%. This data was corrected based on standard recoveries. A simple nutrient (Simple Nuts) QC (nitrate + nitrite, ortho-phosphate, and ammonium) was run at the beginning and end of the run. At the beginning, the nitrate recovery was 112% when corrected for cadmium column efficiency. However, when the data was not corrected the recovery was 99%. The nitrate QC at the end of the run did not have a clear peak; therefore, a concentration was not

calculated. Ortho-phosphate QC recovery was 97% at the beginning of the run, but as the standard recoveries increased throughout the run, the QC recovery increased to 143% by the end of the run. Although reasonable corrected ortho-phosphate concentrations were given in Table 2.3, sample baselines were slow to stabilize; therefore, an accurate baseline was not achieved and concentrations presented from the APNA laboratory analysis were believed to be too high. A comparison of all APNA and Astoria Analyzer samples was given in Table 2.4.

The main goal of this study was to compare in situ APNA and SUNA data to laboratory analyzed grab samples. It was clear from this analysis that SUNA nitrate concentrations were higher than both in situ APNA data and Astoria Analyzer data. Laboratory analyzed grab samples from the Astoria Analyzer matched in situ APNA nitrate concentrations reasonably well, while APNA laboratory analyzed grab samples seemed to be higher. It was possible that the APNA laboratory analyzed grab samples nitrate concentrations were artificially shifted too high when the cadmium column correction was applied. Evidence for this was that the Simple Nuts QC was 99% recovery without correction and increased to 112% after the correction was applied.

Temperature and salinity can affect SUNA nitrate concentrations (Sakamoto et al. 2009). We proposed that this may be one reason the SUNA nitrate concentrations were high compared to in situ APNA data and laboratory analyzed grab sample data. Another reason the data might have been high was that the SUNA's spectra slope was low and the intercept was high (Fig. 2.11). The SUNA deployed during the 12/22/2010 deployment malfunctioned, and a new SUNA was installed at SATURN-03 at the beginning of February 2011. The new SUNA's slope was higher (near 0) and flatter compared to the

old SUNA (Fig. 2.11). The new intercept was lower, indicating a flat curve fit to the spectra. Although it was not possible to compare nitrate concentrations from the old SUNA to the new SUNA because nitrate concentrations are so variable in the estuary, changes in the spectra suggest that nitrate concentrations may have shifted with the installment of the new SUNA at SATURN-03. We suggest that before any conclusions are made about the old SUNA's data quality, a similar experiment to the one conducted on 12/22/2010 should be done with the new SUNA. This may reveal if the offset was due to salinity and temperature artifacts or to instrument failure.

6.0 Troubleshooting

Troubleshooting is one of the most important skills to master when working with new technologies such as the APNA. A complete understanding of chemistries, electronics, and flow schematics is vital when troubleshooting problems. Below are a few of the most common problems and step by step suggestions for troubleshooting. It should be noted that these are only a few of the most common problems and further troubleshooting suggestions can be found in section 5 of the APNA Operating Manual.

6.1 Reagent pumps do not appear to be pumping

Depending on how this problem was discovered, a few options can be investigated that may help diagnose and solve the problem.

- a. Turn all reagent pumps off except for the one of concern. Set the reagent pump of concern to a high set point. Listen for any clicking from inside the APNA. If you can hear clicking, then the pump is most likely working. This may indicate a clog in the line preventing water/reagent from flowing.

- b. Another way to determine if the pump is trying to pull fluid is to attach a small syringe (3 ml) filled with water to the end of the line. If water in the syringe appears to be shifting up and down but not being drawn down, the pump may still be functional. This may indicate a block in the line preventing water/reagent from flowing.
- c. Attach a syringe to the reagent line (preferably a small 3 ml) and **gently** try to push water through the line with the reagent pump turned on at a high set point. **DO NOT force water through, as it can damage pumps.**
- d. If the pump is clicking or it is visibly trying to pull water, try turning the pump on at a high set point and letting it pump for a few hours. The blockage may clear itself.
- e. If the pump is clicking or it is visibly trying to pull water through, and water will not go through the reagent line gently, open the reagent pump valve using the protocol outlined in section 5 of the APNA Operating Manual. With the valve open, it is now safe to use a little more force to clear the line. First, try to clear the line with water. If water does not work and you are sure the pump is operational, try coaxing 10% HCl into the line to clear the blockage. It may take some time (a day or so) for the acid to penetrate a blockage.
- f. If the reagent pump of concern is not clicking and water cannot be pushed through when the valve is open, this may indicate a bad pump. Once all options of external fixing are exhausted it may be necessary to open the APNA to determine if reagent pumps are operational or if there is an electrical problem. Carefully following

protocol found in the APNA Operating Manual open the APNA. Follow the protocol for checking resistance of reagent pumps.

- g. If the reagent pump is deemed bad, the pressure compensation housing may need to be opened to fix the problem. SubChem Inc. does not recommend that the customers open the housing. However, depending on the nature of the problem, opening the housing may or may not be an option.

6.2 Reagent pumps are not delivering proper quantity of fluid

- a. First, check the pressure compensation housing pressure. This can be done by pushing down on the bulb on top of the APNA. The bulb should be firm but not hard. If the bulb is rock hard, there may be too much pressure in the housing for the pumps to work properly. Relieve pressure from the pressure compensation manifold by following the steps outlined in the APNA Operating Manual. NOTE: Pressure can increase because pumps are hot, or if there has been a leak into the fluid. If a leak in the fluid is suspected it should be taken very seriously as water in the pressure compensation fluid can cause electrical shorts that will damage pumps.
- b. If the pressure compensation manifold pressure is ok, there may be a blockage in the line. In this case refer to the steps in section 6.1 of this document for troubleshooting.
- c. If both the first two options do not work there may be a larger problem. Although not ideal, the set point can be increased until the desired delivery rate is reached.
- d. Alternatively, but NOT recommended, the delivery rate of each pump can be controlled by a screw on the pump. The APNA and pressure compensation

manifold would need to be opened to adjust the screw; therefore, is not an ideal option.

6.3 Nitrate channel is noisy after deployment

This was a common problem after each deployment. High sediment load in the Columbia River not only caused the pre-filters to clog quickly, but caused other internal problems to the APNA as water was only pre-filtered to 10 μ M. Particles that were smaller than 10 μ M entered the APNA and were trapped within the cadmium column. When flow was restored after transport, particles were released from the cadmium column.

The first step in avoiding this problem altogether is to detach the cadmium column from the APNA and flush it with water at a high velocity upon return to the laboratory. If this step is omitted the nitrate channel may appear to have a high baseline and the raw data may appear noisy. Check the nitrate waste line for a black precipitate. If a precipitate is present, detach the cadmium column immediately and replace it with bypass tubing. Flush the APNA and cadmium column before reattaching.

NOTE: Due to particles being trapped within the cadmium column during deployment, it was necessary to at least rinse the cadmium and replace the glass wool after each deployment. The cadmium column was reconditioned completely after most deployments (See APNA Operating Manual for instructions).

6.4 Pressure compensation bulb is harder than normal

There are a few obvious reasons for this. The first is that all of the pumps have been pumping at a fast rate for a long time causing the fluid to heat and

expand. The other is more serious. A leak in one of the pumps or pump lines within the pressure compensation fluid can increase the amount of fluid in the housing causing the pressure compensation bulb to harden. See sections 6.1 and 6.2 for instructions on how to troubleshoot this problem.

6.5 Error in file while downloading

- a. There are two options to transfer files from the APNA to the host computer. The first is the Batch File Transfer. This mode will transfer files all at once from the APNA to the host computer. If any file is corrupted and the downloading process is interrupted, it will stop and not be able to be restarted. Options for finishing the download include: deleting files that have been transferred successfully one at a time in File Transfer Mode and repeat the batch download. The other option is to finish transferring files in File Transfer Mode. SubChem Inc. (and I) do not recommend Batch File Transfer.
- b. The second option is File Transfer Mode. This mode is much more user friendly and allows for one or more files to be transferred at a time. The advantage of this mode is that when a file “times out”, and an error message appears, file transferring will continue by clicking ok on the error message. SubChem Inc. (and I) prefer this method of file transferring for these reasons. For file transferring protocol see the APNA Operating Manual.

6.6 Corrupted ANA.* files**

- a. Operating files (ANA.SSF, ANA.INI, ANA.CFG) can become corrupted. There is no known reason for these files to become corrupt; however, if this occurs, auto mode programming will not work. SubChem Inc. has provided detailed

instructions (see APNA Operating Manual) to rename files in the windows program HyperTerminal. Once an operating file is renamed a default file will automatically upload. NOTE: Operating files cannot be deleted in file transfer mode. They must be renamed in HyperTerminal. The default file should be checked for proper settings before continuing.

7.0 Conclusions

Deploying a complex wet chemistry instrument such as the APNA in a physically dynamic environment like the Columbia River estuary was not trivial. A significant amount of time and effort was required to adjust factory suggested protocol to improve performance. Issues I encountered in this study included: bubbles formed by dissolved gasses, high sediment loads, freezing air temperatures, and high river velocities. This chapter explained solutions to many of these challenges that were necessary in the study region of the Columbia River estuary.

Steps were taken to ensure the best possible in situ APNA data whenever possible. These efforts included: pre and post-calibrations, pump calibrations, flow calibrations, pre-deployment blanks, in situ standard addition calibrations, and improved data processing. Detailed methodologies for flow, pump, inlet calibrations, discrete sample analysis, and data processing were developed (see Appendix B for step by step procedures). One of the biggest challenges was the highly variable nutrient concentrations that made automated data analysis challenging. MatLab code was created to improve both data quality and the processing time (see Appendix B for line by line analysis).

Comparisons between APNA and Astoria Analyzer grab samples were challenging to interpret. Despite using identical standards, excellent QC and standard recoveries on both instruments, many samples did not agree. Although many grab samples did not agree between the APNA and the Astoria Analyzer we felt as though this had no effect on our in situ data quality. Our intensive efforts to ensure in situ data quality were confirmed for nitrate from our in depth study on 12/22/2010 where in situ APNA data matched Astoria Analyzer grab samples (Fig. 2.10).

From my research efforts it became clear that the APNA's complexity may limit its ability to be used for monitoring nutrients in extreme environments such as the Columbia River estuary. However, its ability to measure all nutrients (nitrate + nitrite, nitrite, ortho-phosphate, silicic acid, and ammonium) simultaneously at high resolution was crucial to this study. Moving forward, I suggest that the APNA be used as an intermittent research tool to aid in answering specific scientific questions.

8.0 Figures

APNA Flow Check and Pump Calibration

* Performed bi-monthly

Page 1 of 1

Date 12/22/11

Analyst Gilbert

Cd Column SN 5040902

Last cal date 12/16/10

Last pump cal date 12/14/10

Last optics clean date Factory

Flowmeter readings

	Channel 1 (Blue) NOX	Channel 2 (Red) NO2	Channel 3 (Green) PO4	Channel 4 (Yellow) Si	Channel 5 (Black) NH4	Total Flow Calculated
Flow rate w/cd column (mL/2min)	2.10	2.0	1.9	1.1	2.1	9.2
PSI Adjuster on waste line	0 1/2 (1)	0 1/2 (1)	0 (1/2) (1)	0 (1/2) (1)	0 1/2 (1)	

System PSI 1 1.07

System PSI 2 0.31

	Measured Total Flow Mass
Total Flow Measured (3min)	0 g → <u>15.12</u>

Pump Calibration (3 min measurements)

	0.1 Start (mL)	0.1 Stop (mL)	0.2 Stop (mL)	0.3 Stop (mL)	0.4 Stop (mL)	0.5 Stop (mL)	0.6 Stop (mL)
B (CAL) (clear)	300	2.75	2.25	1.50	0.50 → 3.00	1.8 → 3.00	1.50
C (NOx) NH4Cl Buffer (blue 1)		2.70	1.85	0.90 → 3.00	1.65		
D (NOx) NED+Sulfanilamide (blue 2)		2.70	2.00	1.00 → 3.00	1.70		
E (NO2) NED+Sulfanilamide (red)		2.70	2.05	1.20 → 3.00	2.10		
F (PO4) NaMoO4 (green 1)		2.80	2.30	1.60 → 3.00	2.15		
G (PO4) Ascorbic (Green 2)		2.75	2.20	1.40 → 3.00	1.90		
H (Si) NaMoO4 (Yellow 1)		2.80	2.20	1.80 → 3.00	2.10		
I (Si) Oxalic Acid (Yellow 2)		2.80	2.30	1.70	0.75		
J (Si) Ascorbic Acid (Yellow 3)		2.60	1.80	0.65 → 3.00	1.45 → 3.00		
K (NH3) EDTA (Black 1)		2.80	2.30	1.45 → 3.00	1.70		
L (NH3) OPA (Black 2)		2.80	2.50	1.90	1.00		

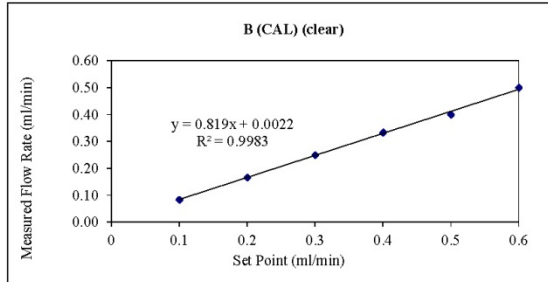
C:\Documents and Settings\NandPlab\My Documents\APNA\Templates\APNA_pumpcal_log

Figure 2.1. An example of a completed Flow and Pump Calibration log sheet.

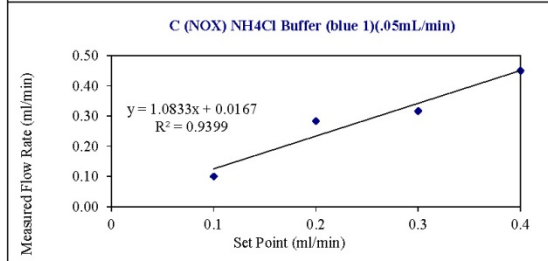
APNA Reagent Pump Calibration

Date 6/22/11

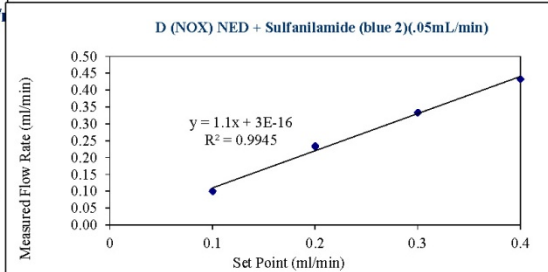
CAL) (clear)				
Set Point (ml/min)	Time (min)	Start mass (g)	Stop mass (g)	Flow rate (ml/min)
0.1	3.0	3.00	2.75	0.08
0.2	3.0	2.75	2.25	0.17
0.3	3.0	2.25	1.50	0.25
0.4	3.0	1.50	0.50	0.33
0.5	3.0	3.00	1.8	0.40
0.6	3.0	3.00	1.5	0.50



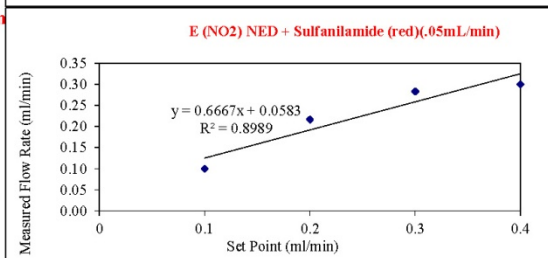
C (NOX) NH4Cl Buffer (blue 1)(.05mL/min)				
Set Point (ml/min)	Time (min)	Start mass (g)	Stop mass (g)	Flow rate (ml/min)
0.1	3.0	3.00	2.70	0.10
0.2	3.0	2.70	1.85	0.28
0.3	3.0	1.85	0.90	0.32
0.4	3.0	3.00	1.65	0.45



D (NOX) NED + Sulfanilamide (blue 2)(.05mL/min)				
Set Point (ml/min)	Time (min)	Start mass (g)	Stop mass (g)	Flow rate (ml/min)
0.1	3.0	3.00	2.70	0.10
0.2	3.0	2.70	2.00	0.23
0.3	3.0	2.00	1.00	0.33
0.4	3.0	3.00	1.70	0.43



E (NO2) NED + Sulfanilamide (red)(.05mL/min)				
Set Point (ml/min)	Time (min)	Start mass (g)	Stop mass (g)	Flow rate (ml/min)
0.1	3.0	3.00	2.70	0.10
0.2	3.0	2.70	2.05	0.22
0.3	3.0	2.05	1.2	0.28
0.4	3.0	3.00	2.10	0.30



Comments:

Proofed 100% _____ Date: _____

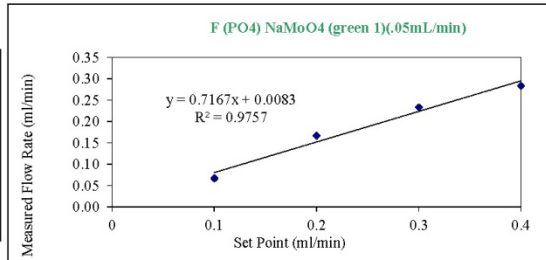
Figure 2.2. An example of a completed Reagent Pump Calibration data sheet.

APNA Reagent Pump Calibration

Date 6/22/11

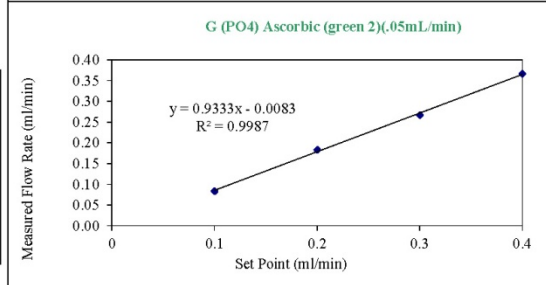
F (PO4) NaMoO4 (green 1)(.05mL/min)

Set Point (ml/min)	Time (min)	Start mass (g)	Stop mass (g)	Flow rate (ml/min)
0.1	3.0	3.00	2.80	0.07
0.2	3.0	2.80	2.30	0.17
0.3	3.0	2.30	1.60	0.23
0.4	3.0	3.00	2.15	0.28



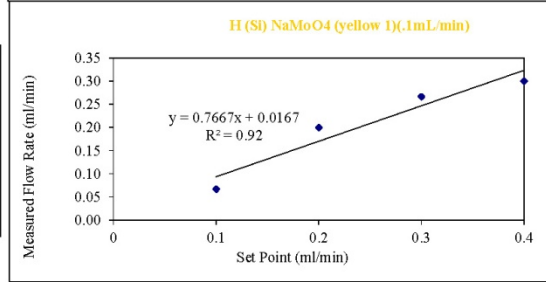
G (PO4) Ascorbic (green 2)(.05mL/min)

Set Point (ml/min)	Time (min)	Start mass (g)	Stop mass (g)	Flow rate (ml/min)
0.1	3.0	3.00	2.75	0.08
0.2	3.0	2.75	2.20	0.18
0.3	3.0	2.20	1.40	0.27
0.4	3.0	3.00	1.90	0.37



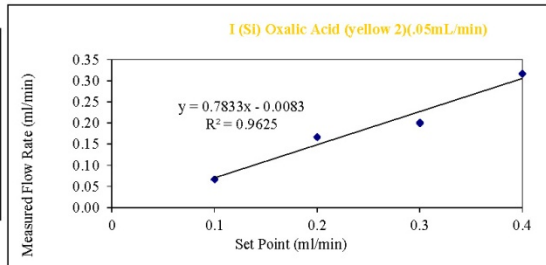
H (Si) NaMoO4 (yellow 1)(.1mL/min)

Set Point (ml/min)	Time (min)	Start mass (g)	Stop mass (g)	Flow rate (ml/min)
0.1	3.0	3.00	2.80	0.07
0.2	3.0	2.80	2.20	0.20
0.3	3.0	2.20	1.40	0.27
0.4	3.0	3.00	2.10	0.30



I (Si) Oxalic Acid (yellow 2)(.05mL/min)

Set Point (ml/min)	Time (min)	Start mass (g)	Stop mass (g)	Flow rate (ml/min)
0.1	3.0	3.00	2.80	0.07
0.2	3.0	2.80	2.30	0.17
0.3	3.0	2.30	1.70	0.20
0.4	3.0	1.70	0.75	0.32



Flow Meter (mL/min)	5.0
Total Flow (mL/ 3 min)	15.12
Total Flow (mL/min)	5.04
% Rec	100.80

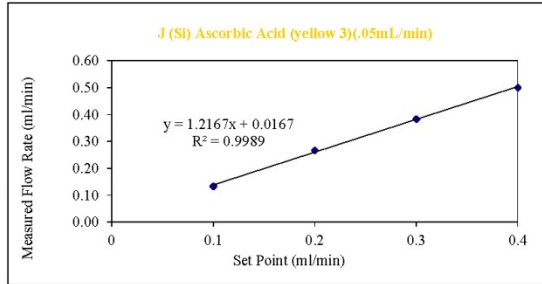
Proofed 100% _____ Date: _____

Figure 2.2. (Continued)

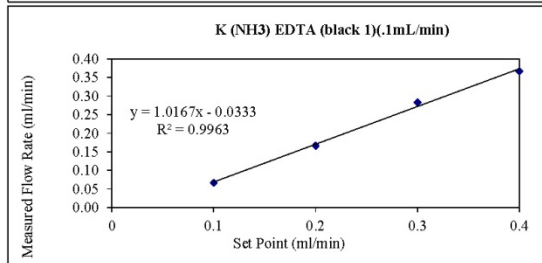
APNA Reagent Pump Calibration

Date 6/22/11

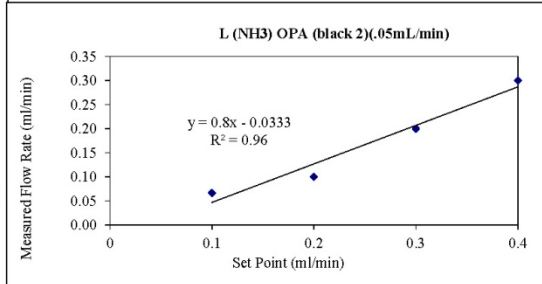
J (Si) Ascorbic Acid (yellow 3)(.05mL/min)				
Set Point (ml/min)	Time (min)	Start mass (g)	Stop mass (g)	Flow rate (ml/min)
0.1	3.0	3.00	2.60	0.13
0.2	3.0	2.60	1.80	0.27
0.3	3.0	1.80	0.65	0.38
0.4	3.0	3.00	1.50	0.50



K (NH3) EDTA (black 1)(.1mL/min)				
Set Point (ml/min)	Time (min)	Start mass (g)	Stop mass (g)	Flow rate (ml/min)
0.1	3.0	3.00	2.80	0.07
0.2	3.0	2.80	2.30	0.17
0.3	3.0	2.30	1.45	0.28
0.4	3.0	3.00	1.90	0.37



L (NH3) OPA (black 2)(.05mL/min)				
Set Point (ml/min)	Time (min)	Start mass (g)	Stop mass (g)	Flow rate (ml/min)
0.1	3.0	3.00	2.80	0.07
0.2	3.0	2.80	2.50	0.10
0.3	3.0	2.50	1.90	0.20
0.4	3.0	1.90	1.00	0.30



Comments:

Proofed 100% _____ Date: _____

Figure 2.2. (Continued)

APN Inlet Calibration Oregon Health and Science University 2000 NW Walker Rd. Beaverton OR, 9

Date 7-26-10 Analyst Gilbert Cal. column SN 05040902

Last cal date 6/17/10 Last pump cal date 7-21-10 Last optics clean date 6/18/10

	NH4Cl Buffer	NED	Sulfanilamide	Ascorbic Acid (0.14M-PO4)	NaMoO4 (43.8mM-PO4)	Ascorbic Acid (0.806M-Si)	NaMoO4 (64.1mM-Si)	Oxalic Acid	EDTA	OPA
Lot number	7-21-10	7-21-10	7-21-10	7-22-10	7-22-10	7-22-10	7-26-10	7-27-10	7-21-10	7-22-10
Expiration date	10-21-10	8-21-10	8-21-10	8-22-10	8-22-10	8-22-10	8-26-10	10-21-10	10-21-10	8-22-10

Stock Standards Used (One Month Expiration)	Lot Number	Expiration	Standard curve standards (prepared from working stock)	Working stock std. vol.	Final volume	Final conc. resp. (uM)	Time made (elapsed)
PO4/NO2/NH4 (2,000/2,000/2,000 uM)	7-26-10	8-26-10	S1 - PO4/NO2/NH4/Si	2.50mL	100 mL	0.5/0.5/0.5/12.5	354
NO3 (10,000 uM)	7-26-10	8-26-10	S2 - PO4/NO2/NH4/Si	5.00mL	100 mL	1.0/1.0/1.0/25	1421
Si (100 mM)	5-9-10	11-9-10	S3 - PO4/NO2/NH4/Si	10.0mL	100 mL	2.0/2.0/2.0/50	2233
			S4 - PO4/NO2/NH4/Si	20.0mL	100 mL	4.0/4.0/4.0/100	2955

Working stock standards (prepared daily from stock standards)	Stock std. volume	Final volume	Final conc. resp. (uM)	Time made (PST)
PO4/NO2/NH4 (2,000/2,000/2,000 uM)	1.00 mL	100mL	20.20/20/500	1014
Si (100 mM)	0.500 mL			
NO3 (10,000 uM)	1.00 mL	100 mL	100	1019

*Flows are hard to balance. This was the best I could do.

Flow rate readings (w/cd column)	Channel 1 (Blue) NOX	Channel 2 (Red) NO2	Channel 3 (green) PO4	Channel 4 (Yellow) Si	Channel 5 (black) NH3	Total flow calculated
Flow rate (mL/min)	1.20	2.30	0.90	1.50	2.50	8.40

System PSI 1 0.91
System PSI 2 -0.16

File name 00726_inletcal *save as date_inletcal (YYMMDD_inletcal)

Start time (PST) 1023 End log time (elapsed time) 5202

Standard curve	DI	DI-RG	S1	S2	S3	S4	S5	DI-RG	DI
Elapsed time (sec)	0	107	837	1557	2318	3021	3630	4219	4760
Channel 1 (Clear) 540 Reference	1.24	1.31	1.30	1.29	1.33	1.30	1.27	1.26	1.15
(Blue) NOX	66.58	67.37	67.21	19	68.23	76.71	73.17	64.52	64.41
Channel 2 (Red) NO2	16.77	22.82	19.30	19.98	21.83	32.89	13.	15.95	12.50
Channel 3 (Clear) 820 Reference	1.39	3.75	62.49	2.00	4.33	3.07	3.20	2.48	4.15
(Green) PO4	1.53	18.86	62.30	7.80	13.76	110	6.52	10.55	12.87
Channel 4 (Yellow) Si	11.79	10.00	30.58	37.98	55.39	15.16	21.06	21.49	47.88
Channel 5 (Clear) FL Reference	-125	-133	-144	-137	-137	-141	-136	-133	-129
(Yellow) NH3	31	53	49	70	88	114	75	73	72

C:\Documents and Settings\NandPlab\My Documents\APNA\Templates\inletcal_log.APNA *1873 change DPI to 0.10

Figure 2.3. An example of a completed Inlet Calibration log sheet.

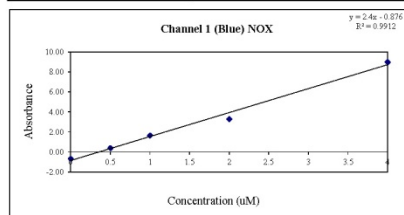
APNA Inlet Calibration

Date: 7/26/2010

Cadmium column: 5040902

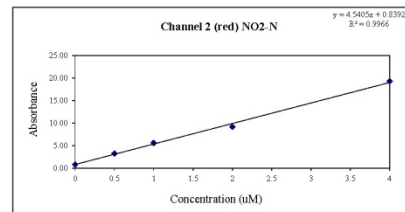
Channel 1 (Blue) NO_x

Conc. (uM)	Background	Raw	Abs	Actual Slope:
0	64.46	63.76	-0.70	2.4
0.5	64.46	64.84	0.38	Theoretical Slope:
1	64.46	66.10	1.64	
2	64.46	67.76	3.30	% Recovery:
4	64.46	73.46	9.00	#DIV/0!
			Intercept: -0.876	
4	64.46	72.28	7.82	(NO ₃ -N only)
Cd column reduction efficiency:				90.5833



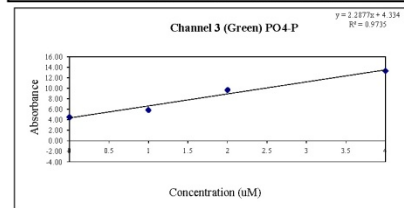
Channel 2 (Red) NO₂-N

Conc. (uM)	Background	Raw	Abs	Actual Slope:
0	12.31	13.16	0.85	4.5405
0.5	12.31	15.61	3.30	Theoretical Slope:
1	12.31	17.94	5.63	
2	12.31	21.50	9.19	% Recovery:
4	12.31	31.59	19.28	#DIV/0!



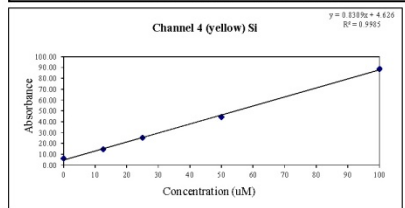
Channel 3 (Green) PO₄-P

Conc. (uM)	Background	Raw	Abs	Actual Slope:
0	1.51	6.03	4.52	2.2877143
1	1.51	7.37	5.86	Theoretical Slope:
2	1.51	11.19	9.68	% Recovery:
4	1.51	14.80	13.29	#DIV/0!



Channel 4 (Yellow) Si

Conc. (uM)	Background	Raw	Abs	Actual Slope:
0	11.88	17.92	6.04	0.83088
12.5	11.88	26.40	14.52	Theoretical Slope:
25	11.88	37.20	25.32	
50	11.88	56.20	44.32	% Recovery:
100	11.88	100.60	88.72	#DIV/0!

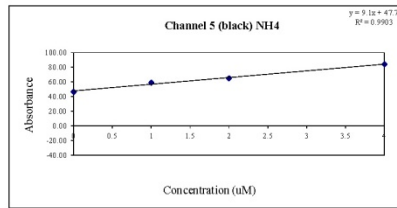


Proofed 100% Date: _____

Figure 2.4. An example of standard curves from an Inlet Calibration.

Channel 4 (black) NH4				
Conc. (uM)	Background	Raw	Abs	Actual Slope:
0	17.00	63.50	46.50	9.1
	17.00			-17.00 Theoretical Slope:
1	17.00	76.00	59.00	
2	17.00	82.00	65.00	% Recovery:
4	17.00	101.00	84.00	#DIV/0!

Comments: The NH4 slope is low even after the pump rate was changed from 0.05 to 0.1.



Proofed 100% _____ Date: _____

Figure 2.4. (Continued)

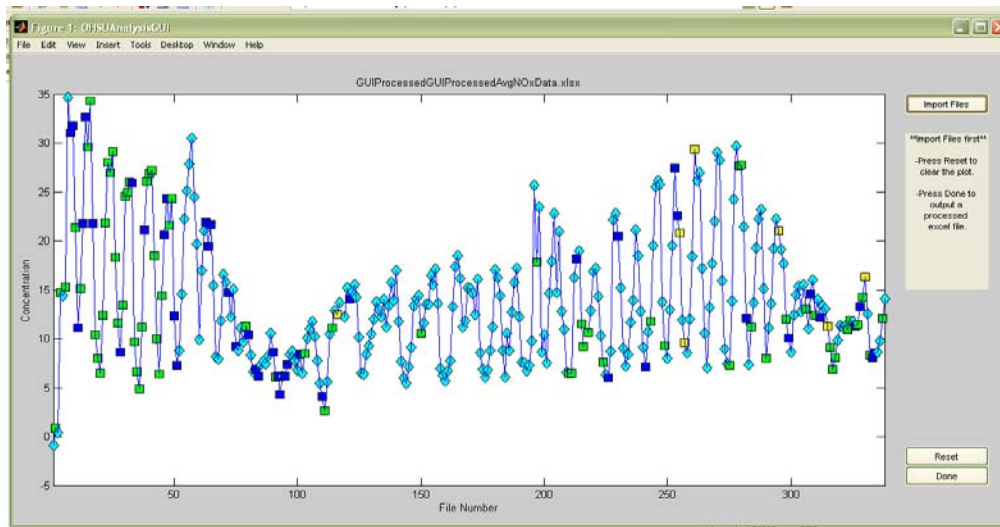


Figure 2.5. A screen shot of nitrate data from summer 2010 at SATURN-03 mid water depth (8.2 m) 7/28/2010 – 8/19/2010. Note the three blank samples at the beginning of the run at 0 μM . The green squares were data points that were deemed “good” by the program. The dark blue squares and yellow squares indicated one or more assumptions were made. These data points were checked for errors. When the program could not find one or more of the desired baseline, sample or calibration regions data was flagged as red squares (not shown). Light blue diamond’s indicated that some alteration had been made to the original placement of the baseline, sample or calibration spike.

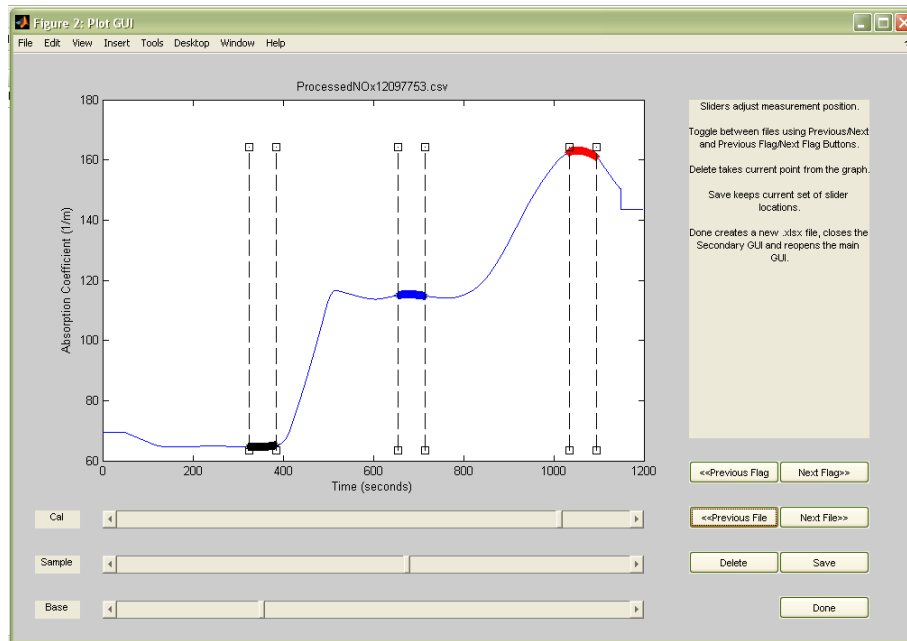


Figure 2.6. A screen shot of the secondary GUI displaying raw APNA data. This GUI allowed the user to change the baseline (black), sample (blue), or calibration (red) location by using slider bars under the plot. Buttons in the lower right hand corner changed files by moving to the next file, moving to the next flagged file, or deleted bad data.

APNA Discrete Analysis

Page ___ of ___

Analyst _____ Date _____ Cadmium column SN: _____
 Last cal date _____ Last pump cal date _____ Last optics clean date _____

	NH4Cl Buffer	NED	Sulfanilamide	Ascorbic Acid (0.14M-PO4)	NaMoO4 (43.8mM-PO4)	Ascorbic Acid (0.806M-Si)	NaMoO4 (64.1mM-Si)	Oxalic Acid	EDTA	OPA
Lot number										
Expiration date										

Stock Standards (Exp. 3 Months)	Lot Number	Expiration
NO3 = 1000 uM		
NO2 = 1000 uM		
PO4 = 1000 uM		
Si = 100 mM		
NH4 = 1000 uM		

Working stock standards	Stock std. volume	Final volume	Final conc. (uM)	Time made (PST)
PO4/NO2/NH4	10.0 mL	100mL	100/100/100/500	
Si	2.0 mL			
NO3	10.00 mL	100mL	100	

	S4	S5
Work Stk Vol	4.00 mL	4.00 mL
Final Volume	100 mL	100 mL
Final Conc uM	4.0/4.0/4.0/100	4.00
Time Made (Elapsed)		
Time Made (Elapsed)		
Time Made (Elapsed)		
Time Made (Elapsed)		

Flow rate readings (w/cd column)	Channel 1 (Blue) NOX	Channel 2 (Red) NO2	Channel 3 (Green) PO4	Channel 4 (Yellow) Si	Channel 5 (Black) NH4	Total flow calculated
Flow rate (mL/min)						

System PSI 1 _____
 System PSI 2 _____

File Name:									
Elapsed time (sec)									
Channel 1 540 Reference (Blue) NOX									
Channel 2 (Red) NO2									
Channel 3 820 Reference (Green) PO4									
Channel 4 (Yellow) Si									
Channel 5 FL Reference (Black) NH3									
Sample ID									
Elapsed time (sec)									
Channel 1 540 Reference (Blue) NOX									
Channel 2 (Red) NO2									
Channel 3 820 Reference (Green) PO4									
Channel 4 (Yellow) Si									
Channel 5 FL Reference (Black) NH3									

C:\Documents and Settings\NandPlab\My Documents\APNA\Templates\APNA_discrete_log

Figure 2.7. An example of a Discrete Analysis log sheet.

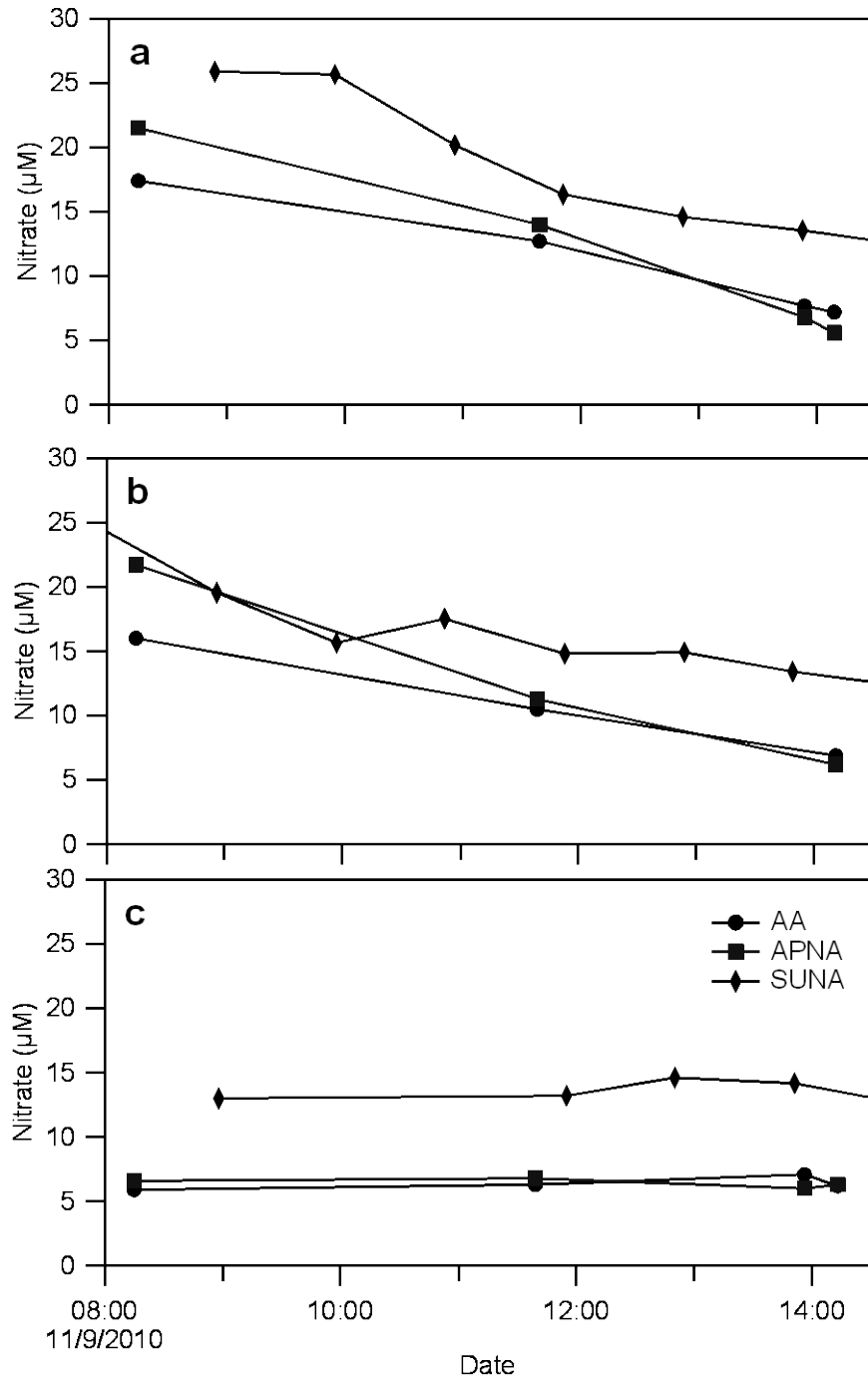


Figure 2.8. A graphical comparison of APNA and Astoria Analyzer (AA) grab samples to in situ SUNA nitrate data at SAUTRN-03 on 11/9/2010. **a**: near surface (2.0 m), **b**: mid water (8.2 m), **c**: near bottom data (13.0 m).

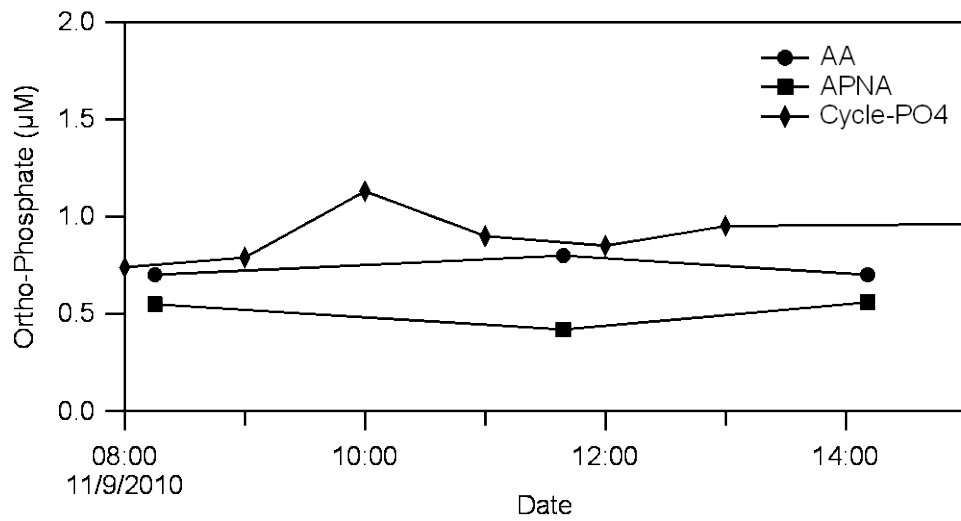


Figure 2.9. Laboratory analyzed Astoria Analyzer (AA) and APNA ortho-phosphate samples compared to in situ Cycle-PO4 ortho-phosphate data from SATURN-03 mid water (8.2 m) depth on 11/9/2010.

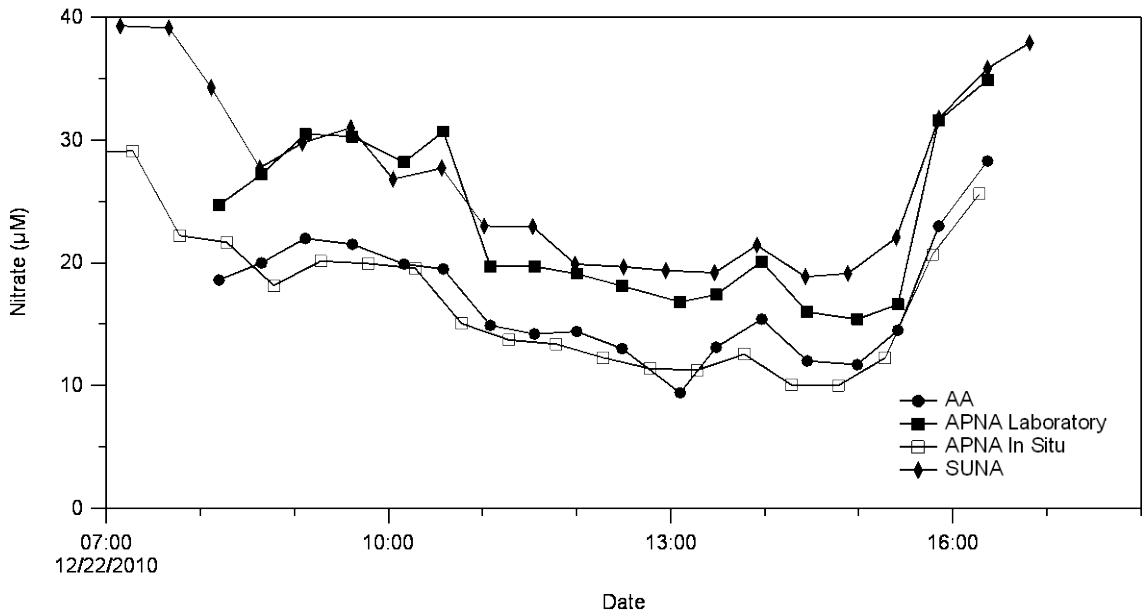


Figure 2.10. A comparison of Astoria Analyzer (AA), APNA field and laboratory data, and SUNA data from SATURN-03 mid water depth (8.2 m) on 12/22/2010. This plot shows an agreement between APNA Laboratory data and the in situ SUNA data and an agreement of APNA in situ data to Auto Analyzer (AA) data.

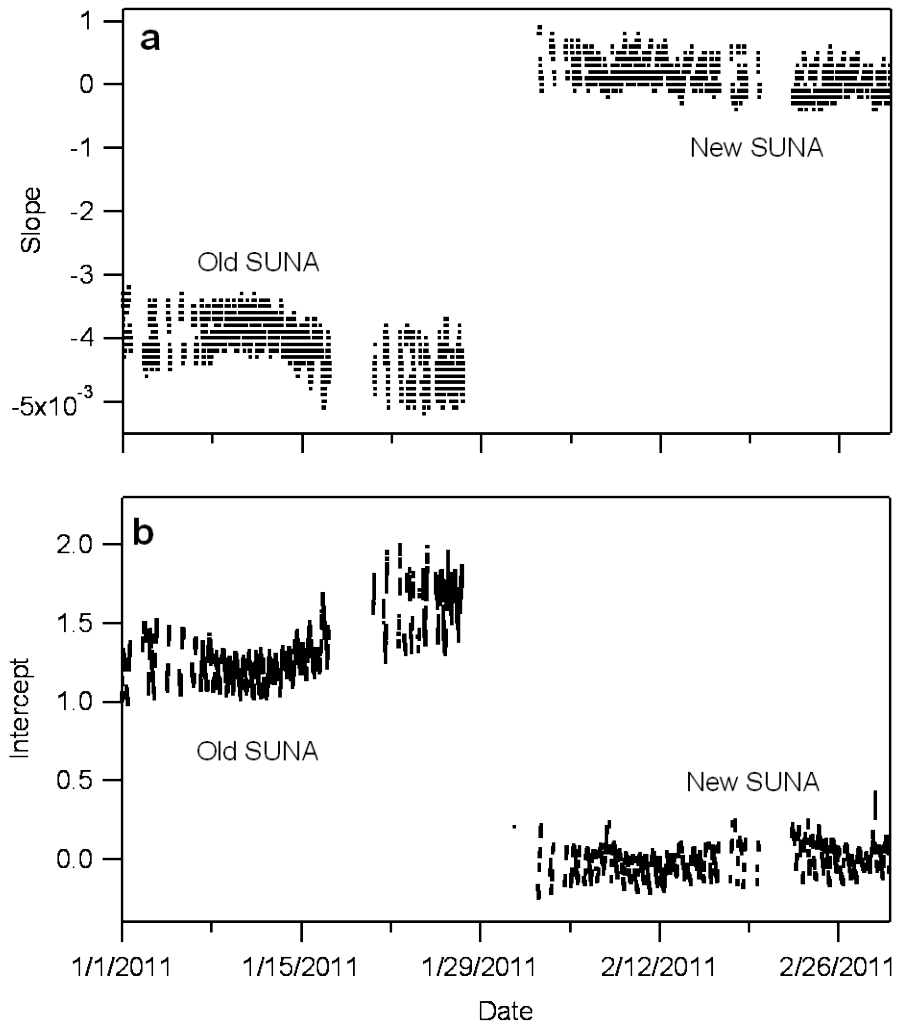


Figure 2.11. Slope and intercept plots of SUNA spectra from mid water (8.2 m) depth at SATURN-03.

9.0 Tables

APNA Grab Samples and Standards											
Sample ID	Sample Depth	Nitrate (μM)		Nitrite (μM)		Ortho-phosphate (μM)		Silicic Acid (μM)		Ammonium (μM)	
		Conc.	Standard % Rec	Conc.	Standard % Rec	Conc.	Standard % Rec	Conc.	Standard % Rec	Conc.	Standard % Rec
DI		0.1		0.3		0.3		2.8		0.1	
S5		3.7	90.7								
S4		4.1	98.1	4.2	99.1	4.2	96.9	100.2	97.5	4.0	103.4
11/9/2010 0815	Surface	21.5		0.4		0.4		193.1		4.1	
11/9/2010 0815	Middle	21.7		0.8		0.5		201.4		3.4	
11/9/2010 0815	Bottom	6.6		0.8		0.4		47.6		0.9	
11/9/2010 1139	Surface	14.0		1.0		0.4		146.1		1.9	
11/9/2010 1139	Middle	11.3		0.9		0.4		116.6		1.6	
11/9/2010 1139	Bottom	6.8		1.0		0.4		59.3		1.1	
S5		3.6	89.6								
S4		4.0	98.4	3.9	97.0	3.8	91.2	114.9	113.3	4.3	111.0
DI		0.1		0.0		0.1		1.6		0.2	
11/9/2010 1354	Surface	6.8		1.0		0.6		76.9		0.9	
11/9/2010 1356	Bottom	6.0		1.0		0.4		70.0		1.0	
11/9/2010 1409	Surface	5.6		1.3		0.2		72.0		1.0	
11/9/2010 1411	Middle	6.2		1.2		0.6		68.7		0.9	
11/9/2010 1413	Bottom	6.3		1.1		0.5		67.8		0.9	
S5		3.1	84.0								
S4		3.7	87.8	4.1	95.6	3.9	96.8	114.5	112.4	4.1	104.0
DI		0.2		0.2		0.0		2.2		0.2	

Table 2.1. Nutrient data from APNA grab samples collected at SATURN-03 on 11/9/2010. Standards were run at the beginning and end of all the samples as well as after every 5-6 samples.

APNA and Auto Analyzer Grab Sample Agreement																
Sample ID	Sample Depth	Nitrate (μM)			Nitrite (μM)			Ortho-phosphate (μM)			Silicic Acid (μM)			Ammonium (μM)		
		APNA	AA	Agreement	APNA	AA	Agreement	APNA	AA	Agreement	APNA	AA	Agreement	APNA	AA	Agreement
11/09/2010 08:15	Bottom	6.6	5.9	YES	0.8	0.3	YES	0.4	0.7	YES	47.6	26.4	NO	0.9		
11/09/2010 11:39	Bottom	6.8	6.3	YES	1.0	0.3	NO	0.4	0.7	YES	59.3	31.2	NO	1.1		
11/09/2010 13:56	Bottom	6.0	7.1	YES	1.0	0.2	NO	0.4	0.8	YES	70.0	38.2	NO	1.0		
11/09/2010 14:13	Bottom	6.3	6.2	YES	1.1	0.2	NO	0.5	0.7	YES	67.8	32.2	NO	0.9		
11/09/2010 08:15	Middle	21.7	16.0	NO	0.8	0.2	YES	0.5	0.7	YES	201.4	150.4	NO	3.4		
11/09/2010 11:39	Middle	11.3	10.5	YES	0.9	0.3	YES	0.4	0.8	YES	116.6	73.4	NO	1.6		
11/09/2010 14:11	Middle	6.2	6.9	YES	1.2	0.3	NO	0.6	0.7	YES	68.7	36.8	NO	0.9		
11/09/2010 08:15	Surface	21.5	17.4	NO	0.4	0.3	YES	0.4	0.8	YES	193.1	156.4	YES	4.1	5.0	YES
11/09/2010 11:39	Surface	14.0	12.7	YES	1.0	0.3	NO	0.4	0.8	YES	146.1	87.4	NO	1.9		
11/09/2010 13:54	Surface	6.8	7.7	YES	1.0	0.3	NO	0.6	0.8	YES	76.9	44.2	NO	0.9		
11/09/2010 14:09	Surface	5.6	7.2	NO	1.3	0.3	NO	0.2	0.8	YES	72.0	39.0	NO	1.0		

Table 2.2. A comparison of APNA and the Auto Analyzer grab samples collected from SATURN-03 on 11/9/2010. Samples agreed if concentrations were within 3 MDL's or less than 15% relative standard deviation.

APNA Grab Samples and Standards

Sample ID	<u>Nitrate (µM)</u>		<u>Nitrite (µM)</u>		<u>Ortho-Phosphate (µM)</u>			<u>Silicic Acid (µM)</u>			<u>Ammonium (µM)</u>		
	Conc.	Standard % Rec	Conc.	Standard % Rec	Conc.	Corrected Conc.	Standard % Rec	Conc.	Corrected Conc.	Standard % Rec	Conc.	Corrected Conc.	Standard %Rec
DI	0.0		0.0		0.0			0.4			0.1		
S5	3.9	97.5	0.0		0.0			0.0			0.0		
S4	4.0	98.2	4.0	99.2	4.0		100.4	101.8		101.4	3.9		100.9
Simple Nuts QC	9.0	112.1			1.7		97.1				7.4		41.9
Si QC								257.1		102.9			
12/22/2010 8:12	24.7		0.3		2.5	2.5		107.0	105.5		0.8		0.8
12/22/2010 8:39	27.2		0.4		2.2	2.3		123.7	109.7		0.9		0.9
12/22/2010 9:07	30.5		0.4		2.5	2.7		147.8	116.3		1.3		1.4
12/22/2010 9:37	30.3		0.5		3.0	3.3		142.9	98.3		1.3		0.9
12/22/2010 10:10	28.2		0.5		3.2	3.6		139.1	81.9		1.4		1.7
DI	0.1		0.0		2.9			0.3			0.3		
S5	4.2	96.2	0.0		0.0			0.8			0.0		
S4	4.4	106.9	4.3	107.5	6.4		88.1	141.4		141.1	3.5		84.2
12/22/2010 10:35	30.7		0.5		2.6	3.0		165.6	97.5		1.0		1.2
12/22/2010 11:05	19.7		0.5		2.0	3.3		86.0	57.1		0.8		0.9
12/22/2010 11:33	19.7		0.5		2.0	1.9		81.9	60.6		0.5		0.6
12/22/2010 12:00	19.1		0.5		2.3	2.1		85.5	69.7		0.6		0.7
12/22/2010 12:29	18.1		0.5		2.3	1.9		100.2	89.3		0.6		0.7
DI	0.2		0.1		1.5			0.0			0.5		
S5	4.3	96.0											
S4	4.5	107.6	4.4	107.6	6.2		117.8	110.9		110.9	4.2		99.6
12/22/2010 13:06	16.8		0.5		2.0	1.6		58.8	52.4		0.6		
12/22/2010 13:29	17.4		0.6		1.8	1.5		72.1	58.7		1.0		
12/22/2010 13:58	20.1		0.5		2.0	1.6		99.6	73.2		1.1		
12/22/2010 14:27	16.0		0.4		2.3	1.8		65.3	42.9		1.5		
12/22/2010 14:59	15.4		0.4		2.2	1.7		54.8	31.7		1.5		

DI	0.0		0.1		1.3		2.5		0.3	
S5	4.2	107.8	0.0		0.0		0.0		0.0	
S4	3.9	96.9	4.2	102.1	6.2	120.6	144.5	142.0	4.4	108.8
12/22/2010 15:25	16.6		0.2		2.6	2.1	69.5	40.3	0.8	
12/22/2010 15:51	31.6		0.2		1.0	0.8	126.3	90.5	1.8	
12/22/2010 16:22	34.9		0.3		1.3	1.0	150.9	128.8	2.7	
Simple Nuts QC					2.5		143.4	0.0	19.5	111.2
Si QC							251.3		100.6	
DI	0.1		0.0		1.0		2.1		0.5	
S5	4.1	92.3								
S4	4.5	110.2	4.3	107.2	5.8	120.6	116.7	114.6	4.4	103.3

Table 2.3. Nutrient data from APNA grab samples collected from mid water depth (8.2 m) at SATURN-03 on 12/22/2010. Standards were run at the beginning, and end of each run as well as after every five samples. A Simple Nuts QC (nitrate + nitrite, phosphate, and ammonium) as well as a silicic acid QC were run at the beginning and end of the run. Samples between standards that were outside 90-110% recovery were corrected based on the standard recovery. All nitrate data, including standards were corrected for a cadmium column efficiency of 87%. Final concentrations used for data comparison are bolded.

APNA and Auto Analyzer Grab Sample Agreement															
Sample ID	<u>Nitrate (µM)</u>			<u>Nitrite (µM)</u>			<u>Ortho-Phosphate (µM)</u>			<u>Silicic Acid (µM)</u>			<u>Ammonium (µM)</u>		
	APNA	AA	Agreement	APNA	AA	Agreement	APNA	AA	Agreement	APNA	AA	Agreement	APNA	AA	Agreement
12/22/2010 8:12	24.7	18.6	NO	0.3	0.3	YES	2.5	0.8	NO	105.5	77.7	NO	0.8	4.0	NO
12/22/2010 8:39	27.2	20.0	NO	0.4	0.2	YES	2.3	0.8	NO	109.7	89.5	YES	0.9	3.7	NO
12/22/2010 9:07	30.5	22.0	NO	0.4	0.3	YES	2.7	0.8	NO	116.3	103.5	YES	1.4	3.8	NO
12/22/2010 9:37	30.3	21.5	NO	0.5	0.3	YES	3.3	0.8	NO	98.3	101.0	YES	0.9	3.6	NO
12/22/2010 10:10	28.2	19.9	NO	0.5	0.3	YES	3.6	0.4	NO	81.9	89.3	YES	1.7	3.9	NO
12/22/2010 10:35	30.7	19.5	NO	0.5	0.3	YES	3.0	0.6	NO	97.5	84.5	YES	1.2	3.9	NO
12/22/2010 11:05	19.7	14.9	NO	0.5	0.3	YES	3.3	0.6	NO	57.1	57.4	YES	0.9	4.0	NO
12/22/2010 11:33	19.7	14.2	NO	0.5	0.2	YES	1.9	0.6	NO	60.6	53.5	YES	0.6	3.9	NO
12/22/2010 12:00	19.1	14.4	NO	0.5	0.2	YES	2.1	0.7	NO	69.7	54.7	NO	0.7	4.0	NO
12/22/2010 12:29	18.1	13.0	NO	0.5	0.3	YES	1.9	0.7	NO	89.3	46.3	NO	0.7	4.8	NO
12/22/2010 13:06	16.8	9.4	NO	0.5	0.2	YES	1.6	0.7	NO	52.4	32.1	NO	0.6	3.2	NO
12/22/2010 13:29	17.4	13.1	NO	0.6	0.2	YES	1.5	0.9	YES	58.7	44.6	NO	1.0	4.4	NO
12/22/2010 13:58	20.1	15.4	NO	0.5	0.3	YES	1.6	0.5	NO	73.2	57.6	NO	1.1	4.4	NO
12/22/2010 14:27	16.0	12.0	NO	0.4	0.4	YES	1.8	0.5	NO	42.9	35.2	YES	1.5	4.6	NO
12/22/2010 14:59	15.4	11.7	NO	0.4	0.6	YES	1.7	1.0	YES	31.7	34.8	YES	1.5	4.4	NO
12/22/2010 15:25	16.6	14.5	YES	0.2	0.2	YES	2.1	0.8	NO	40.3	55.1	NO	0.8	3.9	NO
12/22/2010 15:51	31.6	23.0	NO	0.2	0.2	YES	0.8	1.1	YES	90.5	111.1	YES	1.8	3.2	NO
12/22/2010 16:22	34.9	28.3	YES	0.3	0.2	YES	1.0	0.8	YES	128.8	148.9	YES	2.7	3.1	YES

Table 2.4. A comparison of APNA and Astoria Analyzer grab samples collected from SATURN-03 on 12/22/2010 from mid water depth (8.2 m). Samples agreed if concentrations were within 3 MDL's or less than 15% relative standard deviation.

10.0 References

Code of Federal Regulations (CFR) 40, Ch. 1, Pt. 136, Appendix B.

Sakamoto, C.M., K.S. Johnson, and L.J. Coletti, 2009. Improved algorithm for the computation of nitrate concentrations in seawater using an in situ ultraviolet spectrophotometer. *Limnology and Oceanography: Methods* 7:132-143

Chapter 3

Nutrient Loading and Transformations in the Columbia River Estuary Determined by High Resolution In Situ Sensors¹

¹This chapter will be submitted to Estuary and Coasts for publication.

Corresponding Authors: Melissa Gilbert^{1,3}, Joseph Needoba^{1,3}, Corey Koch², Andrew Barnard², Antonio Baptista^{1,3}

¹ Institute of Environmental Health, Oregon Health and Science University, Beaverton, USA

² WET Labs, Inc., Philomath, OR

³ NSF Science and Technology Center for Coastal Margin Observation and Prediction, Beaverton, OR, USA

1.0 Abstract

The Columbia River estuary is physically dynamic and has water residence times typically shorter than one week. These and other environmental conditions tend to suppress water column productivity and enhance the export of river borne nutrients to the coastal ocean; however, hotspots of biological activity may be significant regions for nutrient transformation and removal. We conducted a high resolution time series study of biogeochemical measurements in order to quantify nutrient transformations within the salinity mixing regime of the estuary. During 2010, three autonomous nutrient sensors (Satlantic SUNA, SubChem Systems Inc. APNA, WET Labs Cycle-PO4) that together measured nitrate + nitrite, ortho-phosphate, ammonium, silicic acid, and nitrite were deployed on fixed observatory platforms. Hourly measurements captured tidal fluctuations and therefore permitted an analysis of river and ocean end-member mixing. The results suggested that during summer, the estuary contained high concentrations of ammonium and phosphate despite low concentrations in the river and coastal ocean. This was likely from organic matter accumulation and remineralization in the estuarine turbidity maximum and lateral bays.

2.0 Introduction

Estuaries are regions of enhanced biogeochemical activity that provide important ecosystem services and support complex food webs. In many estuaries, the estuarine turbidity maximum (ETM) and intertidal regions are important sites for nutrient transformations and therefore can significantly alter riverine nutrient export to the coastal ocean (Garnier et al. 2010; Beusekom and Brockmann 1998; Caffrey 1995, Jensen et al. 1990, Small and Prahl 2004). In particular, dissolved inorganic nitrogen can undergo a variety of transformations, such as nitrification, denitrification (Galloway et al. 2003) and dissimilatory nitrate reduction to ammonium, or DNRA, (Buresh and Patrick 1978). Nutrient transformations can also include: assimilation during primary production, remineralization during organic matter degradation, and dissolution, as in the case of diatom frustule decay (Garnier et al. 2010).

ETMs are sites of relatively high biological activities and nutrient transformations due to the particle trapping characteristics that function to concentrate organic material and facilitate microbiological activity (Garnier et al. 2010; Abril et al. 2000). Tidal marshes and mudflats can be a significant nitrogen sink in many coastal systems (Smith et al. 1985), and potentially account for the removal of 30-70% of riverine nitrate inputs, depending on the residence time of water within the system (Galloway et al. 2003). As anthropogenic sources of reactive nitrogen (Nr) have increased in many watersheds around the world, the importance of denitrification in estuaries has become apparent, as estuaries are the last buffer zone to remove Nr before it is transported to the coastal ocean where it can result in eutrophication (Galloway et al. 2003). In addition to removal processes, organic matter remineralization from intertidal regions provides an important

source of nutrients for water column phytoplankton growth (Caffrey 1995). Studies in temperate estuaries have shown that remineralization can supply as much as 30-80% of the N_r required by phytoplankton (Blackburn and Henriksen 1983; Rowe et al. 1977).

Estuarine water residence time is tightly coupled with nutrient transformations such that as water residence time increases, nutrient transformations increase (Galloway et al. 2003). The most widely studied example is the observed increase in denitrification with an increase in residence time (Howarth et al. 1996). Other studies have demonstrated that rates of nutrient release from organic matter in sediments are influenced by the water residence time (Abril et al. 1999; Abril et al. 2002; Ferguson et al. 2004)

The Columbia River estuary is characterized by ETM formation in several regions of the main channel and has numerous freshwater and saltwater intertidal regions that together may act as important regions of biogeochemical activity. Previous research has demonstrated that nutrients in the Columbia River typically follow a seasonal pattern, with high nitrate and phosphorus concentrations during winter and significant depletion by phytoplankton during summer that are likely linked to an increase in particulate organic matter (Sullivan et al. 2001). However, these nutrients were never fully depleted, suggesting something else ultimately limited phytoplankton growth (Sullivan et al. 2001). Despite significant agricultural and urban influences in the watershed, anthropogenic eutrophication is thought to be mild in the Columbia River estuary (Bricker et al. 2007). Previous studies of nutrient spatial gradients in the fresh water stretch of the lower Columbia and Willamette Rivers identified variability within these fresh water sources to the estuary (Prahl et al. 1998). Elevated levels of nutrients were identified in runoff from

the Willamette River Valley, where agricultural practices are prevalent. However, the effect on the Columbia River nutrient flux was minimal due to a relatively low contribution of Willamette River discharge to the total Columbia River discharge during summer months (Prahl et al. 1998).

Bruland et al. (2008) demonstrated a conservative mixing relationship between river and ocean water for nitrate and silicic acid in the estuary. This study consisted of transects that spanned the coastal plume to freshwater river region, and suggested that biogeochemical transformations in the estuary were minimal. However, Small and Prahl (2004) provided evidence for organic matter degradation as identified by a “thick bottom fluff layer” associated with the ETM that can accumulate from aggregation of organic matter and is likely a site of high microbial activity. They concluded that during summer low river flow conditions, the Columbia River estuary ETM acts as a “particle conveyor belt” transporting organic material toward the ocean during spring tides while selectively trapping particles during neap tides. However, despite the presence of ETMs and intertidal regions, the short estuarine water residence times (Bottom et al. 2005) and previously observed conservative mixing behavior (Bruland et al. 2008; Sommerfield 1999) implies that biogeochemical transformations within the estuary are limited and thus not important to the biogeochemical export of riverborne material. However, few studies have attempted to quantify nutrient transformations over extended periods in the estuary, and no comprehensive analysis of nutrient loading or biogeochemical cycling in the Columbia River estuary is available (Bricker et al, 2007). This is in part due to the practical challenges of quantifying nutrient concentrations of multiple water masses encountered in the estuary.

Here we report a study of inorganic nutrients in the Columbia River estuary using autonomous nutrient sensors that are capable of providing the temporal resolution and continuous long term record needed to assess changes in concentration across all periods of the tidal cycle and across different seasons. By also measuring salinity and temperature, we were able to calculate the daily extent of river and ocean mixing and assess conservative mixing behavior associated with ebb and flood tides. Our high temporal as well as spatial coverage of inorganic nutrients yielded insight into the complexity and importance of the Columbia Rivers' salt water estuary acting as a "bioreactor" for nutrient transformations, despite low residence times in the water column. The technologies and methods described in this study allowed us to identify organic matter remineralization as the dominant estuarine processes acting on riverborne inorganic nutrients during export to the coastal ocean. Furthermore, we identified the ETM and lateral bays as areas where nutrient transformations occurred along the gradient from the Columbia River to the coastal plume.

3.0 Materials and Methods

3.1 Study Area

The Columbia River has the second largest drainage basin in the continental United States and is the largest source of fresh water from the U.S. west coast to the Eastern Pacific Ocean (Simenstad et al. 1990). The drainage basin encompasses 660,480 km² including the Columbia, Snake, and Willamette Rivers (van der Leeden et al. 1990). The estuary is river-dominated and characterized as a salt wedge estuary (Barnes et al. 1972). It becomes highly stratified during neap periods of the monthly tidal cycle and has a dynamic ETM at the density front of the salt wedge in both the North and South

Channels. The reaches of the ETM depend on temporal variability in tidal stage, wind direction, and river flow.

In order to identify specific regions of nutrient transformation from the river to the coastal plume, and understand how transformations influence nutrient budgets along the Oregon/Washington coastal zone, we studied three Reaches defined by the Lower Columbia River Estuary Partnership (2005) (Fig. 3.1). Reach A is defined as the entrance to the estuary and the lower salt water estuary, and was the most saline part of the estuary. This includes lateral bays Bakers Bay and Youngs Bay. Reach B encompassed the fresh water tidal flats of Cathlamet Bay and Grays Bay, and is the inland extend of salt water intrusion (NPCC 2004). Reach C is in the fresh water river, in which tidal influences can affect river flow.

3.1.1 Estuary Sampling Location: SATURN-03

The Center for Coastal Margin Observation and Prediction (CMOP) biogeochemical platform SATURN-03 (Reach A) is located just inside the Columbia River on the south side of the estuary near Point Adams ($46^{\circ}12.0' \text{ N } 123^{\circ}56.4' \text{ W}$) (Fig. 3.1). This station was equipped with a variety of physical, biological, and biogeochemical sensors that were housed at the end of a pier. Water was pumped up to the pier from three depths: near surface (2.4 m), mid water (8.2 m) and near bottom (13.0 m). Large salinity and tidal variations at this site reflect its close proximity to the estuary entrance and necessitate the use of high resolution sensors to resolve hourly (and faster) temporal variability associated with tidally modulated, net seaward advected water masses. The majority of the data from this station is available on the CMOP website (http://www.stccmop.org/datamart/observation_network).

3.1.2 River Sampling Location: SATURN-05

The SATURN-05 infrastructure is located on the United States Geological Service (USGS) station 14246900 which is near the northern bank of the Columbia River 53 miles from the entrance ($46^{\circ} 10.916' \text{ N}$, $123^{\circ} 10.83' \text{ W}$) (Fig. 3.1). The estuary salt wedge does not reach this location (Reach C). It is restricted geographically to Reaches A and B. The water level can change on the order of 0-3 m and river flow can reverse from daily tides. All data from this station is available on-line (http://www.stccmop.org/datamart/observation_network).

3.1.3 CMOP Campaign

In addition to in situ measurements, nutrient samples were collected throughout the Columbia River, estuary, and plume aboard the R/V Wecoma during August 2010. Samples were collected during both a neap and spring tidal outwash (one ebb tide) at RM-17 (Reach B), located 17 miles from the river mouth and just south of the main channel ($46^{\circ} 12.66' \text{ N}$, $123^{\circ} 46.44' \text{ W}$) (Fig. 3.1). Situated upriver of the city of Astoria, and downriver from Cathlamet Bay (freshwater tidal flats), this site was chosen to capture water quality conditions immediately downstream of the major fresh water tidal flat region of the Columbia River estuary.

3.2 Instrumentation on Observatory Platforms

3.2.1 Autonomous Profiling Nutrient Analyzer (APNA)

The APNA is a submersible wet chemistry instrument (SubChem Systems Inc.), in which colorimetric methodologies for nitrate + nitrite (nitrate), nitrite, ortho-phosphate, and silicic acid (Grasshoff and Koroleff 1983) are applied autonomously. A fluorometric ammonium method was adapted by SubChem Systems Inc. for seawater

sampling (Genfa and Dasgupta 1989; Holmes et al. 1999; Aminot et al. 2001). In preparation for each deployment, multiple calibrations (flow balance, reagent pump, standard curves) were performed to ensure the best possible data quality. To achieve an equal and calibrated flow, sample was pumped into the APNA and the amount of water flowing out each channel was measured. Backpressure regulators were added to outflow lines until all flows were balanced. All reagent pumps were calibrated by pumping at four different settings and measuring the volume of water pumped to ensure accurate reagent addition to the sample stream. Once flows were balanced and pumps were calibrated, the APNA was calibrated with at least four standards per channel. The cadmium column (for nitrate reduction) efficiency was checked, and if the recovery was less than 90%, the column was reconditioned and the APNA was recalibrated. Variations in the sampling scheme were employed throughout the year, but a baseline (sample only), sample (sample plus reagents), and standard addition calibration (sample plus reagents plus standard) were conducted for each sample (Fig. 3.2). Standards and blanks were run in the laboratory prior to each deployment to ensure reagents were stable and free of contamination.

The CMOP biogeochemical platform SATURN-03 was used to house the APNA for selected dates between December 2009 and January 2011. Samples were collected every 1-1.5 hours at mid water depth (8.2 m) to capture changes in nutrient concentrations over tidal cycles. While deployed, the APNA filtered sample through a 10 μm filter, heated the sample to 30° C and separated it into 5 flow channels, where the appropriate reagents for each analysis were added and allowed to react before passing through the detectors. Data was stored internally as well as telemetered to the CMOP

online database. After each deployment, data was analyzed using a MatLab program which allowed for a fast preliminary assessment of data quality. Baseline, sample and calibration peaks were identified based on the timing and slope of the plots (Fig. 3.2). The software identified baseline and calibrant peaks by using the minimum and maximum values in the data set. Sample location was determined as the largest plateau region between the minimum (baseline) and maximum (calibrant) values in the data set (Fig. 3.2). Data was flagged as “bad” if the program could not identify all three regions needed to calculate the samples concentration or if more than one plateau was found between the minimum (baseline) and maximum (calibrant) values. “Bad” data was manually quality controlled in which peaks could be adjusted using software-created control slider bars (Fig. 3.2). Due to the possibility of slight changes in the standard pump delivery volume to the sample stream, standard addition calibrations were not used to calibrate the instrument. However, for additional quality control, the stability of the standard addition calibration spike was monitored.

3.2.2 Cycle-PO4

The Cycle-PO4 (WET Labs, Inc.) is a submersible wet chemistry sensor that measures ortho-phosphate colorimetrically with methods adapted from Murphy and Riley (1962) and EPA method 365.5. Prior to each deployment, the Cycle-PO4 was calibrated and characterized at the WET Labs factory in Philomath, OR, using established manufacturer protocols. Optical, electronic, and fluidic parameter values were recorded and the instrument was subjected to shake and vacuum tests. Standards including an ultrapure water blank, 0.5, 2.6, and a National Institute of Standards and Technology (NIST) traceable 10.5 μM phosphate standard were evaluated (7-10 runs) to determine

calibration and ensure the instrument met or exceeded specifications. The instrument underwent an overnight mock deployment at ~5 m depth. Afterwards, a NIST traceable 5.3 μM phosphate standard was evaluated as a calibration check.

The Cycle-PO4 was deployed above water at SATURN-03 (Fig. 3.1) where it sampled mid water (8.2 m) for selected dates between November 2009 and January 2011. Sample was pumped into the Cycle-PO4 through a 10 μm filter, mixed with reagents and pumped into the detector flow cell. The Cycle-PO4 used a factory calibration as well as a periodic standard addition calibration for quality control. Final data was quality controlled by WET Labs using automated algorithms to detect bubble signatures and evaluate raw data precision as an indicator of stability.

3.3 Bench Top Nutrient Sampling Methods

Grab samples of water were manually collected from a variety of locations and depths throughout the Columbia River, estuary, and plume. Each sample location required a unique method of sample collection due to environmental conditions and station access. Water was pumped to the surface from mid water depth (8.2 m) at SATURN-03, and collected in 10% HCl washed dark Nalgene bottles. Samples were stored on ice at 4° C no longer than 24 hours until they were filtered. During an oceanographic cruise, Niskin bottles, an electric pumping system, and a shipboard laboratory flow through from a submersible instrument package were all used to collect samples. All bottles for collection and storage of samples, syringes, and filter housings were washed with 10% HCl before use. Bottles, syringes and filter housings were dried, capped and stored in clean Ziploc bags until use. Collection bottles were rinsed three times with sample and filled by gently pushing sample through a Swinnex filter holder

and combusted 25 mm glass fiber filter (GFF) using a 60 ml syringe. Storage bottles were rinsed three times with filtered sample before final filling, leaving sufficient head space for freezing. Samples were immediately placed upright in a -20° C freezer until analysis. All samples were thawed in a water bath (55° C) and then cooled to room temperature to remove any silicic acid polymerization. An Astoria Analyzer (Astoria-Pacific, Clackamas, OR) for nitrate + nitrite (nitrate), ortho-phosphate, ammonium, silicic acid, and nitrite analysis (APHA 1981, APHA 1975, Armstrong et al. 1967; Atlas et al. 1971; EPA Method 350.1, EPA Method 365.1; EPA Sample Preservation; Fox 1978; Sakamoto et al. 1990). These methods have detection limits (MDL) of 0.5, 0.3, 0.3, 1.0, and 0.2 μM respectively.

3.4 Data Analysis

3.4.1 Conservative Mixing End Member Calculation

An accepted approach for assessing biogeochemical changes in estuaries involves conducting shipboard transects across an estuary salinity gradient and determining deviations from a linear end member mixing relationship that are indicative of estuarine sources or sinks of nutrients and trace metals (Bruland et al 2008; Garnier et al. 2010). Here we describe a complimentary approach to identifying sources and sinks of nutrients within an estuary by analyzing high resolution data from autonomous sensors at a fixed location.

All APNA and Cycle-PO₄ in situ nutrient data was matched with the closest corresponding salinity value (sampled every 3 minutes) from the mid water depth (8.2 m) at SATURN-03. An example of nitrate, phosphate, and salinity fluctuations can be seen in Fig. 3.3a. Note the parallel rise and fall of nitrate and phosphate with salinity (Fig.

3.3a). Nutrient versus salinity plots were created for each ebb tide from the highest to the lowest salinity in which a regression line was calculated and termed Conservative Mixing Regression (CMR) (Fig. 3.3b). For each CMR, the y-intercept, or 0 salinity, gauged the River End Member (REM) nutrient concentration, while the calculated Ocean End Member Salinity (OEMS) (see below) was used to define the Ocean End Member (OEM) nutrient concentration (Fig. 3.3b). To achieve more accurate end members and avoid variability from one tidal cycle to another, CMR were calculated for each ebb tide (Fig. 3.3b). Some ebb tides during neap tides did not have a sufficient salinity range and were not included in the calculations due to the very limited dynamic range of the data set. This generally included cases in which there were less than four data points, or if there were two points around the same salinity value and one at another.

Values for the coefficient of variance (R^2) were calculated for each regression, and any regression that had a value less than 0.75 was not used in data analysis. If either the predicted REM or OEM was negative, it was assumed that the concentration was zero. During time periods when conservative mixing did not occur, nutrient concentrations were averaged for salinities <10 and termed the Estimated River End Member (EREM). Nutrient concentrations were averaged for salinities >20 and termed the Estimated Ocean End Member (EOEM).

The combination of large salinity ranges and instrumentation for high resolution sampling employed here (APNA, SUNA, and Cycle-PO₄) allowed for a unique approach in which nutrient transformations were identified through changes in REMs, not only temporally in a fixed location, but spatially as well by comparing REMs from different locations throughout the river and estuary. These methods are based on the premise that

given a short enough time scale and a small enough geographical location, water will mix conservatively. Large salinity ranges that accompanied each tide allowed for the calculation of CMRs as well as REMs and OEMs for most nitrate and phosphate tidal cycles during the late summer of 2010 (Fig. 3.3).

3.4.2 Calculation of Ocean End Member Salinity

The location and depth of the highest salinity water entering the estuary on any given day, Estuarine Source Water (ESW), changes with tidal phasing (spring/neap) and the upwelling/downwelling nature of the coastal ocean. A regression analysis yielded a quantitative OEMS estimate for each day during the summer time period. In order to calculate an OEMS and facilitate the conservative mixing OEM calculation, temperature and salinity data from SATUN-02 (plume) and SATURN-03 (estuary) were compared (Fig. 3.1). A linear regression equation was derived for SATURN-03 temperature (T) and salinity (S) data for each day, where m was the slope and b was the intercept or expected river water temperature (Equation 1.0).

$$T = m * S + b \quad 1.0$$

SATURN-02 salinity data was entered into equation 1.0 for S to yield an extrapolated temperature. The extrapolated temperatures were compared to real SATURN-02 temperatures to find the minimum difference and identify the water mass with the corresponding salinity. This salinity was the highest salinity or ESW entering the estuary on that day and referred to as the OEMS (Table 3.1).

3.4.3 Nitrate: Change in River Concentration

Hourly measurements of nitrate (SUNA (Satlantic)) were averaged for each day to determine the nitrate concentration at SATURN-05. Given the downstream river

velocity, a one-day lag was taken into account for the transit time between SATURN-05 and SATURN-03 to improve the accuracy of the intersite comparison. Thus, each REM concentration calculated from SATURN-03 was compared with the daily average nitrate concentration from the previous day at SATURN-05. The differences between the SATURN-05 and SATURN-03 nitrate measurements for each tidal cycle were calculated and all tidal cycles were averaged for each deployment yielding the average change in nitrate from SATURN-05 to SATURN-03.

3.4.4 Phosphate: Change in River Concentrations

There were no in situ phosphate measurements at SATURN-05 during this study. Therefore, water samples (two) during the summer analysis period (8/4/2010 and 8/11/2010) were used to calculate the phosphate concentration and compute nitrate:phosphate ratios. Daily average nitrate concentrations from the SUNA, and nitrate:phosphate ratios from the water samples were used to calculate daily average phosphate concentrations for the summer analysis period. Each water sample's nitrate:phosphate ratio yielded a set of phosphate concentrations; however, there was no statistical difference ($P = 0.101$) found between the daily average phosphate concentrations using the two different ratios. The difference in phosphate concentration from the river (SATURN-05) to the estuary (SATURN-03) was calculated using both ratios. All values were averaged to achieve a final difference between the SATURN-05 and SATURN-03.

3.4.5 Statistical Analysis

Student t-tests were performed on REM from estuary (SATURN-03) and river data (SATURN-05), termed the True River Concentration (TRC), to determine if there

were any statistical differences in nutrient concentrations along this gradient. Tests resulting in a P value of < 0.050 were verified as statistically significant relationships. During some times of the year there was only one sample from the river, which was insufficient to make any meaningful statistical conclusions.

4.0 Results

4.1 Seasonal Patterns at SATURN-03

4.1.1 Salinity

Salinity typically varied from near zero to over 30 during each tidal cycle (Fig. 3.4a). Slight variations were observed with season and river flow. During high-flow winter periods, salinity ranged from ~5 to ~30. The spring freshet decreased salinity maximums and minimums (May-Jun) while low flow periods had a slightly increased minimum salinity (Aug-Nov) (Fig. 3.4a).

4.1.2 Nutrients

Nitrate concentrations typically ranged from near 0 to $>20 \mu\text{M}$ within each tidal cycle, but the relationship with salinity changed seasonally (Fig. 3.4b). During fall and winter, river nitrate concentrations (filled light circles) were higher than ocean nitrate concentrations (filled dark circles). During periods of upwelling, ocean nitrate (filled dark circles) concentrations were higher than river concentrations (filled light circles) (Fig. 3.4b).

Phosphate showed a clear seasonal pattern that was associated with summer upwelling (Fig 3.4c and e). There was a correlation between phosphate and salinity during upwelling (summer), in which high salinity water corresponded with high phosphate concentrations (Fig. 3.4c and e). During periods of downwelling (fall-spring),

there was no correlation between phosphate and salinity. A few spikes in Cycle-PO₄ phosphate data were observed in which concentrations reached almost 10 μM (data not shown). Although we do not believe phosphate values reached these levels in the estuary, this data had no signatures to trip a QC flag and visually was typical of a good run. Removal of these points could be based on time series analysis or that phosphate concentrations were too high to be reasonable, but sufficient evidence was not generated to remove these points from the data set.

Ammonium appeared to have no significant correlation with salinity during downwelling or upwelling periods (Fig. 3.4d). The lowest concentrations of ammonium were seen in winter through spring (typically $<10 \mu\text{M}$). Summer ammonium concentrations in the estuary were higher than concentrations observed at any other time of year. Average summer ammonium concentrations in the estuary were $15.3 \pm 8.5 \mu\text{M}$ ($n = 329$), and concentrations reached as high as $60 \mu\text{M}$ (7/28/2010 – 8/19/2010) (Fig. 3.4d). As with the high phosphate concentrations presented above, we have no reason to discount the very high ammonium measurements based on the quality control measures in place for determining obviously erroneous values.

Large ranges in silicic acid were seen throughout the year in the estuary (Fig. 3.4g). High silicic acid concentrations were from the river (filled light circles) and low concentrations were from the ocean (filled dark circles) throughout downwelling and upwelling periods (Fig. 3.4g). Silicic acid concentrations were never fully depleted in the estuary and typically remained $>30\mu\text{M}$.

4.2 Seasonal River and Ocean End Members at SATURN-03

The wide range of salinities observed at SATURN-03 (Fig. 3.4a) allowed for OEMS to be calculated (see Methods) during the summer. However, OEMS could not be calculated all year long because SATURN-02 salinity and temperature data was not available. To compare OEMs across seasons a salinity of 32.5 was used for all OEM calculations including summer.

Nitrate demonstrated conservative mixing behavior at SATURN-03 throughout the year, during both upwelling and downwelling conditions. The average OEM nitrate concentration during late winter was $4.9 \pm 3.9 \mu\text{M}$ compared to the REM of $41.9 \pm 4.9 \mu\text{M}$ (Fig. 3.5a). The nitrate OEM remained low in the spring, while the REM decreased to $14.1 \pm 1.2 \mu\text{M}$ (Fig. 3.5a). Summer upwelling caused the nitrate OEM to increase to $24.3 \pm 7.5 \mu\text{M}$, while the REM was at its lowest at $3.7 \pm 1.8 \mu\text{M}$ (Fig. 3.5a). During the winter, nitrate OEM concentrations dropped while REM concentrations increased to $25.8 \pm 4.1 \mu\text{M}$.

It should be noted that although the error in these calculations seems high, it was not a measure of the accuracy of the calculation, but an artifact of the highly dynamic system in which concentrations can vary greatly. There was a statistically significant difference between the TRC (SATURN-05) and the nitrate REM concentration (SATURN-03) for all seasons except spring (Fig. 3.5a). Late winter showed a statistically significant ($P = <0.001$) gain in nitrate from the river (SATURN-05) to the estuary (SATURN-03). During the summer ($P = <0.001$) and winter ($P = <0.001$), a statistically significant loss in nitrate was observed between the river (SATURN-05) and the estuary (SATURN-03) (Fig. 3.5a).

Using the “Nitrate: Change in River Concentration” method (see Methods), a gain of $10.4 \pm 4.5 \mu\text{M}$ nitrate was measured between SATURN-05 and SATURN-03 during late winter ($P = < 0.001$). There was no statistical difference in the nitrate REM concentration from SATURN-03 and the TRC nitrate concentration at SATURN-05 during the spring season ($P = 0.894$). A statistically significant loss in nitrate was observed from SATURN-05 to SATURN-03 during the summer ($1.7 \pm 1.9 \mu\text{M}$, $P = 0.005$). While this loss seems small, it was $32 \pm 37\%$ of the total riverborne nitrate and was equivalent to a loss of 8.8 ± 9.5 metric tons of nitrate per day based on the river discharge. A loss of $5.7 \pm 4.5 \mu\text{M}$ or $18 \pm 14\%$ nitrate was observed between SATURN-05 and SATURN-03 during the winter.

REM and OEM concentrations could only be calculated for phosphate during periods of upwelling. At other times of the year, phosphate did not vary significantly during estuarine mixing (Fig. 3.4e). Although there was not enough data from the river to statistically evaluate phosphate concentrations during the late winter, the TRC was the same ($0.7 \mu\text{M}$) as the EREM at SATURN-03 (Fig. 3.5b). Therefore, there was most likely no significant gain or loss of phosphate from the river to the estuary during late winter. A lack of data from the river during the spring and winter prevented a comparison of the TRC with the EREM at SATURN-03. Summer upwelling caused the phosphate OEM at SATURN-03 to increase to $1.8 \pm 0.3 \mu\text{M}$ (Fig 3.5b). During summer, when conservative mixing allowed for the calculation of REMs and OEMs, there was a statistically significant gain of $0.4 \pm 0.2 \mu\text{M}$ phosphate from the river (SATURN-05) to the estuary (SATURN-03) ($P = < 0.001$). This was equivalent to a gain of 4.7 ± 1.8 metric tons of phosphate per day based on the river discharge.

REM and OEM ammonium concentrations could not be calculated for any season because ammonium did not mix conservatively, thus the EREM and EOEM were used for all seasons (see methods). Large error bars for the EREM and EOEM indicated that ammonium concentrations in the estuary were highly variable throughout the salinity range (Fig. 3.5c). A lack of data from the river during late winter prevented any statistical analysis, but the EREM from SATURN-03 was higher than the TRC, suggesting that there may have been a slight increase in ammonium from the river to the estuary in late winter (Fig. 3.5c). During spring, one sample from the river was taken just after the peak of the spring bloom and had an unusually high ammonium concentration (Fig. 3.5c). This was the only sample collected in the river during 2010 that was greater 3 μM . Thus, it was most likely not representative of the spring time period. The largest and most statistically significant ($P = <0.001$) difference between the TRC and the EREM was in the summer when the ammonium EREM (SATURN-03) was 15.5 ± 9.4 μM and the TRC (SATURN-05) was 0.3 ± 0.2 μM (Fig. 3.5c).

4.3 Summer 2010 at SATURN-03

More than three hundred nutrient measurements taken over 1.5 spring/neap tidal cycles from 7/28/2010 to 8/19/2010 and this time series revealed the dynamic variability of the Columbia River estuary (Fig. 3.6). The salinity ranged from about 5 to 30 over almost every tidal cycle (Fig. 3.6a and b). Temperature ranged from about 10-17° C with the high temperatures originating from the river, and low temperatures from the ocean (Fig. 3.6c). Higher turbidity was observed during spring tides than the neap tides (Fig. 3.6d). Higher concentrations of both nitrate and phosphate were observed during spring tides than during neap tides (Fig. 3.6g and h). Slightly smaller variations in salinity,

nitrate, and phosphate were observed during neap tides from 8/1/2010 to 8/5/2010 (Fig. 3.6g and h). Ammonium did not show consistent conservative mixing throughout the summer time period (Fig. 3.6i), but a more conservative mixing trend was observed between 8/6/2010 and 8/9/2010 than during any other time. During this time, river-like (low salinity) ammonium concentrations were lower than ocean (high salinity) concentrations (Fig. 3.6i). Silicic acid displayed some conservative mixing during the summer. Two large spikes from 7/31/2010 to 8/2/2010 and from 8/9/2010 and 8/12/2010 were observed, during which silicic acid concentrations reached $>120 \mu\text{M}$ in low salinity water (Fig. 3.6j). These spikes correspond to the same two periods of increased ammonium (Fig. 3.6i and j).

One grab sample taken during this time agreed with both nitrate and silicic acid (Fig. 3.6g and j). Unfortunately, a gap in the phosphate data prevented comparison (Fig. 3.6h). Ammonium was the only parameter in which the grab sample did not match the in situ APNA data. This discrepancy may be due to a difference in filter size and the adsorption of ammonium to particles between 0.7 and $10 \mu\text{M}$ (Fig. 3.6j). Nutrient data from other grab samples (filtered to $0.7 \mu\text{M}$) collected in the Columbia River estuary confirmed that concentrations in Baker Bay were typically $> 10 \mu\text{M}$ and could have reached as high as $60 \mu\text{M}$ during late summer (Lydie Herfort personal communication and CMOP Combined Campaign Water Sample Database).

Figure 3.7 illustrates REMs and OEMs for nitrate and phosphate as well as the nitrate:phosphate ratio from SATURN-03 during the summer. The combination of high resolution data, a large salinity range, different REM and OEM concentrations, as well as conservative tidal mixing were all necessary for this calculation. We have demonstrated

that we can calculate REM and OEM with confidence, as the majority of the correlation coefficient values (R^2) associated with the CMR used to calculate REMs and OEMs were >0.90 (Fig. 3.7a and b).

High R^2 values and low standard error of the regression (error bars) (Zar 1984) for both nitrate and phosphate CMR indicated that end member concentrations were highly conservative and accurate (Fig 3.7a and b, see Fig. 3.3 for graphical example of calculation). Data with R^2 values below 0.75 were not used in calculations, but are shown in Fig. 3.7. An average standard error of regression for all acceptable summer nitrate regressions was $1.7 \mu\text{M}$. Phosphate had an average standard error of regression of $0.07 \mu\text{M}$ for all regressions with acceptable correlation coefficients.

The REM for both nitrate and phosphate remained relatively constant throughout the neap-spring tidal cycle compared to the OEM (Fig. 3.7a and b). Nitrate OEMs ranged from $9.7 \mu\text{M}$ during the neap tides to $38.6 \mu\text{M}$ at the peak of the spring tides (Fig. 3.7a). The phosphate OEM decreased during the neap tide (Fig. 3.7b), but did not decrease in a 16N:1P Redfield proportion (Redfield et al. 1963), which caused the nitrate:phosphate ratio to drop during the neap tides (8/1/2010 – 8/9/2010) (Fig. 3.7c). The OEM nitrate:phosphate ratio was higher than the REM nitrate:phosphate ratio during almost every tidal cycle (Fig. 3.7c). The highest REM and OEM nitrate:phosphate ratios occurred during spring tides, during which the ratio reached a value of ~ 16 , while the lower ratios persisted during neap tide periods (Fig. 3.7c).

4.4 Neap Tide Versus Spring Tide Outwash at RM-17

Surface, middle, and bottom samples from a neap and spring tidal outwash study at RM-17 aboard the R/V Wecoma gave CMR for nitrate, phosphate, and ammonium

(Fig. 3.8). The nitrate REM concentration during the neap tide outwash was 1.6 ± 0.2 μM (Fig. 3.8a). The outwash study during a spring tide gave a nitrate REM concentration of 2.6 ± 0.03 μM (Fig. 3.8b). Phosphate REM concentrations calculated for both neap and spring tidal outwashes were at the MDL of the analysis method of ~ 0.2 μM (Fig. 3.8c and d). Ammonium displayed a more conservative behavior during the neap tide outwash than during the spring tide outwash, with R^2 values of 0.95 and 0.78 respectively (Fig. 3.8e and f). The ammonium REM for the neap tide outwash was 1.6 ± 0.2 μM , while for the spring tide study the ammonium REM concentration was 2.8 ± 0.4 μM . However, an asymptotic behavior of ammonium at higher salinities caused the CMR to yield an artificially high REM (Fig. 3.8c). The lowest salinity values during the spring tide had ammonium concentrations near ~ 0.8 μM increasing to 4-8 μM by a salinity of 10 and remained between 4-8 μM from salinities of 10 and 25 (Fig. 3.8c).

5.0 Discussion

The Columbia River's natural flow was severely altered between 1933 and 1984 by the building of 21 major dams for hydropower, and water impoundments for irrigation and navigational use. These alterations significantly decreased river discharge during spring freshets and allowed for an increased flow during drier times of the year. Ecological impacts of the dams include: a possible increase in water temperature by $\sim 1^\circ$ C (Moore, 1968), reduced suspended particulate matter (van Winkle, 1914; Sullivan et al. 2001), and an increase in phytoplankton growth (Sullivan et al. 2001). Whitney et al. (2005) suggested that the building of dams and altering of seasonal discharge patterns has effected coastal dissolved inorganic nutrient concentrations as far away as the Alaskan Gyre. Nutrient data does not extend back as far as other ecological data, but seasonal

nutrient patterns in the Columbia River have been documented over the last decade (USGS).

Nutrient concentrations in the river reach their lowest during late summer due to low river flow and consumption through high productivity throughout the spring and summer months (Sullivan et al. 2001). Sullivan et al. (2001) and this study showed that by the end of the calendar year, nutrient concentrations in the river had increased. This pattern was seen in low salinity water and REMs from SATURN-03 (Fig. 3.4 and 3.5). According to Redfield ratio (16N:1P) (Redfield et al. 1963), phytoplankton growth in the Columbia River should be limited by phosphate. However, phosphate was detected throughout the summer and was never fully exhausted in the river. Ammonium remained low in the river throughout the year. Thus, nitrate was the dominant source of Nr available for phytoplankton assimilation in the river.

Seasonal patterns of nutrients in the Columbia River can yield valuable information, but quantifying nutrient transformations within a tidally dynamic estuary is much more difficult and requires long term high resolution monitoring to decipher cause-effect. This study utilized a unique approach to confirm nutrient transformations from the river to the ocean, in which a time series of CMRs from multiple fixed locations throughout the estuary provided a REM, which was compared to the TRC to determine if sources or sinks existed between locations.

5.1 River to Ocean Nutrient Gradients and Transformations

While many estuaries have a residence time of 0.5-3 months or longer which allows for water properties to change (Garnier et al. 2010; Etcheber et al. 2007), the Columbia River estuary is relatively unique in that the residence time is typically less

than a few days (Sommerfield 1999; Bottom et al. 2005). Despite this fact, dissolved inorganic nutrient transformations were observed along the lower 53 miles of the Columbia River.

5.1.1 Nitrate

High resolution temporal and spatial data gave the first insight into inorganic nutrient gradients across all three Reaches of the lower Columbia River. During the neap and spring tidal outwash studies conducted at RM-17 on 8/4/2010 and 8/8/2010 respectively, high resolution data was available at three locations. The river (SATURN-05, Reach C) provided a TRC, the upper estuary (RM-17, Reach B) yielded insight into processes of the fresh water tidal flats of Cathlamet Bay, and the lower estuary (SATURN-03, Reach A) revealed the final transformation of nutrients before entering the coastal plume and the significance of estuarine processes.

For the neap tide outwash study, the daily average nitrate concentration at SATURN-05 (Reach C) from 8/3/2010 was $4.3 \mu\text{M}$ (Table 3.2). Nitrate REM concentrations on 8/4/2010 from RM-17 (Reach B) and SATURN-03 were $1.6 \pm 0.2 \mu\text{M}$ and $1.2 \pm 0.4 \mu\text{M}$ respectively (Fig. 3.8a, Fig. 3.7a, and Table 3.2). Note that there was a one day lag between the SATURN-05 and RM-17/SATURN-03 concentrations to account for water transit time. The difference between nitrate REMs calculated from SATURN-05 (Reach C) to RM-17 (Reach B) was greater than the difference between RM-17 (Reach B) and SATURN-03 (Reach A). This pattern could indicate that during the neap tide outwash, a small amount of nitrate was removed from the water column in the fresh water tidal flats (Reach B) and not in the salt water estuary (Reaches A and B).

During the spring tide outwash study the two day average nitrate concentration at SATURN-05 was $\sim 3.2 \mu\text{M}$ from 8/7-8/8/2010 (Table 3.2). Nitrate REM concentrations on 8/8/2010 from RM-17 and SATURN-03 were $2.6 \pm 0.03 \mu\text{M}$ and $2.6 \pm 0.7 \mu\text{M}$ respectfully (Fig. 3.8a, Fig. 3.7a, and Table 3.2). Unlike the neap tide outwash, the loss of nitrate during the spring tide outwash seemed to all occur in the fresh water tidal flats (Reach B).

Based on the daily average nitrate concentration at SATURN-05, REM concentrations at SATURN-03, and river discharge, we were able to calculate the total percentage of nitrate gained or lost between the river (SATURN-05, Reach C) and the estuary (SATURN-03, Reach A). The percentage of nitrate gained/lost varied greatly between tidal cycles, from a gain of 71% to a loss of 100%. During the neap tide outwash study on 8/4/2010 a total of 15.4 metric tons of inorganic nitrate was lost from the water column per day ($1.1 * 10^9 \text{ mol NO}_3^- \text{ day}^{-1}$, 73%) between SATURN-05 (Reach C) and SATURN-03 (Reach A). During the spring tide outwash study, an average of 5.2 metric tons of nitrate per day ($3.7 * 10^8 \text{ mol NO}_3^- \text{ day}^{-1}$), or 28% of the total inorganic nitrate was lost between SATURN-05 and SATURN-03.

In both the neap and spring tide outwash studies nitrate was removed between the river (Reach C) and the estuary (Reach A) which could have been due to denitrification, DNRA, or assimilation by phytoplankton in the fresh water tidal flats or water column (Reach B). Studies have shown that water residence time can have a large impact on the rate of Nr removal from a system (Galloway et al. 2003; Kelly et al. 1987). Nixon et al. (1996) found that estuaries with residence times between 0.5 and 12 months should export 35-70% of Nr entering the estuary. With residence time of water in the Columbia

River estuary typically less than a few days, and the residence time of water from SATURN-05 to the coastal river plume only a few days (Sommerfield 1999; Bottom et al. 2005), an average summer reduction in nitrate of $33 \pm 38\%$ ($1.7 \pm 1.9 \mu\text{M}$) from the river to the estuary was significant ($P = 0.005$) and demonstrated that the Columbia River estuary was acting as a “bioreactor” despite its short water residence time (Fig. 3.5a). Although we cannot discern the process of nitrate removal, we can identify the area of removal as the fresh water tidal flats of the Columbia River (Reach B).

It is known that water residence time in the Columbia River estuary increases during the neap tidal phase compared to the spring tidal phase (Roegner et al. 2011). Nitrate CMRs for both RM-17 (Fig. 3.8a and b) and SATURN-03 (data not shown) had a lower slope during the neap tide outwash than during the spring tide outwash. A lower slope could indicate a poorly flushed system in which more nitrate was removed before being exported to the plume. It could also indicate a “shallowing” of the coastal water entering the estuary could have caused a shift from high nutrient-rich, upwelled waters to somewhat old nutrient-depleted, surface water which could also account for the decrease in the slope of the CMR during the neap tide outwash. This “shallowing” of coastal water entering the estuary or reduction in the ocean nitrate concentration was clearly seen in the temporal trend of the nitrate OEM at SATURN-03, where there was a clear depression during the neap tidal phase (Fig. 3.7a). This pattern was also seen in the phosphate as well as the nitrate:phosphate ratio (Fig. 3.7b and c).

Regardless of the percentage of riverborne nitrate removed in the estuary, it was insignificant compared to the amount of nitrate entrained into coastal surface waters through upwelling. The average daily river discharge during the summer time period

studied was $3.8 * 10^8 \text{ m}^3/\text{day}$, and had an average nitrate concentration of $5.0 \text{ }\mu\text{M}$ (daily average from 7/28/2010 – 8/19/2010 at SATURN-05). Thus, an average of $1.9 * 10^6 \text{ mol}$ nitrate per day would be exported to the coastal plume not accounting for estuarine removal. To calculate an upwelling equivalent a deep water coastal nitrate concentration of $35 \text{ }\mu\text{M}$ was assumed based on measurements from a nearby coastal transect. Assuming that upwelling occurred at a rate of $8.6 * 10^6 \text{ m}^3/\text{day}/100\text{m}$ (Bruland et al. 2008), the average daily export of nitrate not accounting for estuarine removal was or equivalent to 0.6 km of upwelled coastline (range 0.4 to 1.0 km). The estuary removed an average equivalent of 0.2 km of upwelled coastline (range 0.3 to -0.9 km) or $6.4 * 10^5 \text{ mol}$ nitrate per day. Therefore, the amount of nitrate delivered from the river during summer compared to the amount of nitrate entrained through upwelling would have little effect in the coastal ocean. However, nitrate removal may have a more substantial impact on the ecosystem within the estuary.

5.1.2 Phosphate

Phosphate REM concentrations calculated at RM-17 from both neap and spring tide outwash studies (Fig. 3.8c, d, and Table 3.2), and TRC from SATURN-05 (Table 3.2) were at or below our detection limits ($0.2 \text{ }\mu\text{M}$). The REM concentrations from the neap and spring tide outwash studies from SATURN-03 were 0.7 ± 0.3 and $0.6 \pm 0.1 \text{ }\mu\text{M}$ respectfully (Fig. 3.7b, Table 3.2). With no change observed in phosphate concentration between SATURN-05 (Reach C) and RM-17 (Reach B) during either neap or spring tidal outwashes, the statistically significant ($P = < 0.001$) summer average gain of $\sim 0.4 \pm 0.2 \text{ }\mu\text{M}$ phosphate most likely occurred between RM-17 (Reach B) and SATURN-03 (Reach

A) (Fig. 3.5b). Particle desorption, remineralization, and ETM processes could all have a large effect on phosphate concentrations throughout the river and estuary.

The adsorption capacity of phosphate decreases dramatically as the salinity increases. Studies in many estuaries have shown that phosphate desorption occurs in the transition zone from river to ocean (Garnier et al. 2010; Beusekom and Brockmann 1998; Fox et al. 1986). Phosphate can be desorbed from particles within a few minutes to a few hours after coming in contact with high salinity water (Froelich 1988). Low salinities (0-5) were not observed at SATURN-03 at 8.2 m depth, but low salinity water was observed at RM-17. Data from RM-17 showed little salinity effect at the lower end of the CMR during both neap and spring tidal outwash studies (Fig. 3.8c and d), indicating that phosphate desorption may not be a significant process in the lower Columbia River.

Typically, studies on estuarine remineralization and the release of inorganic nutrients into the water column focus on the release of ammonium. According to Redfield ratio (16N:1P) (Redfield et al. 1963), the increase in phosphate for small inputs of ammonium would be too small to be measured. However, ammonium inputs in the Columbia River were large enough that Redfield ratio increases in phosphate could be detected.

Studies from the East Coast of the United States indicate that in shallow estuarine and coastal sediments, phosphate concentrations can reach 150-300 μM within the first few centimeters of sediment (Hopkinson et al. 2001; Klump and Martens 1981). Although nutrient studies on sediment have not been conducted in the Columbia River, this study suggests that high levels of phosphate in subsurface sediment were likely, representing a possible source to the estuary during late summer. This sediment was

most likely from the lateral bays because most of the main channel of the Columbia River is made up of bedrock, large gravel, and sand (Whetten et al. 1969). Small and Prahl (2004) suggested that large quantities of organic matter were hydrodynamically trapped and carried ocean-ward in the ETM (conveyor belt effect) in the Columbia River estuary during summer low flow spring tide periods. If so, then it was possible that during this study, the ETM conveyor belt effect re-suspended, trapped, and remineralized organic material from lateral bay sediments, which may have released high concentrations of remineralized phosphate into the water column.

5.1.3 Ammonium

At RM-17, ammonium displayed a more conservative behavior during the neap tide outwash study than during the spring tide outwash study (Fig. 3.8e and f). During the neap tide outwash study a sharp salinity gradient caused under sampling from salinities 5 to 15, which may have caused the regression to appear more linear (Fig. 3.8e). The spring tide outwash study CMR appeared to have an asymptotic behavior and suggests estuarine processes may be influencing concentrations as far up river as RM-17 (Fig. 3.8f). During the neap tide outwash, low ammonium concentrations persisted from a salinity of 0-5, while during the spring tide study concentrations increased from $<1 \mu\text{M}$ to $>4 \mu\text{M}$ from salinities 0-5 (Fig. 3.8e and f). This difference could indicate that during spring tides, a more turbid estuary disturbed the sediment and released ammonium. Although end members could not be calculated for the majority of the summer ammonium data at SATURN-03, ammonium concentrations at SATURN-03 were higher than those observed at SATURN-05 and RM-17 (Fig. 3.5c).

Studies conducted at SATURN-05, RM-17, and SATURN-03 in the summer of 2010 revealed a slight increase in ammonium (0.4 - 1.2 μM) from SATURN-05 (Reach C) to RM-17 (Reach B), which most likely occurred in the fresh water tidal flats of Reach B (Fig. 3.8e, f, and Table 3.2). Even though a small increase in ammonium in Reach B (0.4-1.2 μM) was observed, according to the Redfield ratio, an increase in phosphate would not have been noticeable in this location (0.03-0.08 μM) due to instrument MDLs.

Ammonium concentrations at SATURN-03 were higher during the two spring tide/high turbidity time periods than during the neap tide/low turbidity time periods (Fig 3.6d and j). After a few days of lower turbidity water in the estuary (8/1/2010 – 8/9/2010), ammonium appeared to revert back to a tidal pattern (8/6/2010 – 8/9/2010) until turbidity increased on 8/10/2010. This correlation of ammonium and turbidity suggests that ammonium may have been released from the sediment during periods of high turbidity associated with spring tides. SATURN-03 and RM-17 are consistent in the suggestion of larger inputs of ammonium into estuarine waters during high turbidity spring tide periods rather than during neap tide periods (using different instrumentation with different chemical methods). However, a longer time series is necessary to discern the importance and correlation between turbidity and ammonium in the lower Columbia River estuary.

During the summer, ammonium accounted for ~10% of the N_r available in the river (SATURN-05, Reach C) (Table 3.2). In the upper salt water estuary, river water enriched with ammonium quickly mixed with salt water from the estuary. In the lower salt water estuary, ammonium concentrations accounted for as much as 85% and an average of ~50% of the available N_r (Fig. 3.5c). A plume survey conducted from

8/6/2010 to 8/8/2010 confirmed this result, with ammonium accounting for ~42% of Nr in the surface plume, but only ~16% in the bottom plume (unpublished results). This suggests that there was more than twice as much Nr available in the estuary and surface plume than was accounted for by measuring nitrate alone. Therefore, it is vital that not only nitrate, but ammonium be taken into account when calculating the Nr flux from the Columbia River to the coastal zone.

The implications of a high ammonium:nitrate ratio in the estuary and surface plume are not clear. However, Kudela et al. (2010) indicated that nutrients from the Columbia River can circulate in the Columbia River plume on the order of 3-4 days and maintain phytoplankton biomass within the plume during periods of suppressed upwelling. With coastal waters in the vicinity of the Columbia River plume being nitrogen (nitrate) limited (Bruland et al. 2008; Kudela and Peterson 2009), an additional source of nitrogen (ammonium) from estuarine remineralization may be significant enough to sustain a phytoplankton population in surface plume waters during periods of suppressed upwelling the late summer.

High ammonium concentrations in the estuary and surface plume suggest that the ammonium source was greater than the sink. Moeller (2011) showed rates of nitrification in the water column at SATURN-05 on 8/11/2010 were low ($493 \pm 430 \text{ nM day}^{-1}$). With an average ammonium concentration in the estuary $15.5 \pm 9.4 \text{ }\mu\text{M}$, and a rate of water column nitrification of $0.493 \pm 0.430 \text{ }\mu\text{M day}^{-1}$, it would take more than 30 days to convert the available ammonium to nitrate assuming that all sources of ammonium were to cease completely. Thus, nitrification in the estuary water column was most likely

insignificant to the relative concentration of ammonium and nitrate being exported from the Columbia River to its plume.

5.2 Denitrification and DNRA

A significant loss of inorganic nitrate was observed from the river (Reach C) to the upper salt water estuary (Reach B) suggesting denitrification or DNRA may be removing inorganic nitrate from the water column in the fresh water tidal flats (Reach B). While nitrate removal was significant in the fresh water reaches of the river, little nitrate removal was observed in the salt water estuary (Reach A and B). Despite the short residence time of water within the estuary, the percent oxygen saturation remained below 100% throughout the summer 2010 time period studied during both high and low tides (Fig. 3.6f), which suggested high biological activity in the water column and sediment. Little nitrate removal and low oxygen in the estuary suggested that other processes such as remineralization may be occurring. Roegner et al. (2011) found evidence of high salinity low oxygen water entering the estuary during upwelling periods. If low oxygen water continues to enter the estuary, it is possible that denitrification (a low oxygen process) may increase. What is not clear yet is: what role nutrient loading, phytoplankton blooms, and remineralization have on the oxygen consumption in the lower estuary. Further studies should be done in the lateral bays on sediment cores themselves to determine rates of denitrification, DNRA, and to identify oxygen consumption due to estuarine nutrient loading.

Ammonium and phosphate concentrations increased from the river to the estuary at a ratio greater than 16N:1P (Redfield et al. 1963), meaning that there was more ammonium available in the estuary than could be accounted for through remineralization

alone. DNRA may have converted some nitrate into ammonium which would have increased ammonium concentrations without increasing phosphate concentrations. Although this data set did not allow for the calculation of denitrification or DNRA sediment flux rates, the more valuable asset of this work was being able to identify and quantify the transformations of inorganic nutrient ratios within the dynamic transition zone from the river to the plume, as significant changes in nutrient ratios can affect the assemblage of phytoplankton in the estuary and plume.

5.3 Remineralization Within the Estuarine Turbidity Maximum (ETM)

The Columbia River is a productive system in the spring and summer in which large quantities of particulate organic carbon (POC) are present (Sullivan et al. 2001). Small and Prahl (2004) identified bottom waters in the Columbia River estuary as having a higher POC concentrations than the surface on a per unit volume basis due to suspension and particle trapping of sediment within the estuary (ETM). Small and Prahl (2004) suggested that in the lower Columbia River estuary, selective particle trapping and recycling occurs during neap stratification, while particle erosion and transport occurs during spring tides. In this study, we observed high concentrations of inorganic ammonium and phosphate in the lower estuary (Reach A) throughout the late summer. Abnormally high concentrations of ammonium and silicic acid were observed at SATURN-03 on 8/1/2010 and 8/11/2010 and appeared to be correlated with high turbidity spring tide periods (Fig. 6d, i, and j). It was possible that a large portion of the increased ammonium, phosphate, and silicic acid observed only in the lower estuary (Reach A) during the summer of 2010 was remineralized or dissolved within the ETM during neap tides and released during spring tides.

5.4 Lateral Bay Remineralization

Our data suggests that lateral bays (i.e. Baker Bay and Youngs Bay) in the Columbia River may be an important site for nutrient transformation processes such as remineralization. Although the main channel is mostly bedrock and sand, the lateral bays in the lower Columbia River estuary are mostly fine grained sediment (McIntire and Amspoker 1984; Whetten et al. 1969). McIntire and Amspoker (1984) found that the most abundant plant found in the lateral bays was microalgae, which were mostly made up of benthic diatoms. The pairing of high ammonium and silicic acid concentrations (Fig. 6i and j) in the lower estuary (Reach A) during spring tides suggests sources other than ETM remineralization. We propose that the high silicic acid concentrations were from remineralization and dissolution of benthic diatom dominated lateral bays. Strong currents, highly turbid water, and a well-mixed water column during spring tides may have agitated lateral bay sediments releasing dissolved and remineralized inorganic ammonium and silicic acid into the water column, which would have only been visible down river of the lateral bays (SATURN-03). Although our data set cannot confirm that the remineralization signal observed was influenced by the lateral bays, evidence suggests this is the case.

Nitrate:phosphate ratios further support strong remineralization within the estuary. We identified a river (SATURN-05) nitrate:phosphate ratio of 24.8 during nitrate depleted summer months. REMs from the estuary (SATURN-03) revealed a decrease from 24.8 in the river to an average ratio of 6.4 in the estuary (Fig. 3.7). Although the reduction in nitrate identified between the river (SATURN-05) and estuary (SATURN-03) contributed to the nitrate:phosphate ratio reduction, the nitrate decrease

was not the major contributor to the ratio decrease. The significant gain in phosphate from the river to the estuary was the main cause for the ratio reduction, indicating a strong source of remineralization within the estuary.

6.0 Conclusions

Despite a short water residence time in the Columbia River estuary, we identified nutrient transformations from the lower Columbia River to the coastal plume during late summer of 2010. Over 23 days, more than three hundred in situ measurements for each inorganic nutrient (nitrate, phosphate, ammonium nitrite, and silicic acid) were generated at SATURN-03 by sampling on an hourly time scale. With large salinity ranges and high frequency nutrient data in the lower estuary, we calculated CMRs for each ebb tide. High correlation coefficient values (R^2) from CMRs allowed for REMs and OEMs to be confidently compared between locations. Along with the sheer size of this data set, shipboard measurements added spatial coverage in the estuary which facilitated conclusions that would have required significant resources (many transects) via traditional methods. Comparing REM and OEM calculations from more than one location allowed us to identify where nutrient transformations occurred along the Columbia River's salinity gradient. This novel technique proved an effective method to elucidate the biogeochemical dynamics and transition zones that is less resource intensive.

Evidence suggested a significant nitrate loss in the fresh water tidal flats (Reach B), which may be accounted for through denitrification, phytoplankton assimilation or conversion of nitrate to ammonium by DNRA. Ammonium accounted for only ~10% of the Nr in the river (Reach C), but accounted for ~ 50% of the Nr in the salt water estuary

(Reach A), as well as the surface coastal plume. While ammonium and phosphate concentrations were elevated throughout the late summer in the lower estuary, high turbidity spring tide periods at SATURN-03 yielded abnormally high ammonium and silicic acid concentrations. We suggested that these elevated inorganic nutrient concentrations resulted from remineralization of organic matter within the ETM and/or lateral bays. Increased concentrations of ammonium, silicic acid and phosphate in the lower estuary suggested high rates of remineralization, and that the estuary was acting as a “capacitor” for organic material. In other words, organic-rich material that accumulates in the estuary throughout the year is remineralized in the estuary and being transported to the coastal plume. Although we have identified significant nutrient transformations within the estuary, significantly more research needs to be done to completely understand the full complexity of nutrient transformations identified in this study and their impacts on the estuarine and coastal food webs.

7.0 Acknowledgments

We are indebted to Oregon Health & Science University and the National Science Foundation (NSF) Science and Technology Center for Coastal Margin Observation and Prediction, specifically the field and cyber teams, as well as our summer intern Ezra-Mel Pasikatan. This research was supported through the National Science Foundation cooperative agreement OCE-0424602 and the M.J. Murdock Charitable Trust. We would like to thank the captain and crew of the R/V Wecoma as well as the chief scientist Frederick Prah. We are also grateful to WET Labs for the use of data from their pilot study in the Columbia River, under NSF contract OCE-0838099.

8.0 Figures

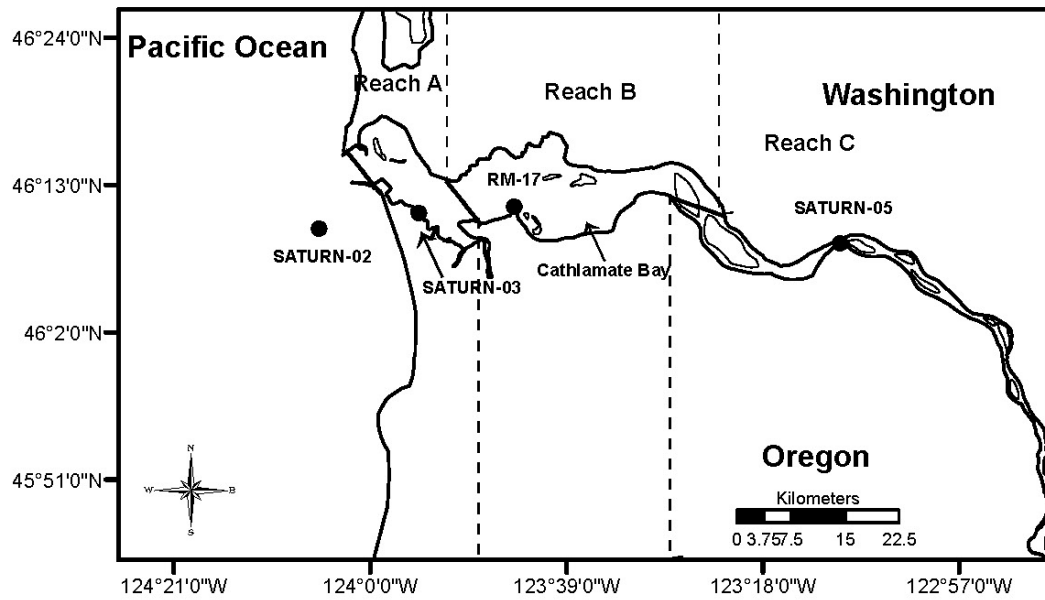


Figure 3.1. A map of the lower Columbia River and coastal Pacific Ocean showing the location of SATURN-05, RM-17, SATURN-03, and SATURN-02. Separations represent Reach boundaries. Reach C: lower river, Reach B: fresh water tidal flats and upper salt water mixing zone, Reach A: salt water mixing zone and estuary entrance.

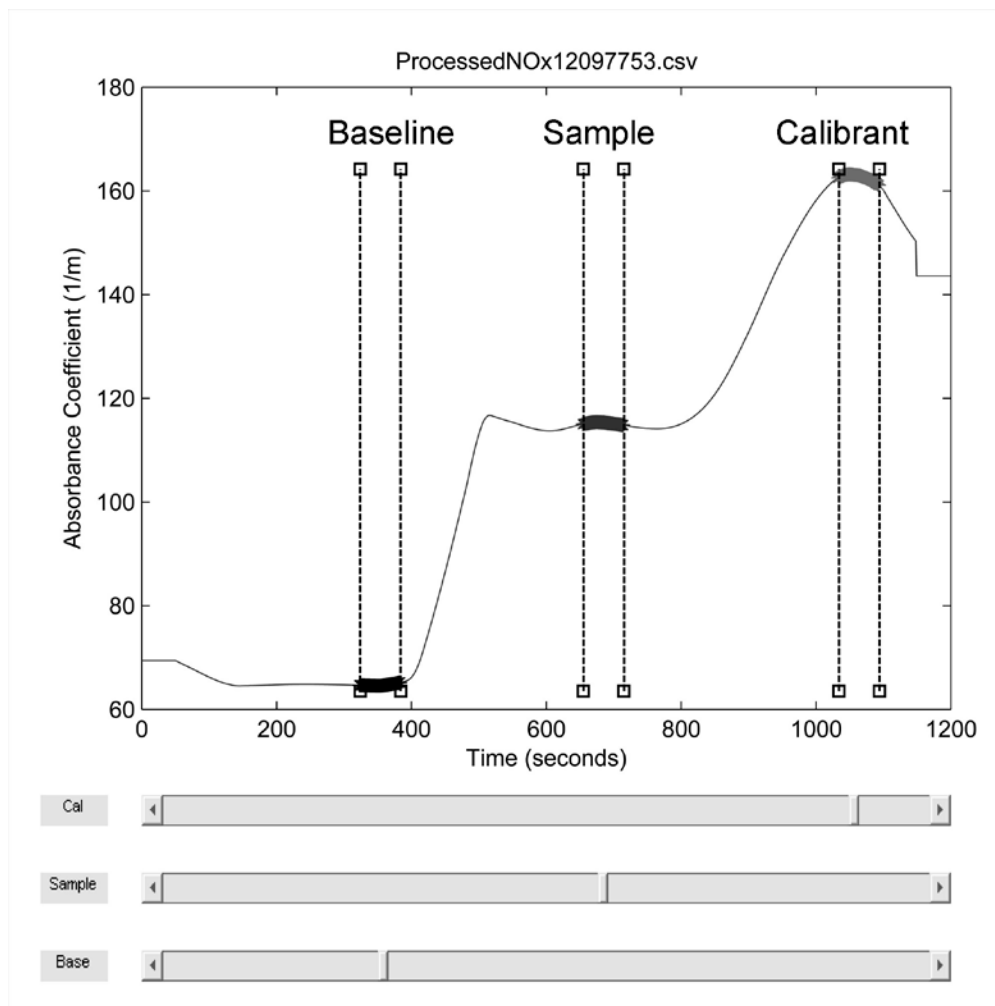


Figure 3.2. An example of APNA in situ data showing baseline, sample and standard addition calibration spike locations identified by bolded line and vertical dashed lines.

Elapsed time (seconds) versus the calculated absorption coefficient (1/m). The absorption coefficient was calculated using the relationship $\text{Absorbance} = -\log(e^{-\alpha x})$ in which x is the path length and α is the absorption coefficient. Slider bars under the plot allow the user to manually move the location of the baseline, sample, and calibrant.

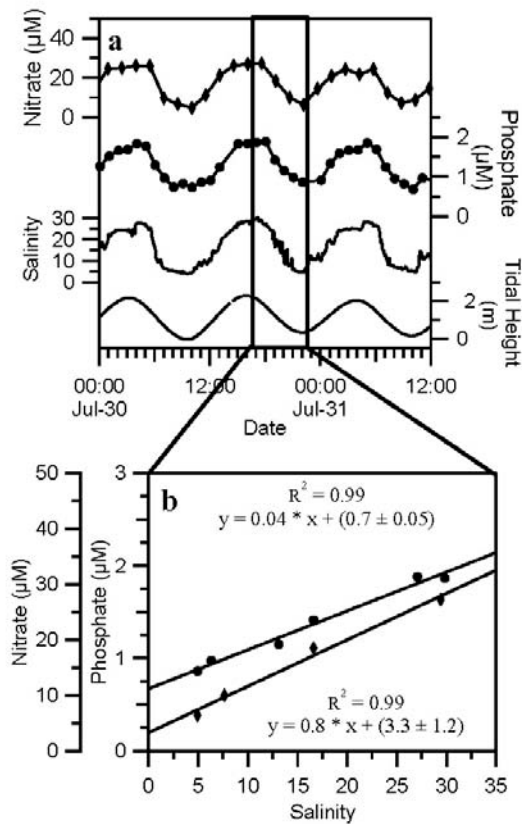


Figure 3.3. An example of a regression of high resolution nitrate (APNA), phosphate (Cycle-PO₄) and salinity data from mid water (8.2 m) at SATURN-03 showing how the river and ocean end members were calculated. **a** Time series of nitrate, phosphate, salinity and tidal height from July 29, 2010 to July 31, 2010. \bullet : individual phosphate measurements, \blacklozenge : individual nitrate measurements. Salinity measurements were taken approximately every 3 minutes. **b** Conservative mixing regressions (CMR) for nitrate and phosphate used to calculate river and ocean end members (REM and OEM) from one ebb tide. Conservative mixing regression includes the regressions intercept \pm one standard deviation.

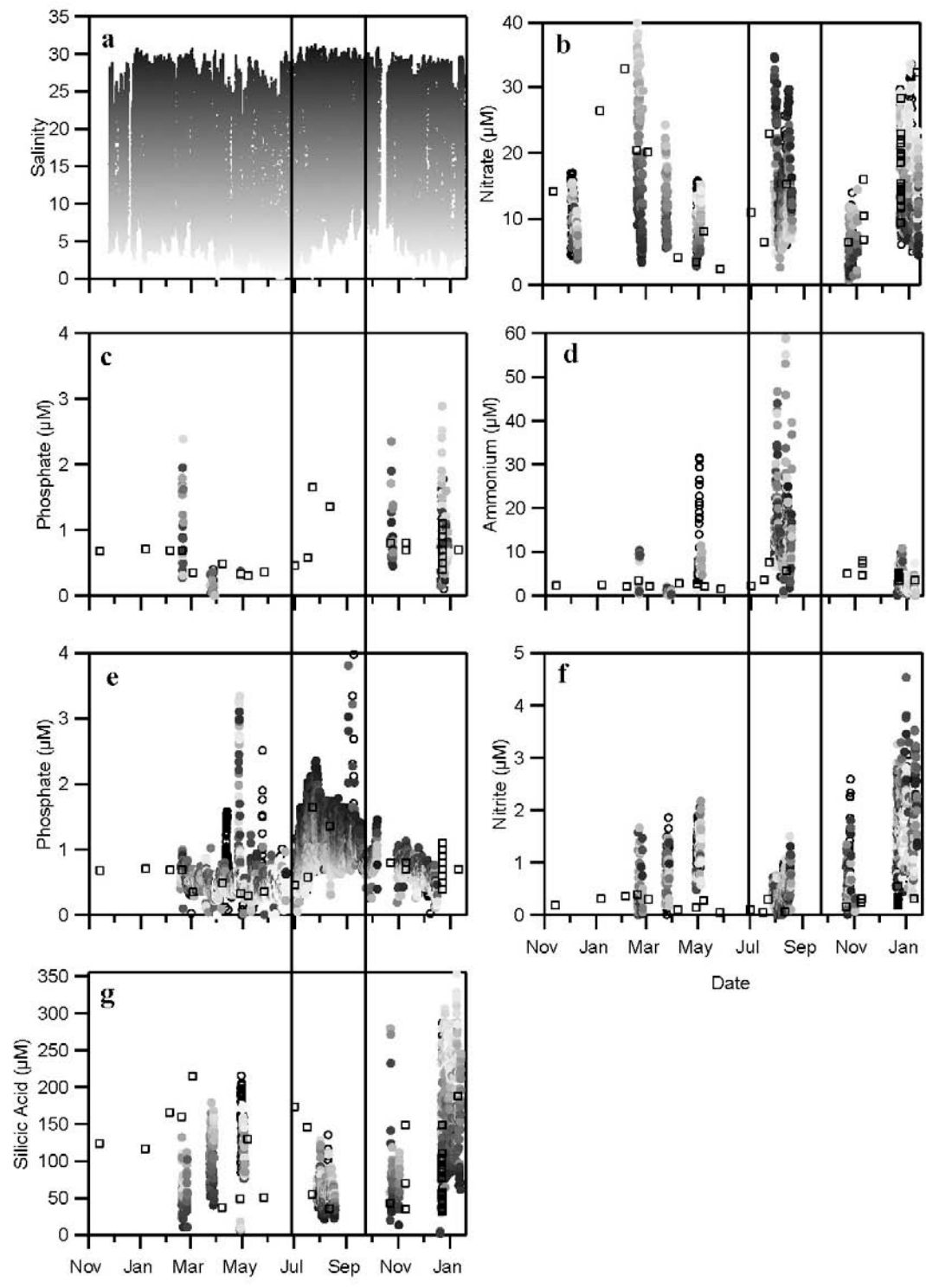


Figure 3.4. High resolution nutrient data from mid-water (8.2 m) at SATURN-03 shaded by salinity from Nov. 2009 to Jan. 2011. ●: (filled circles) individual in situ measurements shaded by salinity where samples associated with low salinity water are shaded light gray and samples associated with high salinity water are shaded dark gray, ○: (open circles) in situ measurements that did not have a corresponding salinity, □: laboratory analyzed grab samples. **a** is salinity, **b, c, d, g, and f** are nutrients from the APNA and **e** is phosphate from the Cycle-PO4. Vertical separations delineate downwelling and upwelling phases. Note: shifts in downwelling/upwelling phases can occur on a much finer scale, and these lines are just a guide to distinguish patterns in seasonal nutrient variability.

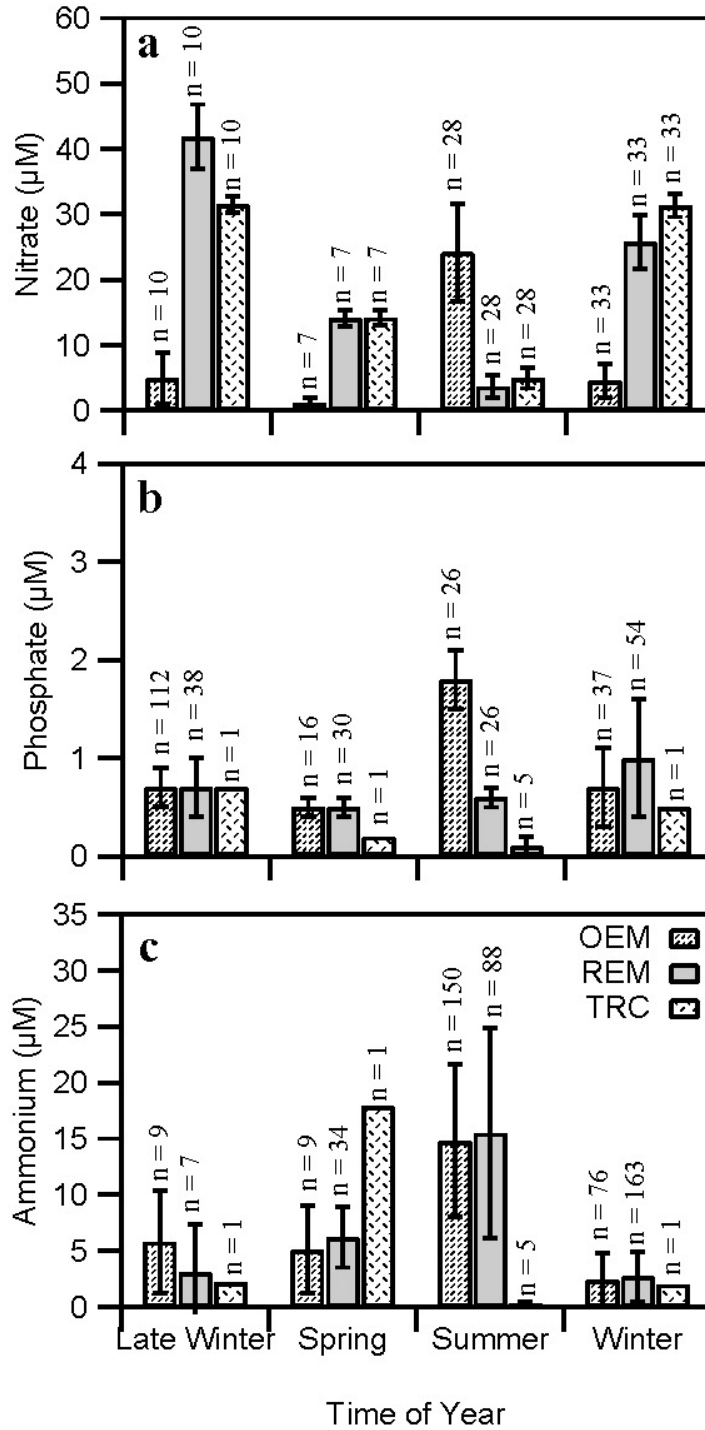

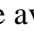
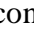


Figure 3.5. Average nutrient concentrations during different seasons from river and ocean end members as well as the true river concentrations (SATURN-05). Late winter was from Feb. 18, 2010 to Feb. 25, 2010. Spring was from Apr. 28, 2010 to May 4, 2010. Summer was from Jul. 28, 2010 to Aug. 18, 2010. Winter was from Dec. 21, 2010 to Jan. 12, 2011. : Ocean End Member (OEM) from SATURN-03. If Conservative Mixing Regressions (CMR) were linear ($R^2 > 0.75$) end members were calculated and averaged for a salinity of 32.5. If CMRs were not linear ($R^2 < 0.75$) the estimated ocean end members were averaged (EOEM) (salinities >20). : River End Member (REM) or if the nutrient was not conservative all nutrient data with salinities <10 were averaged. If mixing was conservative REMs were calculated and averaged. : data from SATURN-05 and considered the True River Concentration (TRC). Nitrate values were averaged over the time period from the SUNA. Phosphate and ammonium concentrations were from grab samples taken during each of the seasons. n was the number of data points averaged or end members from CMRs averaged. The error bars represent the standard deviation of the data collected; therefore, are representative of the variability in the system and not a measure of measurement accuracy.

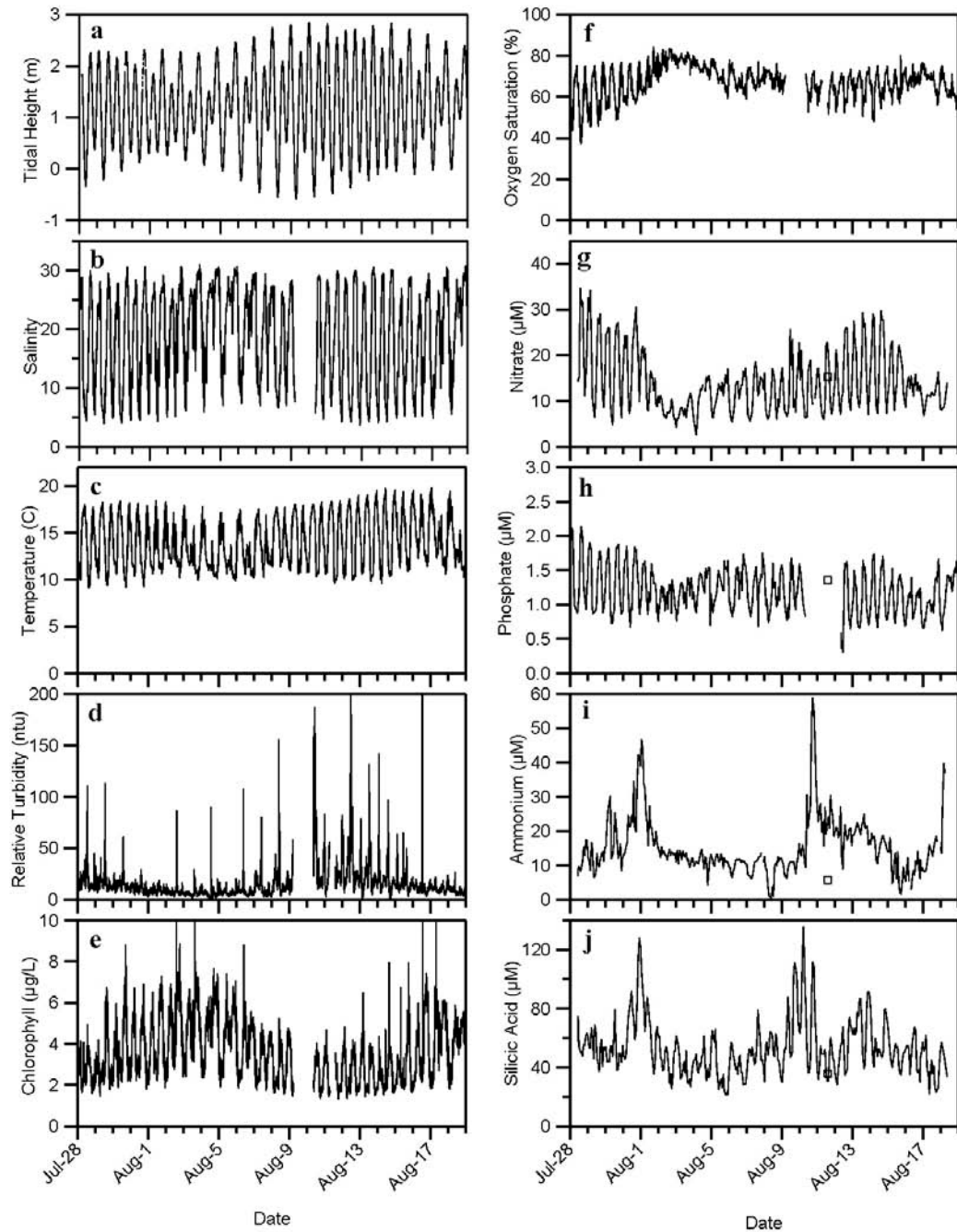


Figure 3.6. High resolution biogeochemical data from mid water (8.2 m) depth SATURN-03 during the summer from Jul. 28, 2010 to Aug. 18, 2010. □: grab samples taken from mid water (8.2 m) depth at SATURN-03. NOTE: **d** is the relative turbidity in which the clear water offset was not taken into account to get the true turbidity.

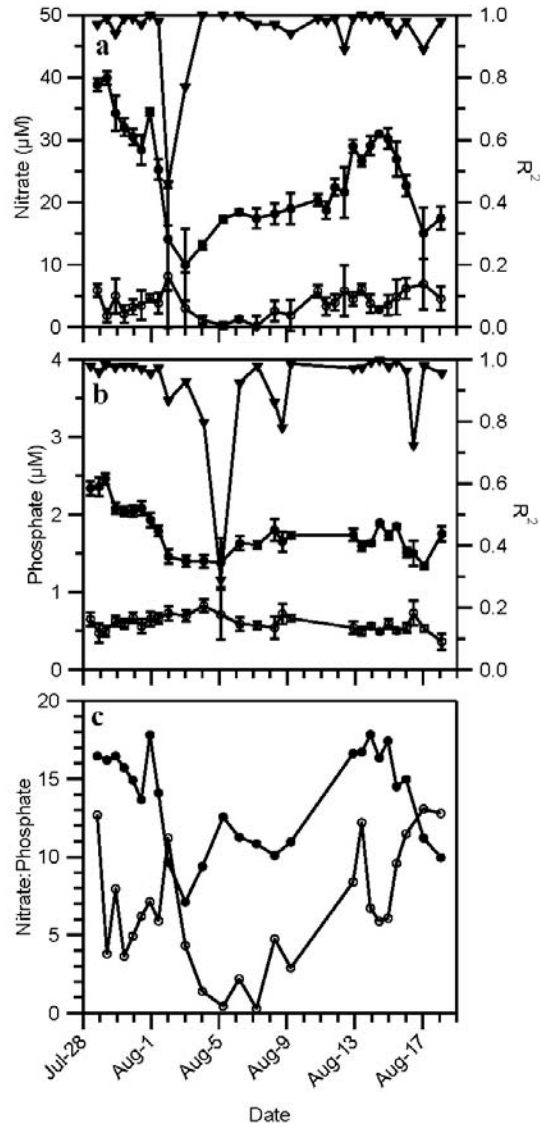


Figure 3.7. REM and OEM along with the corresponding R^2 for nitrate, phosphate, and nitrate:phosphate ratio. Note the high R^2 values for almost all end member calculations.

a Nitrate REMs and OEMs with corresponding R^2 values. Error bars represent the standard error of the regression (Zar 1984). **b** Phosphate REMs and OEMs with corresponding R^2 values. Error bars represent the standard error of the regression (Zar 1984). **c** Nitrate:phosphate ratio end members. ▼: R^2 values, ●: Ocean End Members (OEM), ○: River End Members (REM).

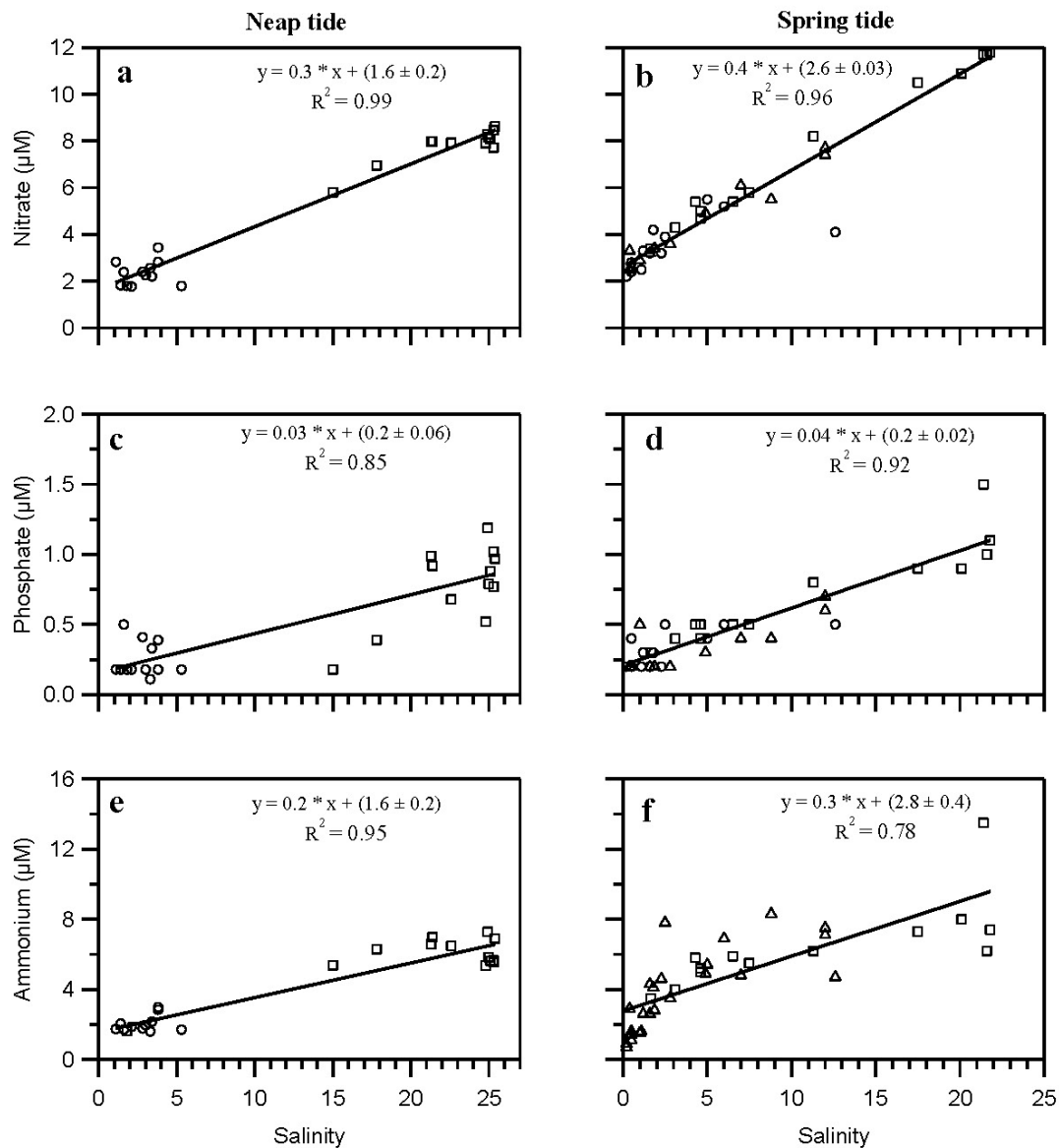


Figure 3.8. Conservative mixing regressions for nitrate, phosphate and ammonium from RM-17 for neap and spring tide outwash studies. \square : bottom samples, Δ : middle water samples, \circ : surface samples. The neap tide outwash was on 8/4/10 and the spring tide outwash was from 8/8/10 to 8/9/10. Note the high R^2 values allowing for the calculation of REMs and OEMs. CMR intercepts are given with one standard deviation.

9.0 Tables

Date	OEMS
7/28/3910	33.41
7/29/3910	33.56
7/30/3910	32.56
7/31/3910	33.70
8/1/3910	33.62
8/2/3910	33.66
8/3/3910	33.69
8/4/3910	33.24
8/5/3910	33.48
8/6/3910	33.32
8/7/3910	30.04
8/8/3910	32.49
8/9/3910	32.86
8/10/3910	32.96
8/11/3910	32.47
8/12/3910	33.08
8/13/3910	32.73
8/14/3910	32.51
8/15/3910	32.91
8/16/3910	33.18
8/17/3910	32.21
8/18/3910	33.70
8/19/3910	33.67

Table 3.1. Calculated Ocean End Member Salinity (OEMS) values from 7/28/2010 to 8/19/2010.

Nutrient	Neap 8/4/2010			Spring 8/8/2010		
	Reach	Reach	Reach	Reach	Reach	Reach
	C	B	A	C	B	A
Nitrate	4.3	1.6	1.2	3.2	2.6	2.6
Phosphate	0.2	0.2	0.7	0.2	0.2	0.5
Ammonium	0.3	1.6	Est. 11.1	0.3	2.8	Est. 7.2
% NH ₄ as Nr	~10	~45	~50	~10	~76	~50

Table 3.2. Nitrate, ortho-phosphate, and ammonium REM concentrations (μM) in Reaches C (SATURN-05), B (RM-17), and A (SATURN-03) during a neap (8/4/2010) and spring (8/8/2010) high resolution tidal outwash studies. The EREM (Est.) ammonium concentrations were given due to non-conservative mixing (see Methods).

10.0 References

- Abril, G., H. Etcheber, P. Le Hir, P. Bassoullet, B. Boutier, and M. Frankignoulle. 1999. Oxic/anoxic oscillations and organic carbon mineralization in an estuarine maximum turbidity zone (The Gironde, France). *Limnology and Oceanography* 44:1304-1315.
- Abril, G., M. Nogueira, H. Etcheber, G. Cabecadas, E. Lemaire, and M.J. Brogueira. 2002. Behavior of Organic Carbon in Nine Contrasting European Estuaries. *Estuarine, Coastal and Shelf Science* 54:241-262.
- Abril, G., S.A. Riou, H. Etcheber, M. Frankignoulle, R. de Wit, and J.J. Middelburg. 2000. Transient, Tidal Time-scale, Nitrogen Transformations in an Estuarine Turbidity Maximum-Fluid Mud System (The Gironde, South-west France). *Estuarine, Coastal and Shelf Science* 50:703-715.
- Aminot, A., R. K erouel, and D. Birout. 2001. A flow injection-fluorometric method for the determination of ammonium in fresh and saline waters with a view to in situ analysis. *Water Research* 35:1777-1785.
- APHA, AWWA, and WEF. 1981. *Standard Methods for Examination of Water and Wastewater*, 15th edition. Washington D.C., USA: American Public Health Association.
- APHA, AWWA, and WEF. 1975. *Standard Methods for the Examination of Water and Wastewater* 14th edition. Washington D.C., USA: American Public Health Association.
- Armstrong, F.A., C.R. Stearns, and J.D. Strickland. 1967. The measurements of upwelling and subsequential biological processes by means of TechniconTM AutoAnalyzerTM and associated equipment. *Deep Sea Research* 14:381-389.

Atlas, E., L.W. Hager, L.I. Gordon, and P.K. Park. 1971. A practical manual for use of the Technicon™ AutoAnalyzer™ in seawater nutrient analysis; revised. Oregon State University, Department of Oceanography. Technical Report 215.

Barnes, C.A., A.C. Dexbury, and B.A. Morse. 1972. Circulation and selected properties of the Columbia River effluent at sea. In *The Columbia River Estuary and Adjacent Ocean Waters*, eds. A.T. Pruter, and D.L. Alverson, 41-80. Seattle, WA: University of Washington Press.

Beusekom, J.E.E., and U.H. Brockmann. 1998. Transformation of Phosphorus in the Elbe Estuary. *Estuaries* 21:518-526.

Blackburn, T.H., and K. Henriksen. 1983. Nitrogen cycling in different types of sediments from Danish waters. *Limnology and Oceanography* 28:477-493.

Bottom, D.L., C.A. Simenstad, J. Burke, A.M. Baptista, A.D. Jay, K.K. Jones, E. Casillas, and M.H. Schieve. 2005. Salmon at river's end: the role of the estuary in the decline and recovery of Columbia River Salmon. U.S. Dept. Commer., NOAA Tech. Memo. NMFS-NWFSC-68.

Bricker, S., B. Longstaff, W. Dennison, A. Jones, K. Boicourt, C. Wicks, and J. Woerner. 2007. *Effects of Nutrient Enrichment In the Nations' Estuaries: A Decade of Change*. NOAA Coastal Ocean Program Decision Analysis Series No. 26 Silver Spring, MD: National Centers for Coastal Ocean Science.

Bruland, K.W., M.C. Lohan, A.M. Aguilar-Islas, G.J. Smith, B. Sohst, and A.M. Baptista. 2008. Factors influencing the chemistry of the near-field Columbia River

plume: Nitrate, silicic acid, dissolved Fe, and dissolved Mn. *Journal of Geophysical Research: Oceans* 113:C00B02. doi: 10.1029/2007JC004702.

Buresh, R.J., and W.H. Jr. Patrick. 1978. Nitrate reduction to ammonium in anaerobic soil. *Soil Science Society of America Journal* 42:913-918.

Caffrey, J.M. 1995. Spatial and Seasonal Patterns in Sediment Nitrogen Remineralization and Ammonium Concentrations in San Francisco Bay, California. *Estuaries* 18:219-233.

EPA. March 1984. "Nitrogen, Ammonium" Method 350.1 (Colorimetric, Automated Phenate). In *Methods for Chemical Analysis of Water and Wastewater*. Cincinnati, OH, USA: Environmental Monitoring and Support Laboratory, Office of Research and Development, U.S. Environmental Protection Agency.

EPA. March 1984. Phosphorus, All Forms Method 365.1 (Colorimetric, Automated Ascorbic Acid). In *Methods for Chemical Analysis of Water and Wastewater*. Cincinnati, OH, USA: Environmental Monitoring and Support Laboratory, Office of Research and Development, U.S. Environmental Protection Agency.

EPA. March 1984. Sample Preservation. In *Methods for Chemical Analysis of Water and Wastewater*. Cincinnati, OH, USA: Environmental Monitoring and Support Laboratory, Office of Research and Development, U.S. Environmental Protection Agency.

EPA. September 1997. Method 365.5. Determination of Orthophosphate in Estuarine and Coastal Waters by Automated Colorimetric Analysis. Cincinnati, Ohio: National Exposure Research Laboratory Office of Research and Development U.S. Environmental Protection Agency.

- Etcheber, H., A. Taillez, G. Abril, J. Garnier, P. Servais, F. Moatar, and M.V. Commarieu. 2007. Particulate organic carbon in the estuarine turbidity maxima of the Gironde, Loire and Seine estuaries: Origin and lability. *Hydrobiologia* 588:245-259. doi: 10.1007/s10750-007-0667-9.
- Ferguson, A., B. Eyre, and J. Gay. 2004. Nutrient Cycling in Sub-tropical Brunswick Estuary, Australia. *Estuaries* 27:1-17.
- Fox, J.B. 1978. The determination of nitrate: A Critical Review. *Critical Reviews in Analytical Chemistry* 51:1493-1502.
- Fox, L.E., S.L. Sager, and S.C. Wofsy. 1986. The chemical control of soluble phosphorus in the Amazon estuary. *Geochimica et Comochimica Acta* 50:783-794.
- Froelich, P.N. 1988 Kinetic control of dissolved phosphate in natural rivers and estuaries: A primer on the phosphate buffer mechanism. *Limnology and Oceanography* 33: 649-668.
- Galloway, J.N., J.D. Aber, J.W. Erisman, S.P. Seitzinger, R.W. Howarth, E.B. Cowling, and J.B. Cosby. 2003. The Nitrogen Cascade. *BioScience* 53:341-356. doi: 10.1641/0006-3568.
- Garnier, J., G. Billen, J. Némery, and M. Sebilo. 2010. Transformations of nutrients (N, P, Si) in the turbidity maximum zone of the Seine estuary and export to the sea. *Estuary Coast Shelf Science* 90:129-141.
- Genfa, Z., and P.K. Dasgupta. 1989. Fluorometric measurements of aqueous ammonium in a flow injection system. *Analytical Chemistry* 61:408-412. doi: 10.1021/ac00180a006.

Grasshoff, K., and F. Koroleff. 1983. Determination of nutrients. In *Methods of Seawater Analysis*, eds. K. Grasshoff, M. Ehrhardt, and K. Kremling, 125-187. Verlag Chemie.

Holmes, R.M., A. Aminot, R. Kerouel, B.A. Hooker, and B.J. Peterson. 1999. A simple and precise method for measuring ammonium in marine and fresh water ecosystems. *Canadian Journal of Fisheries and Aquatic Sciences* 56:1801-1808. doi: 10.1139/f99-128.

Hopkinson, C.S., A.E. Giblin, and J. Tucker. 2001. Benthic metabolism and nutrient regeneration on the continental shelf of Easter Massachusetts, USA. *Marine Ecology Progress Series* 224:1-19.

Howarth, R.W., G. Billen, D. Swaney, A. Townsend, N. Jaworski, K. Lajtha, J.A. Downing, R. Elmgren, N. Caraco, T. Jordan, F. Berendse, J. Freney, V. Kudeyarov, P. Murdoch, and Zhu Zhao-Liang. 1996. Regional nitrogen budgets and riverine N and P fluxes for the drainages to the North Atlantic Ocean: Natural and human influences. *Biogeochemistry* 35:75-139.

Jensen, M.H., E. Lomstein, and J. Sørensen. 1990. Benthic NH_4^+ and NO_3^- flux following sedimentation of a spring phytoplankton bloom in Aarhus Bight, Denmark. *Marine Ecology Progress Series* 61:87-96.

Kelly C.A., J.M. Rudd, R.H. Hesslein, D.W. Schindler, P.J. Dillon, C.T. Driscoll, S.A. Gherini, and R.E. Hecky. 1987. Prediction of biological acid neutralization in acid-sensitive lakes. *Biogeochemistry* 3:129-140.

Klump, J.V., and C.S. Martens. 1981. Biogeochemical cycling in an organic rich coastal marine basin – II. Nutrient sediment-water exchange processes. *Geochimica et Comochimica Acta* 45:101-121.

Kudela, R.M., A.R. Horner-Devine, N.S. Banas, B.M. Hickey, T.D. Peterson, R.M. McCabe, E.J. Lessard, E. Frame, K.W. Bruland, D.A. Jay, J.O. Peterson, W.T. Peterson, P.M. Kosro, S.L. Palacios, M.C. Lohan, and E.P. Dever. 2010. Multiple trophic levels fueled by recirculation in the Columbia River plume. *Geophysical Research Letters* 37:L18607. doi: 10.1029/2010GL044342.

Kudella, R.M., and T.D. Peterson. 2009. Influence of a buoyant river plume on phytoplankton nutrient dynamics: What controls standing stocks and productivity? *Journal of Geophysical Research Letters* 114:C00B11. doi: 10.1029/2008JC004913.

Lower Columbia River Estuary Partnership (LCREP). 2005. Lower Columbia River Estuary Monitoring Project: Annual Report for Year 2. Lower Columbia River Estuary Partnership, Portland, OR.

McIntire, D.C., and M.C. Amspoker. 1984. Benthic Primary Production in the Columbia River. Columbia River Estuary Data Development Program. Oregon State University, Corvallis, OR.

Moeller, F.U. 2011. Biogeochemical and Molecular Biological Characterization of Nitrogen Cycle Processes in the Columbia River and Estuary. A Master's Thesis. Oregon Health and Science University.

- Moore, A.M. 1968. Water Temperatures in the Lower Columbia River. Geological Survey Circular 551.
- Murphy, J., and Riley J.P. 1962. A modified single solution method for the determination of phosphate in natural waters. *Analytica Chimica Acta* 27:31-36.
- Nixon, S.W., J.W. Ammerman, L.P. Atkinson, V.M. Berounsky, G. Billen, W.C. Biocourt W.R. Boynton, T.M. Church, D.M. Ditoro, R. Elmgrene, J.H. Garber, A.E. Giblin'or, A. Jahnkel, N.J.P. Owens, M.E.Q. Pilson, and S.P. Seizinger. 1996. The fate of nitrogen and phosphorus at the land-sea margin of the North Atlantic Ocean. *Biogeochemistry* 35:141-180.
- Northwest Power and Conservation Council (NPCC). 2004. Mainstem Lower Columbia River Estuary Subbasin Plan. In Columbia River Basin Fish and Wildlife Program. Portland, OR.
- Prahl, F.G., L.F. Small, B.A. Sullivan, J. Cordell, C.A. Simenstad, B.C. Crump, and J.A. Baross. 1998. Biogeochemical gradients in the lower Columbia River. *Hydrobiologia* 361:37-52.
- Redfield, A.C., B.H. Ketchum, and F.A. Richards. 1963. The influences of organisms on the composition of sea-water. In *The Sea*, ed. M.N. Hill, 12-37. New York: John Wiley & Sons.
- Roegner, C.G., J.A. Needoba, and A.M. Baptista. 2011. Coastal Upwelling Supplies Oxygen-Depleted Water to the Columbia River Estuary. *PLoS ONE*. 6:e18672. doi: 10.1371/journal.pone.0018672.

- Rowe, G.T., C.H. Clifford, K.L. Jr. Smith, and P.L. Hamilton. 1977. Regeneration of nutrients in sediments off Cap Blanc, Spanish Sahara. *Deep-Sea Research* 24:57-64.
- Sakamoto, C., G. E. Friederich, and L.A. Codispoti. 1990. MBARI procedures for automated nutrient analyses using a modified Alpkem Series 300 Rapid Flow Analyzer, MBARI Technical Report 902.
- Simenstad, C.A., L.F. Small, D.A. McIntire, D.A. Jay, and C. Sherwood. 1990. Columbia River Estuary studies: an introduction to the estuary, a brief history, and prior studies. *Progress in Oceanography* 25:1-13.
- Small, L.F., and F.G. Prahl. 2004. A Particle Conveyor Belt Process in the Columbia River Estuary: Evidence from Chlorophyll a and Particulate Organic Carbon. *Estuaries* 27:999-1013.
- Smith, C.J., R.D. DeLaune, and W.H. Patrick. 1985. Fate of riverine nitrate entering an estuary: I. Denitrification and nitrogen burial. *Estuaries* 8:15-21.
- Sommerfield, W.N. 1999. Variability of residual properties in the Columbia River estuary: Pilot application of emerging technologies. Master's Thesis. Oregon Graduate Institute of Science and Technology, Beaverton.
- Sullivan, B.E., F.G. Prahl, L.F. Small, and P.A. Covert. 2001. Seasonality of phytoplankton production in the Columbia River: A natural or anthropogenic pattern? *Geochimica et Cosmochimica Acta* 65:1125-1139.
- van der Leeden, F., F.L. Troise, and D.K. Todd. 1990. *The Water Encyclopedia* 2nd edition. Lewis Publishers.

van Winkle, W. 1914. Quality of the Surface Waters of Washington. Government Printing Office.

Whetten, J.T., J.C. Kelley, and L.G. Hanson. 1969. Characteristics of Columbia River Sediment and Sediment Transport. *Journal of Sedimentary Petrology* 39:1149-1166.

Whitney, F. A., W. R. Crawford, and P.J. Harrison. 2005. Physical processes that enhance nutrient transport and primary productivity in the coastal and open ocean of the subarctic NE Pacific. *Deep-Sea Research II* 52:681-706.

Zar, J.H. 1984. *Biostatistical analysis*. New Jersey: Prentice-Hall.

Chapter 4

Conclusions and Future Direction

1.0 Conclusions

Biogeochemical changes in highly dynamic, tidally driven estuaries like the Columbia River estuary are difficult to study due to the rapid environmental changes. Environments such as these require high resolution data to decipher cause-effect. As the first multi-location high resolution multi-nutrient study in the Columbia River estuary-plume we described in detail how nutrient transformations were identified through river and ocean end members. Conservative mixing regressions and river and ocean end members allowed for the comparison of high resolution data between locations across the river-plume gradient. We determined that despite a short water residence time, a strong remineralization signal was present in the lower salt water estuary. High ammonium and phosphate concentrations in the estuary compared to the river and coastal ocean throughout the summer indicated the release of organic matter back into the water column. Paralleled spikes in ammonium and silicic acid in the lower estuary (SATURN-03) also supported this theory. We suggested that dissolution and remineralization was occurring within lateral bay sediment and the ETM. These high rates of remineralization led to an increase in the dissolved inorganic ammonium:nitrate ratio being exported to the coastal plume. Therefore, it is vital that ammonium be taken into account when calculating the reactive nitrogen flux to the coastal ocean. Although this work has been a significant leap into understanding nutrient transformations in the Columbia River

estuary significantly more work needs to be conducted to fully understand the implications of the processes identified here.

2.0 Future Direction

Observatory data will play a vital role in not only understanding the complexity of the Columbia River estuary, but other estuarine and coastal systems around the world in the near future. High resolution biogeochemical data from ocean observatories is leading science in a new and exciting direction. However, this is one in which the method of creating scientific hypothesis and testing them is not necessarily the case.

Instrumentation placed on an observatory platform to monitor high resolution changes in dynamic environments can yield unexpected results. Although ocean observatory data is becoming more prevalent and accessible, the challenge is this: What is the best way to use and present observatory data in hypothesis driven science?

This study yielded an unexpected and a novel approach to understanding nutrient transformations. Based on the premise that conservative mixing will occur given a short enough time scale, we were able to create conservative nutrient versus salinity regressions for every ebb tide. Variations in the slope and intercepts of these regressions over the spring/neap tidal cycle revealed that nutrient transformations (i.e. remineralization) were occurring within the estuary.

Identifying a key estuarine process like remineralization in the Columbia River estuary would not have been possible without the use of the CMOP observatories and campaigns; however, this study has also lead to many questions. Questions derived from this study include:

1. Are transformations of ammonium and phosphate occurring in the lateral bays of the estuary and/or within the ETM?

We were able to identify excess ammonium and phosphate in the estuary compared to the river and coastal ocean. Although we were able to determine that sources were located within the salt water estuary, our methods did not allow for the determination of a specific source location. Through an understanding of the estuary we were able to identify possible source locations as the lateral bays and/or within the ETM. Lateral bays in the Columbia River estuary are known to have fine grained sediment with large concentrations of benthic diatoms; therefore, were highly likely to be a site of nutrient remineralization. The ETM in the Columbia River is known to trap and transport particles as well as be a potential site for remineralization. Our results revealed strong pulses of ammonium and silicic acid during high turbidity spring tide events. During these low flow spring tides periods the ETM may be releasing rematerialized nutrients into the estuary. It is not clear from this work if remineralization is occurring in both or just one of these areas, thus more work should be done to determine the importance of the lateral bays and the ETM in nutrient transformations and export to the coastal ocean.

2. How much does particle attachment affect the nutrient measurements within the lower Columbia River estuary?

The Columbia River is highly turbid and may be affecting in situ nutrient measurements. In situ sensors (APNA and Cycle-PO₄) that were deployed filtered water to 10 μM , while samples that were collected to run in the laboratory

were filtered to 0.7 μM . Although some of our data suggests that particle attachment did not make a substantial difference in the nutrient concentrations, it should still be investigated to determine the appropriate filter size for in situ instruments in the Columbia River.

3. What are the true rates of denitrification, DNRA, and remineralization in fresh water tidal flat and lateral bay sediment?

Our study suggested that nitrate was lost mostly in the fresh water tidal flats of the Columbia River, while large sources of ammonium, phosphate and silicic acid were identified in the salt water estuary. Although we were able to determine a general area, we were not able to specifically identify the process in which nitrate was removed. To determine specific rates of denitrification, DNRA, and remineralization studies should be conducted on sediment cores from the fresh water tidal flats and lateral bays. This will aid in determining not only nitrate fluxes to the coastal ocean, but allow for further quantifying of nutrient transformations within a low water residence time estuary.

4. What are the consequences of high ammonium:nitrate ratios on the phytoplankton community in the Columbia River estuary and plume?

This study identified high concentrations of ammonium in the estuary and showed that ammonium accounted for approximately half of the Nr available in the estuary and coastal surface plume compared to the river and deep plume, in which ammonium only accounted for about ten to twenty percent of the Nr available. Nitrate fluxes to the coastal ocean have become much easier to determine due to in situ measurement such as SUNA and ISUS. This study

showed that in the Columbia River, especially during low flow summer months, it is vital that ammonium concentrations be taken into account when calculating the Nr flux to the coastal ocean. Furthermore, as the ratio of ammonium:nitrate changes from the river to the surface plume it will influence and potentially alter phytoplankton speciation and survival. Further studies should be done on the influence of the ammonium:nitrate ratio in the Columbia River plume.

5. How does estuarine silicic acid consumption, dissolution, and burial during the summer months influence the coastal ocean silicic acid budget?

During this study we identified a possible silicic acid dissolution signal as well as possible consumption within the salt water estuary (see Appendix A).

Although we were able to identify a consumption signal in the estuary, we were not able to determine if the silicic acid was being buried and removed from the system within the estuary or being dissolved back into the water column and transported to the coastal ocean. Further studies on biological silicic acid and sediment cores would identify if silicic acid is being buried or exported from the estuary. As damming of the Columbia River has increased summer discharge to the coastal ocean, burial of silicic acid in the estuary could significantly affect the coastal oceans silicic acid budget.

There is no doubt that coastal and ocean observatories like SATURN will play a key role in coastal ocean science in the near future. This study has shown that observatories can not only lead to scientific conclusions, but will be vital in generating explicit hypothesis for coastal systems.

Appendix A

Silicic Acid Data and Results

As part of this study silicic acid data was collected. Although silicic acid is vital to the environment and should be studied in much more detail most of this data was not vital to conveying the message in Chapter 3. Data tables and figures presented here will aid in the comprehension and discussion of the hypotheses in Chapter 3.

Neap Tide Outwash			
Station Name	Date Time (PST)	Depth	Silicic Acid (μM)
RM17-1	8/3/2010 17:46	12	55
RM17-2	8/3/2010 18:09	12	58
RM17-3	8/3/2010 19:08	12	58
RM17-4	8/3/2010 20:10	12	57
RM17-5	8/3/2010 21:10	12	54
RM17-6	8/3/2010 22:12	12	60
RM17-7	8/3/2010 23:09	12	52
RM17-8	8/4/2010 0:14	12	68
RM17-9	8/4/2010 1:09	12	72
RM17-10	8/4/2010 2:10	12	72
RM17-11	8/4/2010 3:12	12	79
RM17-12	8/4/2010 4:07	12	94
RM17-1	8/3/2010 17:46	0	136
RM17-2	8/3/2010 18:09	0	134
RM17-3	8/3/2010 19:08	0	134
RM17-4	8/3/2010 20:10	0	130
RM17-5	8/3/2010 21:10	0	131
RM17-6	8/3/2010 22:12	0	133
RM17-7	8/3/2010 23:09	0	139
RM17-8	8/4/2010 0:14	0	141
RM17-9	8/4/2010 1:09	0	141
RM17-10	8/4/2010 2:10	0	143
RM17-11	8/4/2010 3:12	0	115
RM17-12	8/4/2010 4:07	0	131

Table A.1.a. This data was collected from RM-17 in the Columbia River estuary (See Chapter 3 Figure 3.1). Samples were processed according to “Bench Top Nutrient Sampling Methods” in Chapter 3 Section 3.3.

Spring Tide Outwash

Station Name	Date Time (PST)	Depth	Silicic Acid (μM)
RM17S 1	8/8/2010 17:14	12	115
RM17S 2	8/8/2010 18:07	12	122
RM17S 3	8/8/2010 19:07	12	120
RM17S 4	8/8/2010 20:03	12	125
RM17S 5	8/8/2010 21:04	12	131
RM17S 6	8/8/2010 22:05	12	123
RM17S 7	8/8/2010 23:07	12	80
RM17S 8	8/9/2010 0:06	12	75
RM17S 9	8/9/2010 1:07	12	73
RM17S 10	8/9/2010 2:07	12	77
RM17S 11	8/9/2010 3:10	12	85
RM17S 12	8/9/2010 4:07	12	100
RM17S 13	8/9/2010 6:00	12	140
RM17S 1	8/8/2010 17:14	5	137
RM17S 2	8/8/2010 18:07	5	144
RM17S 3	8/8/2010 19:07	5	147
RM17S 4	8/8/2010 20:03	5	145
RM17S 5	8/8/2010 21:04	5	142
RM17S 6	8/8/2010 22:05	5	131
RM17S 7	8/8/2010 23:07	5	119
RM17S 8	8/9/2010 0:06	5	114
RM17S 9	8/9/2010 1:07	5	107
RM17S 10	8/9/2010 2:07	5	114
RM17S 11	8/9/2010 3:10	5	129
RM17S 13	8/9/2010 6:00	5	145
RM17S 1	8/8/2010 17:14	0	145
RM17S 2	8/8/2010 18:07	0	147
RM17S 3	8/8/2010 19:07	0	147
RM17S 4	8/8/2010 20:03	0	146
RM17S 5	8/8/2010 21:04	0	145
RM17S 6	8/8/2010 22:05	0	138
RM17S 7	8/8/2010 23:07	0	123
RM17S 8	8/9/2010 0:06	0	119
RM17S 9	8/9/2010 1:07	0	125
RM17S 10	8/9/2010 2:07	0	131
RM17S 11	8/9/2010 3:10	0	140
RM17S 12	8/9/2010 4:07	0	140
RM17S 13	8/9/2010 6:00	0	146

Table A.1.b. This data was collected from RM-17 in the Columbia River estuary (See Chapter 3 Figure 3.1). Samples were processed according to “Bench Top Nutrient Sampling Methods” in Chapter 3 Section 3.3.

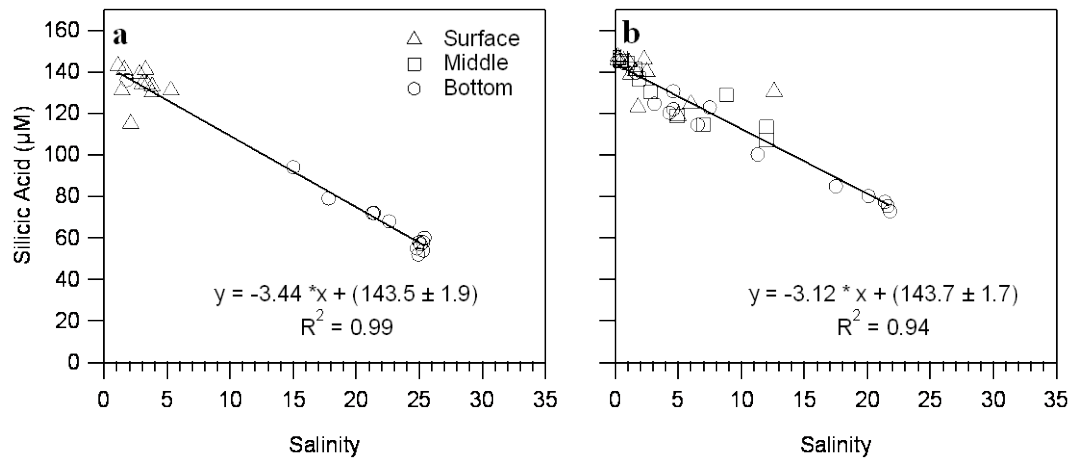


Figure A.1. Silicic acid versus salinity plots for RM-17 during **a** neap outwash (see Table A.1.a) and **b** spring tide outwash (see Table A.1.b) . Figures show conservative mixing of river and ocean end members.

Silicic Acid River and Ocean End Members				
Station Name	Date Time (PST)	Silicic Acid River End Member (μM)	Silicic Acid Ocean End Member (μM)	Silicic Acid Conservative Mixing Regression R^2
SATURN-03	7/28/2010 20:07	57.77	47.38	0.68
SATURN-03	7/29/2010 9:46	59.9	57.15	0.01
SATURN-03	7/29/2010 21:54	47.15	59.33	0.15
SATURN-03	7/30/2010 10:02	54	41.16	0.61
SATURN-03	7/30/2010 22:10	49.35	38.15	0.49
SATURN-03	7/31/2010 10:18	88.06	51.22	0.87
SATURN-03	7/31/2010 22:26	149.91	52.86	0.90
SATURN-03	8/1/2010 10:34	90.57	59.97	0.83
SATURN-03	8/2/2010 0:13	77.59	30.9	0.84
SATURN-03	8/3/2010 0:29	69.49	25.82	0.83
SATURN-03	8/4/2010 0:45	58.45	24.4	0.89
SATURN-03	8/5/2010 5:59	87.88	22.34	0.98
SATURN-03	8/6/2010 4:44	68.04	13.67	0.98
SATURN-03	8/7/2010 5:00	63.16	20.54	0.95
SATURN-03	8/8/2010 6:47	63.83	24.38	0.76
SATURN-03	8/9/2010 5:32	68.16	21.86	0.90
SATURN-03	8/10/2010 19:47	129.34	22.84	0.98
SATURN-03	8/11/2010 7:55	57.57	30.74	0.67
SATURN-03	8/11/2010 19:59	66.92	26.61	0.90
SATURN-03	8/12/2010 9:38	58.98	21.88	0.95
SATURN-03	8/12/2010 21:46	79.47	29.74	0.95
SATURN-03	8/13/2010 9:54	85.08	56.55	0.83
SATURN-03	8/13/2010 22:02	105.02	29.36	0.99
SATURN-03	8/14/2010 10:40	54.55	43.2	0.19
SATURN-03	8/14/2010 22:48	88.35	47.5	0.69
SATURN-03	8/15/2010 10:56	58.29	33.36	0.92
SATURN-03	8/16/2010 0:35	56.71	31.84	0.94
SATURN-03	8/17/2010 1:18	59.73	31.36	0.67
SATURN-03	8/18/2010 1:34	67.25	21.54	0.97

Table A.2. Silicic acid river and ocean end members and correlation coefficients (R^2) from SATURN-03 during the summer of 2010. End members were calculated using the “Conservative Mixing End Member Calculation” (See Chapter 3 Section 3.4.1).

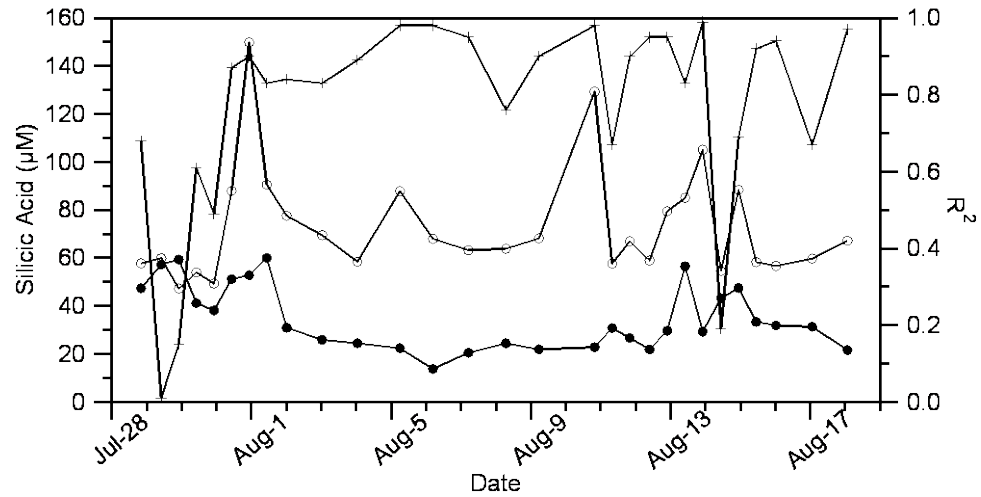


Figure A.2. Silicic acid river and ocean end members from SATURN-03 during the summer of 2010. ●: ocean end member, ○: river end member, +: correlation coefficient values (R^2). This graph shows that the ocean end member was lower than the river end member when correlation coefficients values (R^2) were acceptable. River end members at SATURN-03 were lower than river end members observed at RM-17 (see Fig. A.1 for RM-17 river end members), suggesting consumption of silicic acid in the salt water estuary. End members were calculated using the “Conservative Mixing End Member Calculation” (See Chapter 3 Section 3.4.1).

Plume Survey

Station Name	Date Time (PST)	Depth (m)	Latitude	Longitude	Silicic Acid (μM)
Plume 1	8/5/2010 12:30	3.23	46.181	-124.164	16
Plume 2	8/5/2010 20:30	N/A	46.375	-124.23	45
Plume 3	8/5/2010 21:40	14.57	46.496	-124.36	14
Plume 4	8/6/2010 2:06	21.88	46.285	-124.184	41
Plume 5	8/6/2010 3:06	5.42	46.262	-124.173	65
Plume 6	8/6/2010 3:59	18.28	46.23	-124.156	31
Plume 7	8/6/2010 5:03	0.55	46.195	-124.139	26
Plume 8	8/6/2010 5:57	25.63	46.191	-124.138	45
Plume 9	8/6/2010 7:09	3.53	46.226	-124.155	27
Plume 9 D	8/6/2010 7:09	3.53	46.226	-124.155	27
Plume 10	8/6/2010 8:11	5.84	46.255	-124.168	42
Plume 11	8/6/2010 8:18	0.83	46.259	-124.17	39
Plume 12	8/6/2010 9:04	24.84	46.281	-124.182	43
Plume 13	8/6/2010 9:10	2.91	46.284	-124.183	43
Plume 14	8/6/2010 10:13	25.53	46.282	-124.182	45
Plume 15	8/6/2010 10:19	1.53	46.279	-124.181	26
Plume 16	8/6/2010 11:16	21.57	46.252	-124.167	30
Plume 17	8/6/2010 11:18	2.95	46.25	-124.166	43
Plume 18	8/6/2010 13:13	20.19	46.19	-124.137	35
Plume 19	8/6/2010 13:21	1.86	46.186	-124.134	51
Plume 20	8/6/2010 21:04	23.58	46.264	-124.173	46
Plume 21	8/6/2010 21:00	4.00	46.262	-124.173	20
Plume 22	8/6/2010 22:07	3.05	46.294	-124.189	30
Plume 23	8/6/2010 22:12	23.78	46.297	-124.19	39
Plume 24	8/6/2010 23:12	3.00	46.288	-124.186	36
Plume 25	8/6/2010 23:05	20.93	46.291	-124.188	35
Plume 26	8/7/2010 0:02	3.98	46.267	-124.176	33
Plume 27	8/7/2010 0:08	19.81	46.264	-124.175	34
Plume 28	8/7/2010 1:05	3.74	46.241	-124.164	59
Plume 29	8/7/2010 1:02	12.38	46.243	-124.164	35
Plume 30	8/7/2010 2:07	3.50	46.211	-124.147	27
Plume 31	8/7/2010 2:01	16.80	46.214	-124.149	21
Plume 32	8/7/2010 3:07	3.72	46.182	-124.133	20
Plume 33	8/7/2010 3:01	33.49	46.185	-124.135	48
Plume 34	8/7/2010 12:05	2.47	46.206	-124.146	35
Plume 35	8/7/2010 12:09	25.54	46.205	-124.145	40
Plume 36	8/7/2010 13:51	38.14	46.174	-124.129	48
Plume 37	8/7/2010 13:57	2.01	46.177	-124.131	34
Plume 38	8/7/2010 16:04	1.93	46.242	-124.163	37

Plume 39	8/7/2010 16:07	19.98	46.244	-124.164	30
Plume 40	8/7/2010 18:13	23.87	46.309	-124.195	44
Plume 41	8/7/2010 18:19	7.35	46.312	-124.196	41
Plume 42	8/7/2010 22:34	1.78	46.222	-124.154	17
Plume 43	8/7/2010 22:37	22.13	46.22	-124.154	46
Plume 44	8/8/2010 0:03	7.44	46.182	-124.134	48
Plume 45	8/8/2010 0:13	3.86	46.182	-124.133	31
Plume 46	8/8/2010 1:04	0.93	46.199	-124.142	25
Plume 47	8/8/2010 1:10	31.60	46.202	-124.143	42
Plume 48	8/8/2010 2:06	23.54	46.228	-124.157	27
Plume 49	8/8/2010 2:09	1.75	46.23	-124.159	42
Plume 50	8/8/2010 3:11	12.67	46.261	-124.172	28
Plume 51	8/8/2010 3:12	3.15	46.262	-124.173	53
Plume 52	8/8/2010 3:57	3.87	46.246	-124.165	71
Plume 53	8/8/2010 4:00	15.84	46.244	-124.164	34
Plume 54	8/8/2010 4:32	14.08	46.221	-124.153	25
Plume 55	8/8/2010 4:37	1.10	46.217	-124.151	48

Table A.3. Silicic acid concentrations with corresponding latitude and longitude from the Columbia River plume during the summer of 2010. Samples were collected via a submersible underwater instrument package (Burke Hales and Oregon State University) and processed according to “Bench Top Nutrient Sampling Methods” in Chapter 3 Section 3.3.

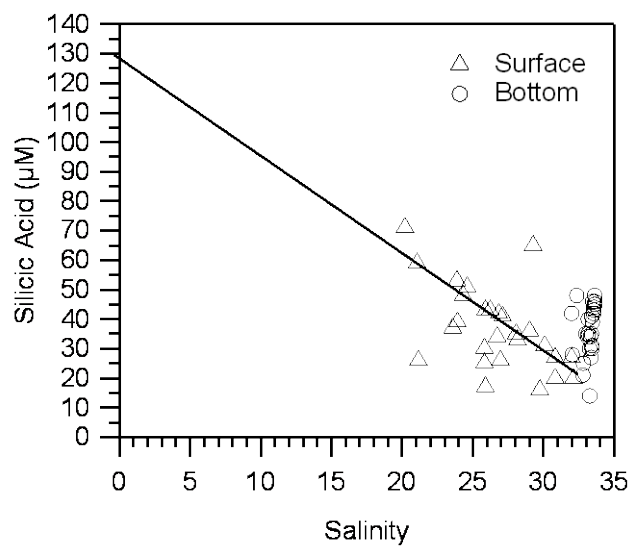


Figure A.3. Silicic acid versus salinity mixing regression from the Columbia River plume on 8/6/2010 to 8/8/2010. The – represents a hypothetical conservative mixing regression.

Note that some data points from the surface do not fall directly on the conservative mixing regression suggesting non-conservative mixing within the estuary.

Appendix B

Autonomous Profiling Nutrient Analyzer Procedures

1.0 Pre Deployment Procedure

Read through the ENTIRE APNA Operating Manual version 3.13 before moving forward with this procedure, as there are important details about operation that may not be covered in this procedure.

1.1 Cadmium column preparation

Preparation instructions for packing a new cadmium column are located on page 48 of the manual.

****All cadmium waste must be collected in the cadmium waste bottle in the hood and disposed of properly.**

A new column should be packed and conditioned if:

- a. Any air gets into the column
- b. The recovery is less than 90%

OR - The column should be flushed externally of the APNA if it has been sitting without use for more than a few days.

It is also a good idea to flush it externally after each deployment before the post calibration.

Additional Notes:

Cadmium can be re-used. Flush the used cadmium with Milli-Q and proceed to step iii of the cadmium column prep section of the APNA Operating Manual.

About 10-15 ml of 2 N HCl and 10% Cu sulfate should be enough to rinse the cadmium.

After 10% Cu sulfate is added, you should look for a brownish red precipitate to form. It will make the water cloudy. At this point the copperizing is done.

When rinsing the copperized cadmium, be sure to get rid of all of the fine particles in the water, as they can get through the glass wool and into the instrument.

When packing glass wool into the column it is ok to put a little more on the outflow side of the column (flow direction should be marked). Pack the glass wool loosely into the column.

Use Teflon tape to seal the column.

1.2 Reagent Pump Calibration

This should be done with the cadmium column that will be used for the deployment attached. It is a good idea to do the reagent pump calibration before any reagents are made in case any reagent pumps are not working properly.

Use the APNA_pumpcal_log.xls log sheet.

Fill out all relevant header information.

1.2.1 Flow meter Readings

Be sure all cables are properly attached to the APNA and power box. Plug the USB connector into the back USB port on the left side of the computer.

Place the inlet line in the 1 L MilliQ bottle and attach to the right port of the three port manifold. Prime the line using a syringe attached to the center port of three port manifold.

Follow instructions in section 4b of the APNA Operating Manual to open ChemView software to test mode. Select COM 3 and be sure that 115200 baud rate is selected, click the "OK" button. Turn on the power to the APNA. Follow instructions in section 4b of the APNA Operating Manual to turn on the "HEATER" and the "MZR SWP" at 5.0 ml/min. Let the APNA pump for at least 10 minutes to clear any air in the lines. NOTE: It is always a good idea to turn on the heater every time you turn on the seawater pump so it is not forgotten when an inlet calibration is performed.

Be sure that all waste lines are free of air and then insert each waste line into a 3 ml syringe for 2 minutes and record the volume of water on the log sheet. Also record if there is 0, ½, or 1 psi adjuster on the waste line. All waste lines should have a flow of about 1 ml/minute.

If the flows are not balanced repeat the step above altering the PSI adjusters on each waste line until a balanced flow is achieved.

NOTE: DO NOT add more than one 1 psi adjuster to each waste line as it will not allow for air bubbles to clear from the line.

Record the system PSI 1 and 2 on the log sheet.

1.2.2 Total Flow Measured

Obtain a small beaker and zero it on the 200 g balance. Place all waste lines in the beaker for 3 minutes. Record the weight on the log sheet.

1.2.3 Pump Calibration

Click on the "REAGENTS" tab.

All reagent lines should be filled with MilliQ and free of air bubbles. If they are, skip the rest of this step. If they are not air free put all the reagent lines in a beaker of MilliQ (This should NEVER be the same as the inlet line). Follow the instructions in section 4b of the APNA Operating Manual to set all reagent pumps to 0.5 and turn them on. Check to make sure all the lines are pumping. Let the lines pump for at least 5 minutes. Follow instructions in section 4b of the APNA Operating Manual to turn off the reagent pumps.

Attach 3 ml syringes to all reagent lines and fill with water to 3 ml. Record the 0.1 Start (ml) on log sheet.

Follow the instructions in section 4b of the APNA Operating Manual to set all of the reagent pumps to 0.1 including the cal pump. Simultaneously turn on all the reagents and start the timer for 3 minutes.

Before the 3 minutes is up switch off all the reagents. When the timer sounds, click the “SEND UPDATE” button.

Record the new volume for all reagents in the 0.1 Stop box on the log sheet.

Set all pumps to 0.2, turn them on and start the timer. Record the stop mass on the log sheet. Repeat for the remainder of the boxes on the log sheet.

NOTE: It may be necessary to refill the syringe if it gets low and will not have enough volume to pump for all three minutes.

1.2.4 Analyzing the Data

Open “APNA_pumpcal_template.xls”

Save the file as YYMMDD_pumpcal.

Enter all of the information from the log sheet into the proper boxes.

NOTE: If slopes do not look linear perform the calibration again.

Print the file and check for errors. Sign off at the bottom of the page that the file has been proofed. The most current pump cal is kept in section 4 of the APNA Operating Manual. All others are filed by date in the data notebook.

1.2.5 Update ANA.CFG file

The pump set points located in the CFG file are used in the ChemView software in Test mode and Auto mode. They are also the settings that appear in the reagent tab when test mode is loaded.

Follow directions in section 4c of the APNA Operating Manual to open ChemView and enter file transfer mode.

Click on the picture of a folder and select the CHEMVIEW SUPPORT folder. There should be an ANA.CFG file located in this folder. Click the “Select Directory” Button.

Click on and highlight in blue the ANA.CFG file on the left side of the screen. This is the file that is on the computer. Click on the “EDIT” button. This will open the file in word pad. Edit the file with the new pump rates and save the changes.

On the left hand side of the screen click on the two arrows that point to the right. This will send the new ANA.CFG file to the APNA. The new date and time stamp of the ANA.CFG file will be displayed in the directory listing on the right hand side of the screen. If it is not there push the “DIRECTORY” button to re-display the files.

Close all of ChemView and re-open. Check the reagent tab to be sure the upload was successful.

1.3 Reagent Preparation

Recipes for reagents are located on page 48-50 of the manual.

See the END CAP PORT LABELS diagram in the beginning of the APNA Operating Manual for port letters and locations.

Other Notes

Record the lot numbers and weights or volumes of each chemical used and the date they are made. The date the chemical is made becomes the lot number. See below for proper expiration dates for each reagent.

Make sure there are enough of all chemicals in stock before starting to make reagents.

Acid wash every piece of glassware, bottle, reagent bag, and syringe before and after each use.

Filter all reagents through a 0.45 μ M membrane filter.

Rinse filter apparatus, storage bottle and reagent bag with reagent before filling.

Once neutralized, all chemicals can be dumped down the drain.

****NOTE: (The NOX and NO2 waste must be collected and returned to the OHSU laboratory to be neutralized and disposed of)** These chemicals are toxic to the natural environment and the MERTS facility does not have an industrial sewage treatment plant to dispose of it.

It is a good idea to keep at least 60 ml of each chemical in the laboratory during the deployment so that if any of the chemicals run out during the deployment the post calibration can still be run.

NED Stock Reagent (27.8 mM) Nitrate/Nitrite – Stable 1 month, Store 4° C

Store this reagent in a dark bottle and cover the reagent bag in aluminum foil or dark trash bag to prevent degradation. This reagent must be neutralized and disposed of down a drain that goes to an industrial sewage treatment plant.

Sulfanilamide Stock Reagent (0.23 M) Nitrate/Nitrite – Stable 1 month, Store 4° C

This reagent must be neutralized and disposed of down a drain that goes to an industrial sewage treatment plant.

Color Reagent Nitrate/Nitrite– Stable 1 month, Store 4° C

The color reagent for NO_x addition #2 (D) and NO₂ addition (E) reagent lines is a mixture of equal parts of NED and Sulfanilamide.

Ammonium Chloride (3.74 M) Nitrate - Stable 3 months, Store 4° C

If two consecutive deployments are planned two liters of this can be made to reduce the amount of waste. It is also good to have a little around in case a cadmium column needs to be conditioned. If other reagents are being made on the same day as this it is a good idea to save this one for last to avoid ammonium contamination not only to the ammonium reagents but others as well. It is also a good idea to double acid wash any container that comes in contact with ammonium chloride as it is hard to wash out of glassware. This is for the NO_x addition #1 (C) reagent line.

Sodium Molybdate (43.8 M) for Phosphate – Stable 1 month, Store 4° C

Dissolve the potassium antimony tartrate in water, dissolve the sodium molybdate. Add the sulfuric acid after both the potassium antimony tartrate and sodium molybdate are completely dissolved. (This prevents a blue color from forming.) This is for PO₄ addition #1 (F).

L-Ascorbic Acid (0.14 M) for Phosphate – Stable 1 month, Store 4° C

This is for PO₄ addition #2 (G).

Phosphate Color Reagent –

This instrument is NOT set up for a color reagent. The sodium molybdate and ascorbic acid are pumped into the sample stream separately to increase longevity of the reagents.

Sodium Molybdate (64.1 mM) Silicate – Stable 1 month, Store Room Temperature

This reagent pumps at 0.10 ml/min so make 2 L of this reagent and fill a Hyclone 2 L reagent bag with about 1500 ml. These reagent bags seem to reduce blue color formation compared to the ones ordered from SubChem. This reagent is for Si addition #1 (H).

Oxalic Acid (0.50 M) Silicate – Stable 3 months, Store Room Temperature

If two consecutive deployments are planned 2 L of this can be made to reduce the amount of waste. This reagent is for Si addition #2 (I).

L-Ascorbic Acid (0.806 M) Silicate – Stable 1 month, Store 4° C

This reagent is for Si addition #3 (J).

EDTA conditioning reagent (0.625 M) Ammonium – Stable 3 months, Store Room Temperature

If two consecutive deployments are planned 2 L of this can be made to reduce the amount of waste. This reagent is pumped at 0.10 ml/min which is twice as fast as the OPA. Be sure there is slightly more than double of this reagent than there is OPA because a precipitate will form when the OPA is added to seawater without this reagent. **Do NOT let this run out before the OPA!** Use a 2 L reagent bag if necessary. DO NOT use a stop cock valve for this chemical as it will eat through the plastic and spill. If storing this reagent in a reagent bag hang the bag upside down with a stop cock on the end for extra protection. This is for NH₃ addition #1 (**K**).

OPA Stock Solution (0.783 M) Ammonium – Stable 1 month, Store 4° C

The OPA solid should be kept in the dark at 4° C. It is vital that this reagent run out before the EDTA so only 500 ml is necessary. The OPA takes a while to dissolve in the methanol so leaving it in a refrigerator overnight to dissolve is a good idea.

****This reagent can penetrate latex, vinyl, and nitrile gloves. For caution use two pair of gloves and dispose of gloves immediately after working with the reagent or if any is spilled on your hands. It will turn your hands a black color if it gets on your gloves.**

OPA Fluorescence reagent - Stable 1 month, Store 4° C

This reagent should be kept in the dark. DO NOT use a stop cock valve for this chemical as it will eat through the plastic and spill. If storing this reagent in a reagent bag hang the bag upside down with a stop cock on the end for extra protection.

1.4 Standard Preparation

Recipes for standards are located on page 48-50 of the manual. Also see APNA_standards.xls or standard preparation sheet in the front of manual.

Standards do NOT need to be filtered.

100 mM Standards (NO₃, PO₄, Si, NH₄) – Stable 6 months, Store 4° C

100 mM Standards (NO₂) – Stable 3 months, Store 4° C

1000 µM Standards – Stable 3 months, Store 4° C

Daily Standards – Stable 1 day

Standard Curve Standards – prepare just before running

Standard Addition for In Situ – Prepare just before deployment and remake for each deployment

This is for calibration addition (**B**). This standard's pH **MUST** be decreased to <8.5 to reduce the risk of precipitation in the reagent line.

1.5 Pre Deployment Inlet Calibration

1.5.1 Inlet Calibration

This should be done with the cadmium column that will be used for the deployment attached.

Use log sheet APNA_inletcal_log.xls

Fill out header information.

Fill in the lot numbers and expiration dates of all reagents and standards.

Prepare working stock standards according to recipe on the log sheet and record the time in PST.

After the inlet line is primed with MilliQ, follow the procedure in the APNA Operating Manual of section 4b to turn on the “MZR SWP” and the “HEATER”.

Let the system run for about 5-10 minutes.

Record the PSI 1 and PSI 2 on the log sheet.

Place each waste line in a 3 ml syringe and measure the volume of outflow for 2 minutes. Record the volumes on the log sheet.

NOTE: If the volumes are significantly different than they were in the pump calibration re-balance the flows and record any changes made to PSI adjusters.

If reagents are not already attached and primed this is the time to do so. Turn on the reagent pumps to a set point of 0.50 and pump for at least 5 minutes.

NOTE: Be sure that there are no stop cock valves on either of the ammonium reagents as they will crack and leak.

Turn off the reagents and let MilliQ pump through the instrument until a stable baseline is reached for at least 3 minutes.

Follow the procedure in section 4b of the APNA Operating Manual to start the logging process in Test mode. Save the file according to the following format:
YYMMDD_inletcal.DAT

Record the file name and start time on the log sheet.

Record the time each new standard is started along with the stable peak value in the appropriate boxes on the log sheet.

Prepare each standard according to the log sheet just before running and record the elapsed time it was made on the log sheet.

Before running each standard, insert a separate inlet line into the standard and attach it to the left port of the three port manifold. Prime the line by using a syringe attached to the center port to pull any air bubbles out of the line.

Continue until all of the standards have been run.

End logging and record the end elapsed time on the log sheet.

NOTE: This number disappears when you push the button so you have to note the time before you push the “DATA LOGGER” button.

1.5.2 Data Processing

Open the data file that was just created and saved as YYMMDD_inletcal.DAT. Highlight and copy only the cells that have data.

Open the APNA_inletcal_template.xls file. Click on the “RAW” tab. Paste copied data into Cell A1. All of the calculations should be performed automatically. NOTE: If all the data is not showing up on the charts, the calculation columns may need to be extended.

Print out all the “filt” charts for each of the five channels.

Drag the cursor over the chart and record the peak height next to each peak for each channel.

Click on the “slopes” tab. Enter the recorded values into the appropriate boxes. Enter the cadmium column serial number and the intercept from the NOX channel into the appropriate boxes.

Record any comments in the comments box.

Print the slopes page and proof it against the peak numbers. Sign and date at the bottom of all the slope pages that they have been proofed.

Review the data to see if a second calibration needs to be performed for any reason.

1.6 AUTO Mode Testing

1.6.1 Upload a new ANA.SSF file

Follow the procedure in section 4c of the APNA Operating Manual or see the **Update ANA.CFG file** section above to transfer an updated ANA.SSF file to the APNA.

NOTE: It is a good idea to keep all instrument commands under the AUTO ON feature. If the instrument loses power for any reason, sampling will continue as soon as the power is restored.

Exit all ChemView software.

Place the inlet line in fresh MilliQ water and prime.

Open ChemView in Auto mode and turn on the power. This should start the sampling. It is a good idea to have at least three blank files run in a row before each deployment. This helps ensure the data quality when processing and also ensures that the APNA runs correctly in Auto mode.

Once three MilliQ measurements are made the power can be switched off at any time while in wait mode.

1.7 Field Instructions – for deployment at SATURN-03

When transporting the APNA be sure it is secure and that all of the reagent line stay connected to the APNA. It is easiest if they are already loaded onto the pole they will be hanging from in the field.

DO NOT take the APNA on a cart that vibrates as it may cause damage to internal parts.

Once at the shack, set up the instrument, attach all cords, inlet lines, and waste lines.

The current inlet line consists of two 47 mm filter housings in parallel. Each housing contains a mesh 30 μ M pre filter and a 10 μ M membrane filter. All housings should be pre-loaded and the remaining ones left with the field team.

Once all lines and cables are attached properly prime the inlet line by following the Changing Filters in the Field.xls procedure.

With the data cable attached to the laptop turn on the APNA in auto mode and watch one file to be sure it is running properly.

If it is running properly turn off the power to the APNA while in wait mode and detach the data cable from the computer and attach it to the top port of the computer at SATURN-03.

Turn the power to the APNA back on and watch for flow. It is a good idea to tape the power button down to be sure it can not be accidentally turned off.

Have the field team turn on the computer with the data output and watch for the mode to change. See APNAHyperterminalCodes.pdf for details.

Once it is clear the APNA is running properly it is ok to close the computer connection and leave.

The data can be viewed via the web and should be checked daily.

2.0 Post Deployment Procedure

2.1 Data Download

There are a few ways to download data, but this is the way that has worked best.

Follow the instructions in section 4c of the APNA Operating Manual to open file transfer mode.

Click on the folder button and select the folder on the computer the data will be put into. NOTE: A good filing system is to store the data in dated folders. (All previous data is kept in the APNA folder on the desktop organized into folders in YYMM format.)

On the left side of the screen will be all the files currently on the APNA. Highlight in blue all of the files that need to be transferred to the computer. NOTE: It is always a good idea to transfer the ANA.CFG and ANA.SSF files with all of the data.)

Click on the double arrow pointing to the right on the left side of the screen. This will start the download process.

During this process errors may occur, so it is important to check back and push ok if an error has occurred.

Once all of the files have been downloaded, sort them by size to see if there are any that are unusually small. If so re-download those specific files by following the same procedure as above.

Once all of the files have been downloaded successfully, highlight only the .DAT files that have been transferred. Click on the “Delete” button. DO NOT delete the ANA.SSF or the ANA.CFG files.

2.2 Post-Deployment Inlet Calibration

Flush the cadmium column with MilliQ externally of the APNA to be sure there is no loose sediment trapped in it that could cause a blockage in the instrument.

Reattach the cadmium column

Use log sheet APNA_inletcal_log.xls

Fill out header information. Fill in the lot numbers and expiration dates of all reagents and standards. It is vital that the same reagents be used for the post deployment inlet cal as was used for the pre-calibration.

Prepare working stock standards according to the recipe on the log sheet and record the time in PST.

After the inlet line is primed with MilliQ, follow the procedure in section 4b of the APNA Operating Manual to turn on the “MZR SWP” and the “HEATER”.

Let the system run for about 5-10 minutes.

Record the PSI 1 and PSI 2 on the log sheet.

Place each waste line in a 3 ml syringe and measure the volume of outflow for 2 minutes. Record the volumes on the log sheet.

NOTE: If the volumes are significantly different DO NOT change where the pressure adjusters are, continue with the procedure. This calibration is supposed to represent what was happening in the field.

Let MilliQ pump through the instrument until a stable baseline is reached for at least 3 minutes.

Follow the procedure of section 4b of the APNA Operating Manual to start the logging process in Test mode. Save the file according to the following format:
YYMMDD_inletcal.DAT

Record the file name and start time on the log sheet.

Record the time each new standard is started along with the stable peak value in the appropriate boxes on the log sheet.

Prepare each standard according to the log sheet just before running and record the elapsed time it was made on the log sheet.

Before running each standard, insert a separate inlet line into the standard and attach it to the left port of the three port manifold. Prime the line by using a syringe attached to the center port to pull any air bubbles out of the line.

Continue until all of the standards have been run.

End the logging and record the end elapsed time on the log sheet.

NOTE: This number disappears when you push the button so you have to note the time before you push the "DATA LOGGER" button.

2.3 Data Processing

Open the data file that was just created and saved as YYMMDD_inletcal.DAT. Highlight and copy only the cells that have data.

Open the APNA_inletcal_template.xls file. Click on the "RAW" tab. Paste the copied data into Cell A1. All of the calculations should be performed automatically. NOTE: If all the data is not showing up on the charts the calculation columns may need to be extended.

Print out all the "filt" charts for each of the five channels.

Drag the cursor over the chart and record the peak height next to each peak for each channel.

Click on the “slopes” tab. Enter the recorded values into the appropriate boxes. Enter the cadmium column serial number and the intercept from the NOX channel into the appropriate boxes.

Record any comments in the comments box.

Print the slopes page and proof it against the peak numbers. Sign and date at the bottom of all the slope pages that they have been proofed. Review the data.

2.4 System Cleaning

2.4.1 Flow Cell Cleaning

Remove the cadmium column and place the cadmium column bypass (a piece of 1/16 in tubing) in its place.

Remove all the reagent bags.

Place the inlet line in MilliQ and attach the inlet line to the right valve on the three valve manifold. Prime the inlet line using the center valve. Follow the instructions in section 4b of the APNA Operating Manual to turn on the “MZR SWP” pump.

Place all reagent lines in a beaker of MilliQ. Under the “REAGENTS” tab in test mode set all of the reagent pumps to 0.5. Follow instructions in section 4b of the APNA Operating Manual to turn on all the reagent pumps.

Let the lines pump for about 10 minutes and then turn off all of the pumps following the instructions in section 4b of the APNA Operating Manual.

Clean the beaker and replace with new water. Follow the instructions in section 4b of the APNA Operating Manual to turn the pumps back on and let pump for another 10 minutes. This ensures that all of the reagent lines are purged with clean MilliQ water.

Once all of the reagent lines have been purged with MilliQ perform the Optical Detector Cleaning Procedure for APNA in section 9d of the APNA Operating Manual. If the detector readings do not return to what they were before the deployment repeat this procedure until they do.

2.4.2 Cadmium column cleaning

During the cleaning procedure, it is a good idea to flush the cadmium column after a deployment. The best way to do this is to actually remove the cadmium from the column and rinse it with water. It may not be necessary to recondition the column but it is important that all of the sediment be flushed out. Use new glass wool to repack the column as it will prevent any of the cadmium stuck on the old glass wool from getting into the APNA and causing a blockage. NOTE: Discard the waste properly (see cadmium column prep in Deployment procedure).

The APNA is now ready to be deployed again!

3.0 MatLab OHSUAutoAnalysisV2 in depth analysis

Developed by Ezra-Mel Paskiatan, from SubChem Systems Inc. program

3.1 Introduction

This document was originally written by Ezra-Mel B. Pasikatan and edited by Melissa Gilbert to add a more in depth line by line analysis. See MatLabCodeSummary.doc for original writing by Ezra-Mel B. Pasikatan.

3.2 Methods—APNA Data Analysis

The data analysis routine for the APNA is an improvement of a Matlab program originally developed by Peter Egli of Sub Chem Systems Inc. The program has been equipped with several improvements, which will be explained further below.

The first improvement to the program called a ‘debubble’ program, a script which takes out ‘bubble spikes’ in absorbance coefficient (1/m) data based on statistical parameters. Second is a subprogram which actively looks for the areas to take measurements from the raw data. Third is full automation of the program with optional manual inputs. Fourth is a graphical User Interface which allows for fast processing of data, as well as human feedback into an otherwise computerized system. This improved system will be used to process the APNA data more accurately.

The novel aspect of this project was to automate the data analysis process and improve the quality of processed data. Therefore, the Matlab code will be heavily discussed. To aid future users of the program, as well as to lower the learning curve for those who would like to improve the program or modify it for other research purposes. Discussion will revolve around the specific function of the code and the reasoning for it, as well as improvements.

3.3 Line by Line Analysis

3.3.1 Program 1: APNADataAutoProcessor.m

APNADataAutoProcessor is a heavily modified version of OHSUAnalysisV2 by Peter Egli of Sub Chem Systems Inc. Essentially, it’s an overhead file that contains scripts for each of the five nutrients analyzed by the APNA.

Line 17-18: ensures that all previous work is cleared.

Line 23-14: The main change from the previous version of this program is a relocation of the uigetfile() function from each script to the header file. Uigetfile() opens a user interface for the user to open the Matlab file the user would like to work with. This has been done to streamline the process of processing the files. Instead of having the user go through this five times, each time having to wait until the previous set of files processes, the user can define the path of the program once, then let the program run by itself.

Line 28: This line allows for the option of either entering all of the input variables into the code or having the program prompt for input variables such as slope and intercept. If running only one nutrient not through this header program “yn=yes” must be set in MatLab for the individual nutrient files to work.

Line 30, 38, 40, 41: These lines calculate how fast the program processed all of the files and prints it out in the MatLab Command Window when the processing is finished.

Line 32-36 These are the individual file names. Each file will be processed one at a time in this order. See the corresponding .m file for details.

3.3.2 Program 2: Nutrient Sub files

NOxAnalysis_autoV2.m, NO2Analysis_autoV2.m, PO4Analysis_autoV2.m, SiAnalysis_autoV2.m, NH3Analysis_autoV2.m

A subroutine exists for each of the five nutrients the APNA analyzes. The file names are above. Each is essentially the same except for input variable numbers so the description will only be discussed once.

Lines 12-15: The program imports all .dat files in the specified file path. The filenames are read into a structure array.

Line 23-61 and 71-103: These lines were inserted into this program for when the leak alarm is on. When the leak alarm is activated an @ symbol is put in the data and MatLab can't read it. This portion of the code increases the amount of time it takes to process files so there is a switch in the code to only activate it if we know there is a leak. The code can be turned off by putting any number other than 1 in line 30 of the code.

Lines 60: The Julian Time Stamp is then extracted from the name of each file.

Lines 64-66 and 104-107: Time, Elapsed Time, and the Raw Data are then extracted in the same manner as the Julian Time stamp.

Line 68-81: Due to a change in the output file on the APNA a subroutine is used to identify the column in which the specific nutrient data resides.

Line 113-138: A yes or no switch case allows the user to either input processing parameters manually or use automatic defaults. Input variables for Cdark and Cref can be found in the APNA manual.

Line 142-183: A second switch case allows the user to input time series measurement placement parameters, or use the defaults.

Line 188-189: The data is then passed through the Debubble_d function.

Line 198: The second filter option is ignored and the filtered data then equals the data from the Debubble_d function.

Line 202-212: All zeros in any of the matrices created so far in the program are then removed and set to non-number placeholders (NaN).

Line 216-222: The Absorption Coefficient is calculated using variables set in the previous switch case. The general formula for the absorption coefficient calculation can be found in the APNA Manual.

Line 226: The actual concentration of the sample is calculated by using the slope and intercept from the input variables.

Line 230: The data is then fed into the PlateauSelectorV2.m, an automatic measurement location finder.

Line 234-258 Comma Separated Value (.csv) files are then written of each file. With the following data in each column:

JD (Julian Day) = column A (1)

Time = column B (2)

ET (Elapsed Time) = column C (3)

RawData (not filtered through debubble_d program) = column D (4)

ACData (absorbance data filtered through debubble_d program) = column E (5)

ConcData (concentration data filtered through debubble_d program) = column F (6)

Baseloc (The center point in ET of the baseline location) = column H (8)

Sampleloc (The center point in ET of the sample location) = column I (9)

Calloc (The center point in ET of the calibration location) = column J (10)

Line 256: Each file is written as with Processed in front of the nutrient and file name in Julian Day.

Line 263-290: Flags are assigned to bad data

Line 269: A flag of 1 is assigned to any data file in which the location selected for the baseline noise is greater than the standard deviation entered in the input variables in the beginning of the process.

Line 276: A flag of 2 is assigned to any data file in which the location selected for the sample noise is greater than the standard deviation entered in the input variables in the beginning of the process.

Line 283: A flag of 4 is assigned to any data file in which the location selected for the calibration noise is greater than the standard deviation entered in the input variables in the beginning of the process.

Line 289: The total flag is calculated by adding the sum of lines 216, 223, and 230.

Line 294-330: The final section of the program outputs an excel summary of the data. Final calculation to adjust the Sample and Calibration measurements are done in this

section Also, Flags are written into the matrix AvgData. This matrix, along with the column names are written into an excel file named AvgNOxData.xlsx .

- Column A (1) = str2double(nameonly) **Filename**
- Column B (2) = JD **Julian Day**
- Column C (3) = Time **Start Time**
- Column D (4) = mean(BaseData) **Avg Baseline (1/m)**
- Column E (5) = std(BaseData) **Baseline Std Dev(1/m)**
- Column F (6) = mean(SampleData) **Avg Sample (1/m)**
- Column G (7) = std(SampleData) **Sample Std Dev(1/m)**
- Column H (8) = mean(CalData) **Avg Cal (1/m)**
- Column I (9) = std(CalData) **Cal Std Dev(1/m)**
- Column J (10) = Column F (6) – Column D (4) **Adj. Sample (1/m) (subtracting out the baseline from the sample)**
- Column K (11) = Column F (6)– column H (8) **Adj. Cal (1/m) (subtracting the sample from the calibration spike)**
- Column L (12) = Column K (11)/spike **In Situ Cal Slope**
- Column M (13) = Column J (10)-intercept)/slope [Lab Cal(uM)] **(the intercept and slope are from the input variables. This calculates the final concentration of the nutrient based on the lab inlet calibration.)**
- Column N (14) = Column G (7)/slope [Lab Slope Error(uM)]
- Column O (15) = Column K (11)-intercept)/column L (12) **[In Situ Cal(uM)]**
- Column P (16) = Column G (7)/column L (12) % **[In Situ Slope Error(uM)]**
- Column Q (17) = TFlag **(Calculated in line 236)**
- Column R (18) = BadData **(These data will appear as red points in the GUI)**
- Column S (19) = DoubleCheck **(These data will appear as yellow points in the GUI)**
- Column T (20) = CaseOtherOther+FewPlat **(These data will appear as blue points in the GUI)**
- Column U (21) = baseloc **(The center point in elapsed time of the baseline location)**
- Column V (22) = sampleloc **(The center point in elapsed time of the sample location)**
- Column W (23) = calloc **(The center point in elapsed time of the calibration location)**
- Column X (24) = slope **(This is from the input variable)**
- Column Y (25) = spike
- Column Z (26) = intercept **(This is from the input variable)**
- Column AA (27) = 0

Changes from previous version

This program has been streamlined to be used for the corresponding GUI. Instead of outputting detailed excel files of each sample, basic .csv files are created. Changes include: only the columns for time, elapsed time, ACData, ConcData, and the locations of the base, sample and calibration measurements. This was done because having all the information for each sample on an excel file was made redundant by the GUI. These .csv files contain information for the GUI to use. The creation of .jpeg files of each plot has been completely eliminated. This is because the GUI will create adjustable plots using the .csv files.

3.3.3 Program 3: Debubble_d.m

The debubble_d.m subroutine was the first part of the program to be improved. Dissolved gasses often come out of solution in the tubing which leads to the reaction chamber. This results in spikes in the transmittance data. The debubble_d.m subroutine was created to smooth these bubble spikes. The program takes out any points that are more than three standard deviation above or below a moving average of n points (n being an arbitrary user defined number), then takes a smoothing function to the data.

Lines 22-30: To obtain the mean and standard deviation, the program takes the 2-D matrix fed into it and creates a 3-D matrix by flipping $2n+1$ point in each row upward into the third dimension.

Lines 40-45: The mean and standard deviation of each column corresponding to a point is taken.

Lines 49-50: The upper and lower standard deviation limits are set using the mean plus or minus 3 multiplied by the standard deviation divided by the square root number of points in the running mean.

Lines 59-77: The matrix is then reset to its original length.

Lines 81-87: The resulting matrix is then compared to the upper and lower limits. If the point around which the running average is not in the limit, it is set to the non-number place holder NaN.

Lines 93-108: A smoothing function is then used, which replaced all NaN points with the mean around that point.

3.3.4 Program 4: PlateauSelectorV2.m

The Plateau Selector routine is a completely new addition to the program. It supplements (and can eventually replace) the time-based parameters used by the original program. The first derivative is used to tell the plateau regions and slope regions apart. Once this is done, a switch case will identify areas to place measurements based on the location of the maximum and minimum and the number of regions between them.

Lines 4-6: The program imports the variable ACData from each of the nutrient analysis file and finds its length and width.

Lines 10-12: It then initializes the output variables which specify the middle of the location of the base, sample, and calibration locations.

Lines 15-26: The derivative of the Y variable is then found and filtered using a moving average filter. This moving average filter creates more even regions by taking out isolated pockets of high or low slope.

Lines 27-29: The moving average filter is shifted so that the average is in the center of the data span being used.

Lines 31-64: A logical array called Bounds is then created which corresponds to Y and defines regions of plateaus (1) and slopes (0). This array is created by applying a threshold to the slope. This threshold is defined by the range of the data file divided by an arbitrarily large number. Plateau regions occurring before 300 seconds are deleted. Plateaus smaller than 10 seconds are deleted from Bounds.

Lines 69-76: The variable Ybounded is created in order to exclude any slope area for data processing purposes later. All slope areas, as defined by the Bounds variable, are set to NaN.

Lines 114-136: The maximum and minimum of the data from each sample is found, as well as their locations. The location of the maximum and minimum is bounded by limits which exclude sections of data where the max and min should not exist.

Lines 138-141: The heart of the code is the regionprops function. This function is actually a part of Matlab's image processing toolbox, but it has been adapted for sample data processing use. The regionprops function creates a label matrix from a logical array. Each region is labeled with a number, and a structure array containing various properties of each region, in this case, the area and pixel locations (PixelIdxList) are created. The first switch case criteria is the number of regions in the image.

Lines 142-146: The label matrix L along with the locations of the maximum and minimum is then used to calculate the second switch case variable, the number of regions between the max and min regions.

Lines 151-177: All variables needed for the switch case are then initialized.

Lines 180-190: The switch case selector uses two criteria to process files: (1) the number of regions total, and (2) the number of regions between the max and min regions. If there are none or only one region, the data is flagged as an error, and the measurement locations are determined using default time series parameters.

Lines 192-201: If there are two regions and the Yminloc occurs after the Ymaxloc the default time series settings are used.

Line 203-215: Otherwise the program looks for the longest region. If the longest region occurs first, it places the base and sample measurement location there. If not, it assumes there has been no calibration spike and places both sample and calibration measurements on the same plateau. In this case the data is flagged as bad because an assumption has been made.

Lines 217-225: A second switch case is nested in the otherwise statement of the first switch case. This switch case uses the number of plateaus between the max and min plateau regions. If the two plateau regions are right next to each other, the data is processed similar to the two regions case in the main switch case, and marked with a special flag which alerts the user that an assumption was made to process that data.

Line 231-241: If there are three or more plateau regions between the min and the maximum. If there are less than two regions the error case is used where the time series default picks the locations.

Line 241-257: If a long baseline plateau or a long calibration plateau is observed with no plateaus in the middle of the min and max. If a long baseline plateau occurs the sample location is placed just to the left of the baseline measurement. If a long cal plateau is observed the sample is placed just to the right of the second area.

Line 259-273: The ideal case is when there is only one region between the min and max regions. The sample measurement is placed in the middle of the center region, and the data is not flagged.

Line 276-284: If there are more than one region between the max and min regions, the longest one is found, and the measurement placed in its middle. The sample is flagged as an assumed data location.

Line 318-324: Output variables are set after the switch case.

Lines 326-348: After those are set, additional files are flagged from criteria based on the output variables.

3.3.5 Program 5: APNADDataGUI

The Graphical User Interface was built to aid in file processing by allowing a user to quickly see trends in the data processed by the first program. It consists of two windows. The first or main window plots the adjusted sample data files as concentration.

This primary window consists of the graph an Import, Click Point, Reset and Done Button, as well as basic instructions for each. The Import Button opens a file import interface that allows the user to import an excel file into the GUI that has been processed by the above program. The adjusted data (concentration) column of that file is then plotted in the main axes, with the points color coded with their flags. Red is bad data, yellow is data that definitely needs to be looked at; blue is that there was an assumption made and may need to be checked and green is good data. The reset button clears the data plotted in the axes. Done writes the current data into an excel file and opens the file. Click Point activates the data cursor mode function, and lets the user click on a point to pull up information about it in a small text box. If the user presses enter while the point is clicked, the secondary GUI window is opened.

The Secondary GUI window opens a plot of the absorbance or fluorescence data used to obtain the point clicked in the main GUI window. The interface allows the user to select the locations of the baseline, sample, and calibration measurements on the plot with the three sliders located at the bottom of the GUI. Once the user is satisfied with the updated measurement location, the save button should be pressed to update the main data variables. If the data is not worth keeping, the delete button allows the user to completely discard the data in the secondary GUI and the point corresponding to it on the main GUI plot (set everything in the row corresponding to plot to NaN except for the time stamps). The previous and next file button allow the user to toggle between files in the secondary

GUI, while the previous and next flag buttons do the same for flagged files. The done button saves all changes to the application data, closes the secondary GUI and reopens the main GUI.

Since the code for the GUI program is essentially described by the function of the buttons, a code summary will not be created.

3.4 Matlab Data Processing Manual

1. Open Matlab. Make sure the folder the program APNADDataAutoProcessor (as well as the Nutrient Subroutines, clickplotter_d, and PlateauSelectorV2) is located in is in the Matlab File Path.

a. To do this right click on the folder and click on add to path and then selected folders and subfolders.

3. If the leak alarm was activated at any point during the deployment line 30 of each nutrient sub file will have to be changed to a 1 before proceeding any further.

2. Type APNADDataAutoProcessor into the command window, or open the .m file and click the run button or see step four for instructions on how to process a single channel.

a. A file open window will appear. Open a .dat in the folder where the batch of downloaded APNA files has been placed.

3. A prompt asking if the user would like to change default settings will appear. Answer yes to activate the pop-up menus to change parameters such as the calibration slope and intercept. Answer no to use the default settings.

4. To process a single channel follow step one above and then open the folder with all of the .DAT files that need to be processed.

a. Type yn= 'yes' into the command prompt if the input variables need to be changed and yn='no' if the default settings will be used.

b. Be sure the "current folder" in the MatLab window is the folder with the data that is going to be analyzed.

c. Type one of the following NOxAnalysis_autoV2; NOxAnalysis_autoV2;
NO2Analysis_autoV2; PO4Analysis_autoV2; SiAnalysis_autoV2; NH3Analysis_autoV2
into the MatLab command window.

d. The pop-up menu will appear if the user has typed yes and it will use default settings if the user has typed yn='no'

Using the GUI: APNADDataGUI

1. Open Matlab. Make sure APNADDataGUI is in the Matlab file path.

2. Type APNADDataGUI into the command window, or open the .m file and click the run button.

3. Click the Import Files Button. Open the Summary (Avg) excel file for a set of data, which was previously processed by APNADDataAutoProcessor.

Note: Any Avg file can be opened in the GUI including ones that have already been processed as long as no changes have been made to them. Thus it is a good idea to save a copy of any Avg file with a different name if it has been altered in any way.

4. If the file you open is not the one you want, or are done with the file, click Reset, then Import another file.

5. Click a point on the graph. A tag with information on the point should appear next to it. When you find the point you would like to check, press enter while the tag of that point is displayed. This will open the secondary GUI.

6. The secondary GUI has a plot, a set of three sliders, and seven buttons. The three sliders control the location of the base, sample, and calibration measurements. The Next/Previous and Next Flag/Previous Flag buttons allow the user to move between files or flagged files while in the secondary GUI. The delete button deletes the point represented by the sample plot in the main plot. The save button saves the current slider locations, and updates the main plot to account for those changes. The done button closes the secondary GUI and opens the main GUI.

7. The secondary GUI can be activated as many times as necessary.

8. When processing is finished, press done in the main GUI to output an excel file.

4.0 Discrete Sample Processing

4.1 APNA Prep

A MINIMUM of 100 ml of filtered sample is needed to obtain accurate concentrations on the APNA.

Before starting to run samples on the APNA a reagent pump calibration (see Pre-Deployment Procedure) and a full inlet calibration (see Pre-Deployment Procedure) should be performed.

4.2 Running Discrete Samples

Samples should be thawed to 55° C and cooled to room temperature before running.

Use log sheet APNA_discrete_log.xls.

Fill out header information.

Fill out lot numbers and expirations of all reagents and standards. Additional QC information can be recorded on the log sheet or in the laboratory notebook.

Prepare working stock standards according to log sheet and record the time made in PST.

After the inlet line is primed with MilliQ, follow the procedure in section 4b of the APNA Operating Manual to turn on the “MZR SWP” and the “HEATER”.

Let the system run for about 5-10 minutes.

Record the PSI 1 and PSI 2 on the log sheet.

Place each waste line in a 3 ml syringe and measure the volume of outflow for 2 minutes. Record the volumes on the log sheet.

NOTE: If the volumes are significantly different than they were in the pump calibration re-balance the flows and record any changes made to PSI adjusters.

Follow the procedure in section 4b of the APNA Operating Manual to start the logging process in Test mode. Save the file according to the following format: YYMMDD_discrete_YYMMDD.DAT, where the first date is the current date of the run and the second date is when the samples were collected.

Record the file name and start time in PST on the log sheet.

The first sample should be DI followed by DI + reagents (RG), S5, and S4.

This is a good time to run a QC sample.

If all standards appear to be at the appropriate heights, continue to run samples.

It may be necessary to run an additional DI baseline before changing to samples.

Each sample should have a background (no reagents) and a sample + RG reading. Each reading will take between 5-7 minutes. Record both the background and the Sample + RG on the log sheet.

A calibration check should be performed at the beginning, end, and between every 5-6 samples.

It is a good idea to run a QC check at the end of the run.

4.3 Discrete Data Processing

Open the data file that was created and saved as YYMMDD_discrete_YYMMDD.DAT. Highlight and copy only the cells that have data.

Open the APNA_discrete_template.xls file. Click on the "RAW" tab. Paste the copied data into cell 1A. All of the calculations should be performed automatically. NOTE: If all data is not showing up on the charts the calculation columns may need to be extended.

Print out the "filt" plots for all five channels. NOTE: It may be necessary to print two plots per channel if the run is long.

Drag the cursor over the chart and record the peak height next to the peak. Repeat this for each channel.

Click on the "Conc." Tab. Enter all of the sample ID's. Enter all the baseline data (no reagents) in the columns labeled "B" and all of the data with reagents into the columns labeled "raw".

Fill in all of the yellow boxes at the top of the spreadsheet. The slopes should be from the inlet calibration. The intercept is set up to detect the lowest value from the day or the intercept from the inlet calibration. Replace the -999 with the intercept from the inlet calibration.

The "final" page is meant to be a summary of all the data with calculations standard percent recoveries. If standards are not within 90-110% it is advisable to correct the data for poor standard recoveries.